

# **DEVICE, ELECTRONIC, TECHNOLOGY TO ALLOW THE EXTRACTION OF VACUUM ENERGY**

SANGOUARD Patrick:

EXTRACTION OF A VACUUM ENERGY CONFORMING TO EMMY NOETHER'S THEOREM OF 1915 ?:  
principle, mathematization, simulation, electronics, and technology

patrick.ps.patrick@gmail.com

. Tel: 06 86 50 78 44

## TABLE OF CONTENTS

### **I / OBTAINING AN ELECTRIC CURRENT FROM VACUUM?**

- I.1 / Introduction
- I.2 / Brief presentation of Casimir's force
- I.3 / extract energy from a vacuum?

### **II / DESCRIPTION OF THE PRINCIPLE USED TO "EXTRACT" ENERGY FROM THE VACUUM**

### **III / CALCULATION OF THE CURRENT GENERATED BY THE CASIMIR STRUCTURE**

- III.1 / calculation of the vibration frequency of the casimir structure
- III .2 / Calculation of the current peak

### **IV / USE OF DIFFERENT PIEZOELECTRIC MATERIALS**

#### **IV.1 = PIEZOELECTRIC MATERIAL = PZT**

- IV-1.1 / Space between Casimir electrodes as a function of time over 2 periods, for different trigger values of MOS transistors
- IV-1.2 / Spatial and temporal evolution of the Coulomb and Casimir forces during an entire period
- IV-1-3 / Variation of the starting interface  $z_0$  between Casimir electrodes: PZT
- IV-1-4 / variation of the length  $l_s$  of the Casimir electrode: PZT
- IV-1-5 / variation of the width  $b_p$  of the piezoelectric bridge: PZT
- IV-1-6 / variation of the thickness  $a_p$  of the piezoelectric bridge: PZT
- IV-1-7 / variation of the proportionality ratio  $p = FCO / FCA$ : PZT

#### **IV-2 / USE OF OTHER PIEZOELECTRIC MATERIALS**

##### **IV-2-1 / Piezoelectric material = PMN-PT**

- IV-2-1-1 / Evolution of the Casimir interface as a function of time during two periods
- IV-2-1-2 / Evolution of the forces of Casimir and Coulomb
- IV-2-1-3 / Ratio variation as a function of Casimir interval and current peak as a function of the ratio: PMN-PT
- IV-2-1-4 / peak current as a function of time and peak voltage at the terminals of the choke for 2 periods: PMN-PT
- IV-2-1-5 / threshold voltage according to the desired FCO / FCA ratio
- IV-2-1-6 / Vibration frequency as a function of the FCO / FCA ratio and peak current as a function of the Casimir interval chosen: PMN-PT

##### **IV-2-2 / Piezoelectric material = AlN**

#### **IV-3 / CONCLUSIONS**

### **V / TRANSFORMATION AND AMPLIFICATION ELECTRONICS WITHOUT EXTERNAL SUPPLY OF A PERIODIC SIGNAL OF A FEW MILLIVOLTS IN A CONTINUOUS VOLTAGE OF A FEW VOLTS**

### **VI / EMBODIMENT TECHNOLOGY OF THE CURRENT EXTRACTOR DEVICE USING THE FORCES OF CASIMIR IN A VACUUM**

### **VII / STEPS FOR THE REALIZATION OF THE STRUCTURE AND ITS ELECTRONICS**

### **VIII / ENERGY BALANCE**

### **IX / CONCLUSIONS BIBLIOGRAPHY APPENDICES**

### **X / A FEW REMINDERS FROM RDM**

- X.1 / Calculation of the deflection of a bridge embedded at its 2 ends X.2 /
- Calculation of the resonant frequency of the piezoelectric bridge
- X.2.1 / Differential equation of a vibrating beam and determination of the eigen modes
- X.2.2 / Eigen modes and frequencies
- X.2.3 / Boundary conditions:

### **XI / MATLAB PROGRAM USED FOR NUMERICAL SIMULATION**

## LIST OF FIGURES

- Figure 1: Casimir effect
- Figure 2: General representation of the structure
- Figure 3: View of the device without electronics
- Figure 4: Different view of the device without electronics
- Figure 4b: Representation of the reference used Axes, Forces, Electrodes Casimir
- Figures 5: general configuration of the device: MOS grid connections (Face 2 of the piezoelectric bridge: red), Source connections (Face 1 of the piezoelectric bridge: green)
- Figure 6: distribution of the threshold voltages of the enriched and depleted N and P MOS switches
- Figure 7: Polarization, applied force and appearing load on a piezoelectric block
- Figure 7b: Piezoelectric coupling mode
- Figure 8: Piezoelectric bridge Cutting Reactions and Bending Moment, Deflection Angle
- Figure 9: Table of characteristics used for MATLAB and ANSYS simulations
- Figure 10: Final structure with the metal oxides surrounding the metal electrodes
- Figure 11: Interval between Casimir electrodes as a function of time for a proportionality coefficient  $F_{CO} / F_{CA} = 2$ : PZT
- Figure 12: Vibrations of the structure for a coefficient of proportionality  $p = F_{CO} / F_{CA} = 200$ : PZT
- Figure 13: Casimir force and Coulomb force during a complete cycle  $f$  (interface between electrodes of the Casimir resonator) and for a coefficient of proportionality  $p = F_{CO} / F_{CA} = 200$
- Figure 14: Casimir force and Coulomb force during a complete cycle  $f$  (time) and for a coefficient of proportionality  $p = F_{CO} / F_{CA} = 200$
- Figure 15: shows the ratio  $p = F_{CO} / F_{CA} = f(\text{time})$  during a complete structural vibration cycle and with a choice of maximum ratio = 200
- Figure 16: Maximum Peak CURRENT =  $f$  (starting interface  $z_0$ ), Maximum selected  $F_{CO} / F_{CA}$   $p$  ratio = 200
- Figure 17: Structure vibration frequency =  $f$  (starting interface  $z_0$ ):  $F_{CO} / F_{CA}$  chosen = 200: PZT
- Figure 18: MOS threshold voltage =  $f$  (starting interface  $z_0$ ):  $F_{CO} / F_{CA}$  chosen = 200: PZT
- Figure 19: maximum current =  $f$  (length of the Casimir electrode  $l_s$ ), starting interface = 200 A °, selected coefficient of proportionality =  $p = F_{CO} / F_{CA} = 2$
- Figure 20: Threshold Voltage =  $f$  (length of the Casimir electrode  $l_s$ ), starting interface = 200 A °, selected coefficient of proportionality =  $p = F_{CO} / F_{CA} = 2$
- Figure 21: threshold voltage =  $f$  (piezoelectric bridge width), Starting interface = 200 A °:  $F_{CO} / F_{CA}$  chosen = 10
- Figure 22: current =  $f$  (piezoelectric bridge width), Starting interface = 200 A °:  $F_{CO} / F_{CA}$  chosen = 10
- Figure 23: CURRENT =  $f$  (the thickness  $ap$  of the piezoelectric bridge), Starting interface = 200 A °:  $F_{CO} / F_{CA}$  chosen = 10
- Figure 24: Threshold of the MOS =  $f$ (Thickness of piezoelectric film ), start Interface = 200 A ° with a choice  $F_{CO} / F_{CA} = 10$
- Figure 25: Structure vibration frequency =  $f$  (the thickness  $ap$  of the piezoelectric bridge), Starting interface = 200 A °:  $F_{CO} / F_{CA}$  chosen = 10
- Figure 25: Peak current =  $f$  (Ratio  $p = F_{CO} / F_{CA}$ ), Starting interface = 200 A ° Piezoelectric material = PZT
- Figure 26: Figure 26; current of the MOS =  $f$  (ratio =  $F_{CO} / F_{CA}$ ), start Interface = 200 A ° piezoelectric material = PZT
- Figure 27 Threshold voltage of the MOS =  $f$  (ratio =  $F_{CO} / F_{CA}$ ), start Interface = 200 A ° piezoelectric material = PZT
- Figure 28: plot of the evolution of the Casimir inter-electrode interval as a function of time over two periods and Ratio  $F_{CO} / F_{CA} = 10000$ : Inter-electrode Casimir interface = 200 A °
- Figure 29: plot of the evolution of the Casimir inter-electrode interval as a function of time over two periods and an  $F_{CO} / F_{CA}$  Ratio = 1000: Casimir inter-electrode interface = 200 A °
- Figure 30: plot of the evolution of the Casimir inter-electrode interval as a function of time over two periods and a Ratio  $F_{CO} / F_{CA} = 2$ . Casimir inter-electrode interface = 200 A °
- Figure 31: Materials = PMN-PT: Coulomb and Casimir force as a function of the inter-electrode interface. Starting interface = 200A °
- Figure 32: Materials = PMN-PT: Coulomb and Casimir force as a function of time. Starting interface = 200A °
- Figure 33: Materials = PMN-PT: Ratio  $p = F_{CO} / F_{CA}$  as a function of time. Starting interface = 200A °
- Figure 34: Materials = PMN-PT: Coulomb Force / Casimir Force ratio as a function of the Casimir inter-electrode interface. Starting interface = 200A °
- Figure 35 Materials = PMN-PT: Peak Current delivered by the structure as a function of the  $F_{CO} / F_{CA}$  Ratio. Starting interface = 200A °
- Figure 36 Materials = PMN-PT: Current peak as a function of time obtained over 2 cycles. Starting interface = 200A °

- Figure 37: Materials = PMN-PT: Voltage peak across the  $2 \cdot 10^{-4}$  H choke as a function of the time obtained over 2 cycles. Starting interface = 200A °
- Figure 38: Materials = PMN-PT: Voltage peak across the  $2 \cdot 10^{-4}$  H choke as a function of the  $F_{CO} / F_{CA}$  Ratio. Starting interface = 200A °
- Figure 39: Materials = PMN-PT: Threshold voltage of the Enriched or Depleted MOTS according to the  $F_{CO} / F_{CA}$  Ratio. Start interface = 200A °
- Figure 40: Materials = PMN-PT: Vibration frequency as a function of the  $F_{CO} / F_{CA}$  Ratio. Starting interface = 200A °
- Figure 41: Materials = PMN-PT: Current peak across the  $2 \cdot 10^{-4}$  H choke as a function of the starting interval between Casimir electrodes. Starting interface = 200A °
- Figure 42: Piezoelectric Material = AlN Casimir, Coulomb Force = f (Time) starts Interface = 200 A °
- Figure 43: Piezoelectric Material = AlN Ratio  $F_{CO} / F_{CA} = f$  (Time) starts Interface = 200 A °
- Figure 44: Material = AlN Interval between Casimir electrodes = f (time) during two complete cycles: Interface between starting electrodes = 200 A °
- Figure 45: Principle of electronics for amplifying and rectifying a weak AC
- Figure 46: Elementary stage for obtaining a negative voltage from the negative part of the alternative signal of the transformer (coil)
- Figure 47: Elementary stage for obtaining a positive voltage from the positive part of the alternative signal of the transformer ( coil)
- Figure 48: SPICE simulations of voltages, current, power of the transformation electronics into a direct voltage (5.4 V) of an alternating input signal of 50 mV
- Figure 49: SPICE simulations of the currents drawn by the transformer and the power consumed by this transformer.
- Figure 50 / DC output voltages as a function of the number of elementary stages for AC input voltages of 20 mV and the other of 100 mV.
- Figure 51: influence of the coupling capacitance on the amplification of the input signal
- Figure 52 / Evolution of the DC output voltage as a function of the amplitude of the AC input signal for a frequency of 150 kHz
- Figure 53 / Evolution of the power supplied in nW by the source as a function of the amplitude of the voltage supplied in mV.
- Figure 54: Summary of the characteristics of the circuit for transforming a voltage of a few millivolts into a direct voltage of a few volts and without any power supply circuit.
- Figure 55: S.O.I technology for making the elements of the “doubler”
- Figure 56 extract de [7]
- Figure 57: Growth of SiO<sub>2</sub> oxide on silicon
- Figure 58: Distribution of thickness
- Figure 59: etching of S.O.I silicon
- Figure 60: Engraving of the protective metal rear face of the S.O.I.
- Figure 61: deposition and etching of the piezoelectric layer
- Figure 62: Metal deposit, Metal engraving
- Figure 63: view of the Casimir device on the rear face, engraving on the rear face of the structures.
- Figure 64: Adjusted growth of metal oxide under the electronic control, front view of the Casimir device
- Figure 65: Position of the mobile Casimir electrode when the Coulomb force appears
- Figure 66: Displacement of the mobile Casimir electrode during the appearance of the Coulomb force
- Figure 67: general appearance of the device studied, forces and applied moments
- Figure 68: view of the deformed bridge
- Figure 69 : width , length , thickness of the bridge
- Figure 70: a / Forces, shear forces and Moments applied on the bridge. b / Variation of bending moment. c / Shape and arrow of the bridge embedded at both ends. With:  $\delta_0$  = inflection points,  $z_{max}$  = arrow of the bridge
- Figure 71; Section, Frenet trihedron
- Figure 72: Numerical solution of equation 18
- Figure 73 : ANSYS simulation of the resonant frequency of the piezoelectric
- Figure 74: ANSYS simulation of the resonant frequency of the complete structure

## ABSTRACT

This theoretical and preliminary work corresponds to the hope of extracting, without contradicting EMMY NOETHER's invariance theorem, an energy that is omnipresent, isotropic, uniform and present in the entire universe: that of the void!

This theoretical work shows that it should be possible to maintain over time a periodic vibration of a piezoelectric structure which generates current peaks during a fraction of the period of vibration. This is achieved by controlling automatically and at the opportune moments the perpetual and omnipresent action of Casimir attractive force between two electrodes, by an opposite and greater Coulomb force of at least a factor of two.

This proportionality factor,  $\text{Coulomb} / \text{Casimir Forces} > 2$ , is determined by the threshold voltage of enriched or depleted MOS transistors and defined during the manufacture of the device.

The attractive Casimir force appearing between the two electrodes of a reflector deforms a piezoelectric bridge, which automatically induces the electric charges used by a Coulomb force on the return electrode.

As long as the electric voltage, generated by the electric charges on one side of the piezoelectric bridge and connected to the gate of an enriched MOS transistor (MOSE) is below its threshold voltage, this transistor remains blocked. The electrical charges on the other side of the bridge are on the source of this transistor and remain confined to the moving electrode of the Casimir reflector. During this phase, the Coulomb return electrode is then grounded by closing the circuit consisting of series depleted MOS (MOSD). Likewise, the fixed electrode of the Casimir reflector is continuously grounded. The Coulomb force between the two electrodes of the Casimir reflector and between the piezoelectric bridge and the Coulomb return electrode is then zero.

Depending on the deformation of the piezoelectric bridge, the electric charges present on the two electrodes of the piezoelectric bridge increase. They therefore increase on the gates of the enriched or depleted MOS and generate an electrical voltage greater than the threshold voltages of the MOSE and MOSD transistors. Thus, the circuit formed by MOSE in parallel closes and that formed by MOSD in series opens, then isolating the fixed return electrode from ground, which allows the charges present on the source to be distributed uniformly over this electrode. recall and be trapped there.

Electric charges of opposite sign are then distributed over the two electrodes, one on one side of the piezoelectric bridge, the other on the return electrode! So, an attractive Coulomb force who can be greater than and in the opposite direction to that of Casimir then develops between these return electrodes. This attractive Coulomb force moves the two electrodes away of the Casimir reflector, reducing then canceling the deformation of the bridge. It automatically disappears when the deformation of the piezoelectric bridge is canceled out, letting the Casimir force again dominate and deform this bridge again for a new cycle!

The device is found in the initial conditions which causes the structure to vibrate.

When homogenizing the electrical charges on both sides of the return electrode, periodic current peaks appear for a fraction of the device's vibration time. These peaks of currents passing through an inductor spontaneously induce peaks of alternating voltages at the terminals of this device.

Electronics without any power supply then transforms these weak alternating signals into a direct voltage of several volts.

To manufacture these different structures, we are proposing an original technology making it possible to produce these electronics without power supply, as well as that of the control of the very weak interfaces between the electrodes of the Casimir reflector and that of the return electrodes of the vibrating structure!

The Casimir and Coulomb forces, the current or voltage peaks appear spontaneously and without input of any external energy, likewise the transformation electronics have no power supply.

The structure automatically enters vibration thus inducing current and voltage peaks converted into a usable direct voltage.

Everything is only a consequence of the existence of the isotropic, homogeneous, and omnipresent Casimir force due to the quantum fluctuations of the vacuum.

This set does not seem to contradict Emily Noether's theorem!

*"In the universe, everything is energy, everything is vibration, from the infinitely small to the infinitely large" Albert Einstein.  
"A person who has never made mistakes has never tried to innovate." Albert Einstein*

# I / OBTAINING AN ELECTRIC CURRENT FROM VACUUM?

## I.1: Introduction

We know that the quantum vacuum, the energy vacuum, the absolutely nothing, does not exist!

This statement has been proven multiple times and noted in particular by:

- Lamb's shift (1947) of atomic emission frequencies.
- By the force of Van der Waals which plays a very important physicochemical role and had an interpretation quantum 1930 [London] when two atoms are coupled to the same fluctuations in vacuum.
- By the experimental verification (1958) of the existence of a force equated by Casimir in 1948. This so-called Casimir force was measured for the first time in 1997
- By Hawking's radiation theory, predicted in 1974 and observed on September 7, 2016.

### Hawking's radiation:

The vacuum of physicists is like a kind of ocean full of energy that constantly fluctuates around a mean value called zero and considered as the benchmark. This vacuum is often pictured and metaphorically compared to a sea of particles and antiparticles, which go in pairs, annihilate, and then endlessly reconstitute. The entire universe would have emerged from it during the BIG-BANG over 13.75 billion years ago! Hawking radiation is radiation that a black hole must emit, due to the laws of quantum mechanics on vacuum, and which causes it to evaporate through loss of mass and angular momentum if the black hole is rotating (black hole of Kerr) and electrically charged. If it is electrically charged (Kerr-Newman).

### Quantum Casimir force:

It is a force appearing between two parallel conductive plates, not electrically charged and very close to each other. It is most often attractive but can also be repulsive depending on the characteristics of the reflectors constituting these two plates.

1 / The quantum fluctuations of the vacuum are present in any quantum field theory. The quantum Casimir effect is due to fluctuations in the electromagnetic field, described by the theory of quantum electrodynamics and theorized by Hendrik Casimir in 1948.

2 / The thermal Casimir effect in vacuum was predicted by Yevgeny LIFCHITS in 1956 when he realized that classical thermal fluctuations should lead to an analogue of the Casimir effect theoretically predicted in the quantum domain. Various physicists in particular considered the forces exerted between solids or liquids separated by a fluid and these theorists predicted in 1961 that if the properties (more precisely, the refractive indices) of materials are well chosen, the Casimir force could then be repulsive. This repulsive force was measured in 2009 by F. Capasso and his colleagues who demonstrated a repulsive Casimir force of the order of 120 piconewtons when a gold plate and a gold microbead are separated by twenty. of nanometers.

## I.2 / Brief presentation of Casimir's force

The vacuum energy is the zero-point energy of all fields (tensorial and scalar) in space, which for the standard model includes the electromagnetic field, gauge fields, fermionic fields, as well as the Higgs field which is responsible for the mass of particles and with which photons do not interact. In quantum field theory, this vacuum energy defined as zero, is the ground state of fields! In cosmology, vacuum energy is a possible explanation for Einstein's cosmological constant.

It has been observed and shown theoretically that this so-called zero-point energy, is non-zero for a simple quantum harmonic oscillator, since its minimum energy is equal to  $E = \frac{h\nu}{2}$  with  $\nu$  the natural frequency of the oscillator, and  $h$  the Planck's constant.

Originally [1], the Casimir effect is derived from statistical fluctuations in total vacuum energy and is revealed by the presence of two perfect and plane reflectors. The Casimir effect is the attraction (in general) between two plates separated by a vacuum. In this approach, this Casimir energy is the  $E_{CA}$  part of the vacuum energy which is a function of the  $z_s$  separation of the Casimir plates with:  $E_{ca} = S \left( \frac{\pi^2 \hbar c}{720 z_s^3} \right)$

This Casimir energy is proportional to the reduced Planck constant  $\hbar$ , to the speed of light  $c$  and to the surface  $S$  of the reflectors (in the limit where the edge effects of the plates are negligible, which then imposes large dimensions of the reflectors compared to that of the separation of the plates).

The force of Casimir  $F_{CA}$  between the two reflectors is then the derivative compared to  $z_s$  of this energy thus:

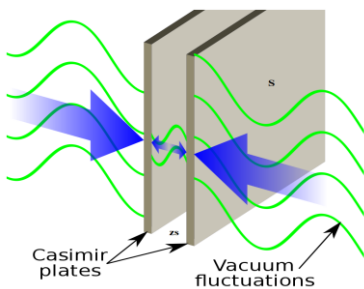
$$F_{CA} = \frac{dE_{ca}}{dz} = S \left( \frac{\pi^2 \hbar c}{240 z_s^4} \right) \quad (1)$$

This Casimir force, proportional to the surface, defines a pressure  $F_{CA} / S$  which depends only on the distance  $z_s^4$  between the reflecting plates. This local approach greatly facilitates the formulations of Casimir's forces [1,2].

The force of Casimir is then attractive and can be understood like a local pressure namely, the so-called virtual radiation pressure and exerted by vacuum fluctuations on the mirrors. These homogeneous, isotropic, and constant fluctuations of the vacuum, manifested by radiation and virtual particles, are modified by the presence of reflecting mirrors. These particles, however real, are called virtual because their lifetimes are noticeably short (for an electron of the order of  $6 \cdot 10^{-22}$  seconds) before recombining to return to a vacuum!

The presence of the reflective plates excludes wavelengths longer than the distance  $z_s$  between the plates. They thus induce a pressure difference of the virtual particles generated by the vacuum between the internal and external space of the 2 plates. This difference results in a force that pushes the plates together.

In other words, the quantum state of a volume of space is different when this volume contains a physical object. This presence causes the existence of the Casimir force which is generally attractive but - as we have mentioned- can also be repulsive, depending on the geometry and the properties of the material!



The Casimir force between two perfectly conductive and smooth plates, without conductive charge, at zero temperature is written as the difference of the radiation pressures calculated outside and inside the cavity and is then written:

$$F_{ca} = S \left( \frac{\pi^2 \hbar c}{240 z_s^4} \right) \quad (1)$$

**Figure 1 Casimir effect**

The surface  $S$  of the mirrors is assumed to be much larger than the square of the distance between plates separated by  $z_s$  in order to be able to neglect any diffraction effect on the edges of the mirrors. In this ideal case, the force depends only on geometric parameters, the speed of light and the reduced Planck constant  $\hbar = h / (2 \pi)$

The famous physicist Evgueni Mikhaïlovitch Lifchits gave a general formula, which supplements that of Casimir because it considers the temperature - [3]. Indeed, when the temperature is no longer zero, the radiation of the black body must then be considered and the Casimir force at temperature  $T$  then becomes that of Lifchits.

This modification is important for large distances, typically  $L \geq 3 \mu\text{m}$  at ambient temperature, we then have:

$$F_{ca} = S \left( \frac{\pi^2 \hbar c}{240 z_s^4} + \frac{\pi^2}{45} \frac{(kT)^4}{(\hbar c)^3} - \frac{kT \pi}{z_s^3} e\left(-\frac{\hbar c}{kT z_s}\right) \right) \quad (2)$$

With  $k$  the Boltzmann constant and  $T$  the temperature.

We will use this equation (1) to calculate and simulate the structure defined in the following diagram (figure 2) because the intervals between electrodes are much smaller than  $3 \mu\text{m}$  and the effect of temperature is negligible.

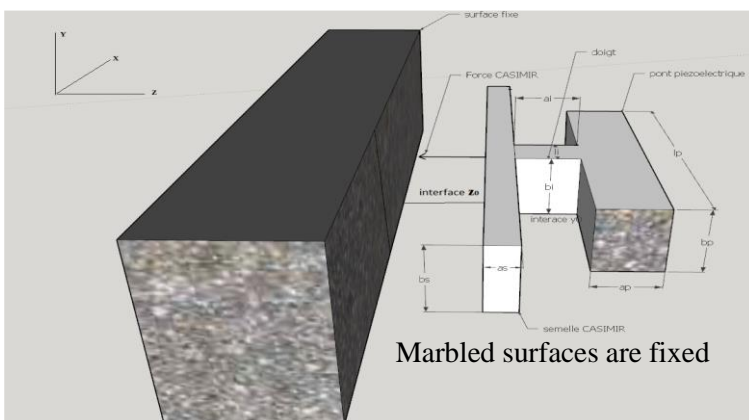


**(Figure 2): General representation of the structure**

### I.3 / EXTRACT ENERGY FROM THE VACUUM?

The term *vacuum energy* is sometimes used by some scientists claiming that it is possible to extract energy - that is, mechanical work, heat...., from the vacuum and dispose thus, ideally, a gigantic and virtually inexhaustible source of energy.

Of course, these different hypotheses arouse great skepticism among many scientific researchers because they call into question a principle demonstrated mathematically by the theorem of the mathematician Emmy Noether in 1915, which involves the conservation of energy (like all invariances).

This theorem is accepted in physics and has never been faulted until now!

In fact, the problem is less to extract energy from the vacuum than to extract it without spending more energy that we cannot hope to recover! For example, in the case of Hawking black holes radiation, it is a mass that is converted ultimately in energy. So, we did not get energy "for free" which is consistent with Noether's theorem.

This principle of Noether's theorem, still observed at the macroscopic scale, suggests that extracting energy from a vacuum would require at least as much energy, even probably more, than the process of its recovery would provide.

Thus, a cyclic system, on the model of a piston engine going from a position  $n^{\circ} 1$  to  $n^{\circ} 2$ , then from  $n^{\circ} 2$  to  $n^{\circ} 1$ , would imply to bring back the reflecting plates of Casimir to their previous positions then to dismiss them again. To do this, the existence of the Casimir force in  $1/zs^4$  therefore greater in position (2) than in (1) would then imply spending more energy to return to (1), which would necessarily require the added energy!!

This problem, like that of perpetual motion, then implies that this hope of extracting energy from a vacuum seems impossible and cannot be done with at least zero energy balance!

These arguments are realistic and suggest that one cannot extract energy from a vacuum.... a priori?

But this is forgetting that an energy is not limited to a force but is, for example, the product of a force (intensity variable) by a displacement (position variable).

Indeed, imagine that the piston is a piezoelectric bridge and that the deformation of this bridge is caused by the Casimir force attracting, for example, the face  $n^{\circ} 1$  of this bridge. The deformation of this piezoelectric bridge induces fixed electric charges of opposite sign on each of its faces 1 and 2 (figure 5).

Consequently, if it were possible to cause mobile electric charges, of the sign of face 1, to appear at the opportune moment, on a surface close and electrically isolated from face 2, then an attractive Coulomb force opposite to the force de Casimir would practice.

If this Coulomb force is greater than the Casimir force, for example by a factor of at least 2, then the total force  $F_t = F_{CA} - F_{CO}$ , applied to the center of this piezoelectric bridge deforms it in the other direction, decreases then cancels out the electric charges on the two faces of the piezoelectric bridge, thus eliminating the coulomb force (see Figures 3 and 4).

The system would then return to its original position and physical characteristics. Everything would start again, causing vibrations of the piezoelectric bridge of the Casimir reflector device without any external energy input!

Thus, if it was possible to produce, at the right time, the same signs, and mobile electric charges on the 2 surfaces of the Casimir reflector, a repulsive Coulomb force would be generated ! (See figure 5). Therefore:

**If** the appearance of a Coulomb force in the opposite direction and greater by a factor  $> = 2$  than the Casimir force is:  
1 /: possible:

2 /: induced spontaneously (therefore without any contribution of an external energy ) by the initial translation from (1) to (2)

3 /: temporary (because it cancels out as soon as the piston returns to position  $n^{\circ} 1$ ).

Then, on the assumption that all the transient states of the system do not require any input of external energy and are only consequences of a primary cause which is the energy of the vacuum, the principle of Emmy Noether should not be contradicts!

In other words, it is necessary that the force of attraction of Casimir initiates the movement of (1) towards  
EXTRACTION OF A VACUUM ENERGY CONFORMING TO EMMY NOETHER'S THEOREM: 29/09/2021 Dr SANGOUARD Patrick



(2), creates by itself and without the contribution of any external energy a higher opposing force of a factor 2 and which can be at an opportune moment to bring the piston back from (2) to (1) then vanishes!

In this case, no external energy being necessary, the overall conservation of energy would not be violated, because the extraction of energy from the vacuum would have an energy balance at least zero.

Indeed, by moving the plates, one modifies the possible wavelengths (because in resonance with the gap between the plates) of the virtual radiations of the radiation leaving the vacuum and at the origin of the Casimir force, thus varying the energy of the void itself!

The fixed electric charges on the two metallized faces of the piezoelectric bridge are of opposite signs and attracts from the mass of the mobile charges of opposite signs (figure 5).

Let us imagine that the whole of the return electrode is in two parts of equal areas but separated by a switch circuit consisting of MOSN and MOSP enriched, in parallel and of threshold voltage  $V_{tNE} = -V_{tPE}$ . (Figure 5) The first part of this metallic return electrode and surface  $S_{p1}$  consists of one of the faces of the piezoelectric bridge and carries mobile electric charges  $Q_m = -Q_F$ .

The second part of this metal electrode is earthed via another switch circuit made up of depleted MOSN and MOSP, in series and of the same threshold voltage as the enriched MOSN and MOSP:  $V_{tND} = V_{tPE} > 0$  and  $V_{tPD} = V_{tNE} < 0$  (See figure 5).

These switch circuits (circuit 1 = MOSN and MOSP enriched in parallel, circuit 2 = MOSND and MOSPD in depletion and in series), are designed so that they open and close in opposition.

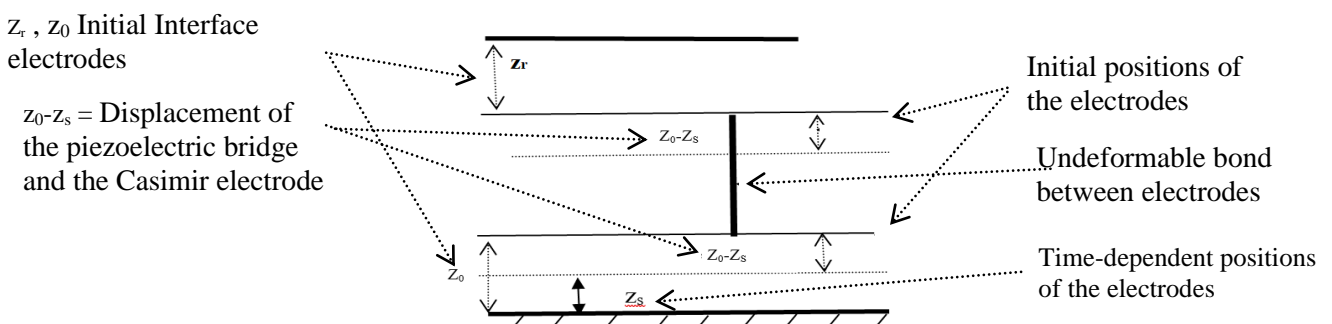
When circuit 1 then opens or closes, at the same time switch circuit 2 closes or opens, thus isolating this return electrode from the ground (see figure 5). This opposite behavior of the switch circuits can be seen in Figure 6. So, when circuit 1 is open, the two parts of the return electrodes are grounded through circuits 2, on the other hand when circuit 1 closes the two parts of the return electrodes are isolated! (Figure 5)

The electric field inside a perfect conductor being zero, the mobile charges attracted to the first part of the return electrode are redistributed on the two parts of this electrode in the ratio of the homogenization surfaces, that is to say  $1/2$  and are opposite the other face  $n^\circ 2$  of the bridge which has an opposite electric charge!

One then develops, between these isolated electrodes an attractive Coulomb force which is in the opposite direction to the Casimir force and can be greater than it! (See figure 3 + 4 + 5)

Now, we know that in the case of a deformation perpendicular to the polarization of a piezoelectric layer and caused by an  $F_{CA}$  force, the fixed charges  $Q_F$  induced by the deformation of this piezoelectric layer are proportional to the Casimir force  $F_{CA}$  and are therefore in  $1/z_s^4$ , with  $Q_F = \frac{d_{31} F_{CA} l_p}{a_p}$  (3), [5] and [6]. With  $d_{31}$  = piezoelectric coefficient ( $CN^{-1}$ ),  $l_p$ ,  $a_p$  respectively length and thickness (m) of the piezoelectric bridge (figure 5). These fixed electric charges on the two metallized faces of the piezoelectric bridge have opposite signs and attract mobile charges of opposite signs from the mass (figure 5).

Thus, when it is effective, the Coulomb return force  $F_{CO}$  is in  $1/z_s^{10}$  because on the one hand in  $(Q_F/2)^2$  (therefore in  $1/z_s^8$ ) but also in  $1/(z_r + z_0 - z_s)^2$  because depending of the distances  $z_r + z_0 - z_s$  between return electrode  $n^\circ 1$  and face  $n^\circ 2$  of the piezoelectric bridge. With  $z_r$  the initial distance between the opposite face of the piezoelectric bridge and the return electrode,  $z_s$  = distance between Casimir electrodes, time dependent, and  $z_0$  = initial distance between Casimir electrodes (see figure 3 + 4 + 5) and figure below. We will choose in the following MATLAB simulations (unless otherwise specified), the same interface between return electrode  $z_r$  as that attributed to the initial interface  $z_0$  between Casimir reflectors



The distances over which the free Casimir electrode moves, correlated with the deformation of the piezoelectric bridge are very small and less than  $100 \text{ \AA}$ . The variations  $z_0$ ,  $z_e$ ,  $z_s$  are therefore  $< 100 \text{ \AA}$  and are very small compared to the dimensions of the piezoelectric bridge and that of the Casimir electrodes. Although the rigorous calculation is possible, for the sake of simplification we will first consider that the Coulomb return electrodes remain strictly parallel (Figure 3,4,5).

Taking into account that the Coulomb force is zero when the piezoelectric bridge has no deformation, we thus obtain an attractive Coulomb force of direction opposite to that of Casimir with

$$F_{CO} = \frac{Q_F^2}{4\pi\epsilon_0\epsilon_r} \left( \frac{1}{(z_r + z_0 - z_s)^2} - \frac{1}{(z_r)^2} \right) = \left( \frac{d_{31} l_p F_{CA}}{2 a_p} \right)^2 \frac{1}{4\pi\epsilon_0\epsilon_r} \left( \frac{1}{(z_r + z_0 - z_s)^2} - \frac{1}{(z_r)^2} \right) = \left| S_s * \frac{\pi^2 h c}{240} * \frac{d_{31} l_p}{a_p} \right|^2 * \frac{1}{16\pi\epsilon_0\epsilon_r} * \frac{1}{z_s} \left( \frac{1}{(z_r + z_0 - z_s)^2} - \frac{1}{(z_r)^2} \right)$$

This Coulomb Force in  $1/z_s^{10}$  can therefore become greater than that of Casimir which is in  $1/z_s^4$ !

Applied to the piezoelectric bridge, it reduces its deformation, and therefore the induced charges.

So, Coulomb's force diminishes and then vanishes when the bridge goes to the starting position  $n^{\circ}1$  since  $z_s = z_0$ !

For these Coulomb return electrodes generate only a Casimir force that is negligible compared to that of the reflector, it will be necessary to choose interfaces  $z_r$  greater than  $2z_0$ . For example, if  $z_r = 2z_0$  and the surface of Casimir reflector  $S_{s2} = 5 * S_p$  then the Casimir force between the return electrodes will be about 100 times weaker than that linked to the reflector, which is negligible (figure 5)!

On the other hand, as  $F_{CO}$  depends on the charge accumulated on the piezoelectric bridge in  $(1/z_s)^3$ , the electric voltage that the MOS switches will have to withstand before being triggered increases with the interface  $z_r$ , since the position where  $F_{CO} = F_{CA}$  decreases with  $z_r$  (see figure 32b). This leads to an increase in the threshold voltages of the different MOS with the increase interface  $z_r$ !

This electrostatic attraction of the piezoelectric bridge is possible because the fixed electric charges generated by the deformation of the piezoelectric bridge attract mobile electric charges  $Q_m$  of opposite signs from the mass.

Note that if switch circuit  $n^{\circ}1$  is open, we have seen that circuit  $n^{\circ}2$  is closed and connected to ground, so the second part of the return electrode is to ground. Conversely, when circuit  $n^{\circ}1$  is closed then circuit  $n^{\circ}2$  is open, isolating the second part of the return electrode.

On the other hand, the mobile loads of face 2 by triggering, at the appropriate moment and depending on the threshold voltages, the automatic closing of circuit 1 and the opening of circuit 2, the charges of face 1 are distributed uniformly over the surfaces of the face  $n^{\circ}1$  of the piezoelectric bridge and the return electrode.

They create an attractive force  $F_{CO}$  of Coulomb opposed to that of Casimir which can be superior to him in modulus. The total  $F_{CA} - F_{CO}$  force then becomes repulsive and, applied to the piezoelectric bridge decreases and cancels out its deformation, which consequently automatically removes the electric charges on it and initiates the reopening of circuit 1 and the closing of circuit 2.

Thus, the repulsive force of Coulomb disappears, and the force of Casimir becomes preponderant again which allows this cycle to start again!

It seems the spatial and temporal omnipresence of the attractive Casimir force, with the spontaneous appearance and at the appropriate moment of the Coulomb force described above, then generate vibrations of the mobile Casimir reflector plate!

We will calculate the frequency of these vibrations with MATLAB.

Note that during the movement of the piezoelectric bridge from (1) to (2), only the force of Casimir  $F_{CA}$  is exerted, because the circuit 2 is conducting and connects the return electrode to the mass suppressing the action of the force Coulomb. Note also that the fixed electrode of the Casimir reflector is constantly earthed (see figure 5).

During the short homogenization time of the mobile charges on the fixed return electrode, an alternating current peak  $I_a$  is recovered which generates an alternating voltage peak  $U_a$  through its crossing of an inductor (therefore without any additional energy).

This weak and ephemeral but always present electric power  $U_a \cdot I_a$  is at the frequency of vibration of the structure. It then activates suitable electronics that must transform - without any external power source - this alternating voltage  $U_a$  into a direct voltage  $U_c$  which can be used (see chapter 5).

This electronics was designed when I was working at ESIEE and on abandoned sensors. This electronics was necessary for this problem sensors which, as their name suggests, are abandoned, therefore without internal energy. It works very well in SPICE simulation (see part V).

If all the components of this project are successful (principle of extracting energy from the vacuum + device generating current peaks at the vibration frequency of the system and converted in peak of voltage by a coil + transformation electronics + technology for realization the device selected) , all without any additional energy, the principle of Noether should be validated and the vacuum could then be considered as a simple medium, with which it is possible to exchange energy!

*This is the aim of this pre-work and this report.*

**II / DESCRIPTION OF THE PRINCIPLE USED TO "EXTRACT" ENERGY FROM THE VACUUM**

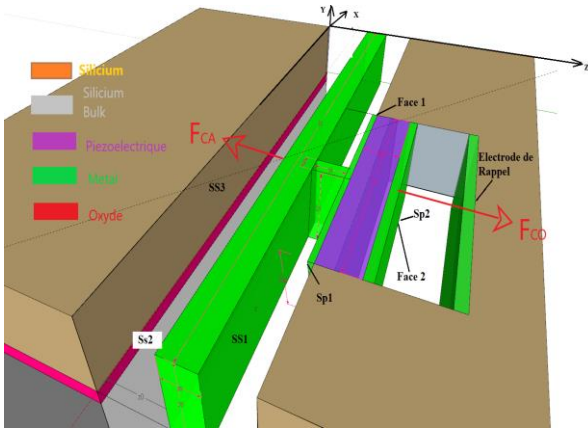


Figure 3; View of the device without electronics

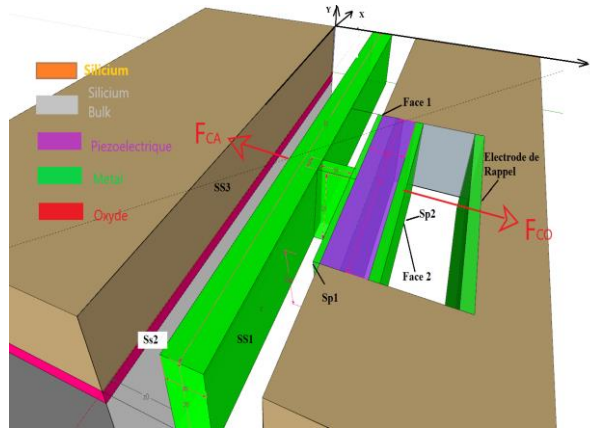
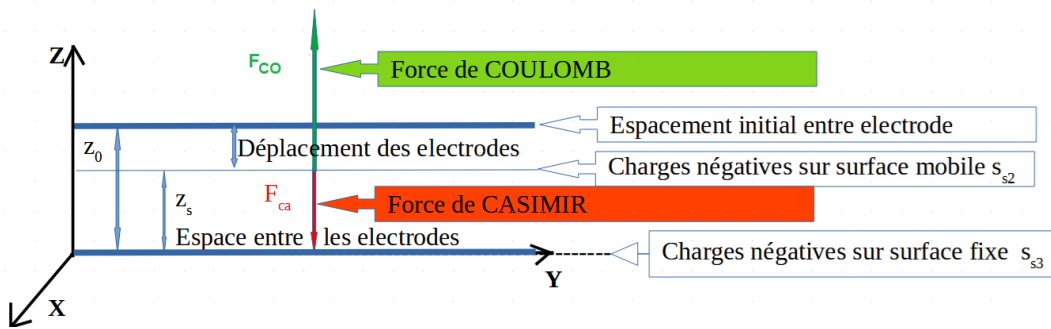


Figure 4: Different view of the device without electronics

figure 4b Axes , forces, électrodes casimir



As a preamble, we hope and suppose that the events which induce the attractive force of Casimir are exerted in a universal, isotropic, perpetual, and immediate way, if the conditions of separation between reflecting Casimir plates are suitable.

Let therefore be a Casimir reflector device consisting of:

- 1 / a metallized and mobile parallelepipedal electrode, of surface  $S_{s1} = S_{s2}$  on its 2 lateral faces
- 2 / of a fixed metallized surface  $S_{s3}$  separated by a distance  $z_0$  (figure 3, 4 and 5)

In order for the movement of the movable plate of this Casimir reflector to create electric charges that can be used to induce an attractive Coulomb force, it is necessary that the movement of this movable plate naturally induces a deformation of a structure creating electric charges.

A piezoelectric device is therefore required, rigidly connected to the mobile Casimir electrode, so that its induced naturally deformation leads to the appearance of electric charges! And this without any other energy being involved (Figure 3,4, 5).

Of course, it is also necessary that the movement of this Casimir reflector mobile plate  $S_{s2}$  can be stopped at a chosen and predefined value before the bonding of the surface  $S_{s2}$  on the fixed surface  $S_{s3}$  takes place! Otherwise, we just definitively collapse the two reflector plates, and no energy extraction is possible! In addition, it is necessary that the mobile system returns to its initial position (or slightly exceeds it)

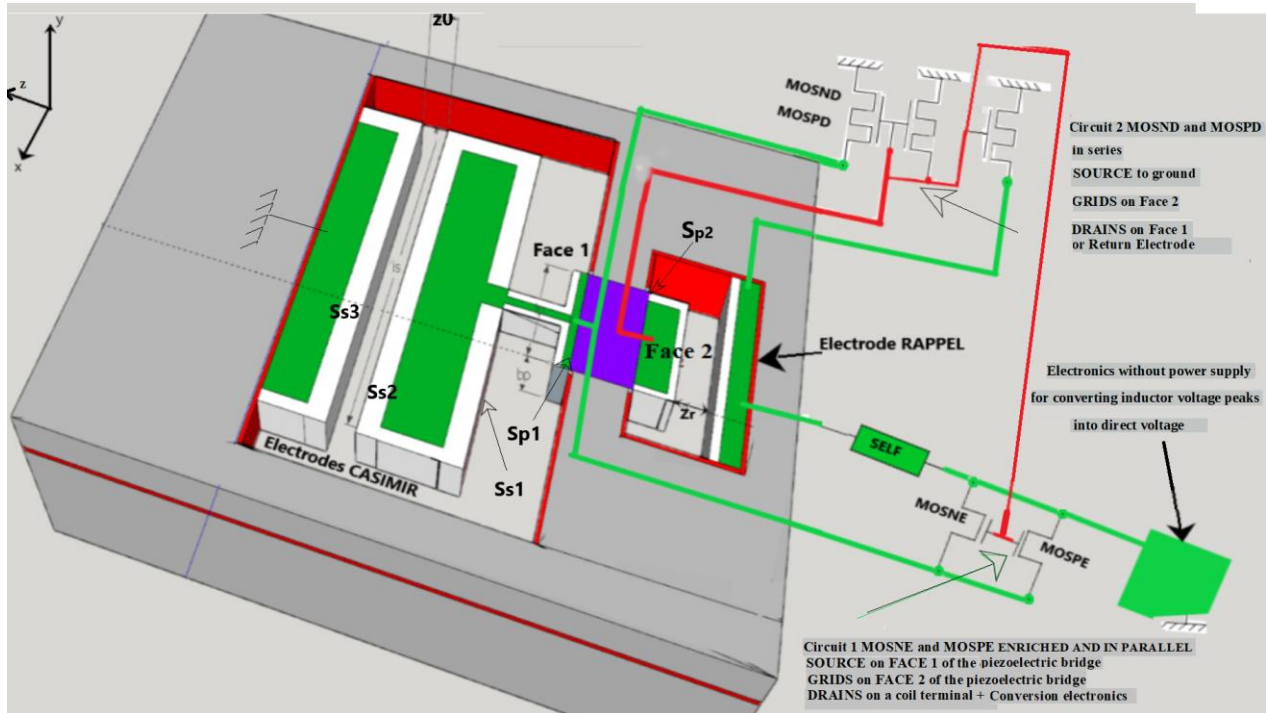
As said previously, we can then imagine that the attractive Casimir force exerted between the facing surfaces  $S_{s2}$  and  $S_{s3}$  and which moves the mobile reflector plate  $S_{s2}$ , induces a deformation of a parallelepiped piezoelectric bridge of surface  $Sp1$  and  $Sp2$ , rigidly linked, by a metal finger, to this reflecting mirror (figures 3,4,5)

We observe, in figure (5), that the surfaces  $Sp1 = Sp2 = b_p * l_p$ , green or red metallic of the insulating piezoelectric bridge, are connected for:

- 1 / for  $Sp1$  on the face n° 1, through the metal finger (green) to the mobile plate of the Casimir surface reflector  $S_{s2} = b_s * l_s = S_{s1}$  which forms one of the electrodes of the Casimir reflector. Thus, the metallic surfaces  $Sp1$  and the metallic parallelepiped  $S_{s1} = S_{s2}$  are equipotential
- 2 / for  $Sp2$  on the face n ° 2, at the grids of the switch circuits n°1 and n°2 .

The deformations caused by the attractive force of Casimir, then produce fixed electric charges for example  $Q_{fn1} = -Q_{fp2}$ , on the faces  $S_{p1}$  and  $S_{p2}$  of the insulating piezoelectric bridge. These fixed charges in turn attract, from the immediate environment (mass or earth) to which they are connected by circuits 2, mobile electric charges  $Q_{mp1}$  and  $Q_{mn2}$ , respectively. These charges are distributed over the metallized surfaces deposited on the insulating piezoelectric bridge, therefore on  $S_{p2}$  and the gates of the transistors of circuits 1 and 2 as well as on  $S_{p1}$ , the metal block, the sources of the transistors of circuit 1 and the two coupling capacitors of the electronic transformation circuit. (See figures 5 +45)

**Figures 5: general configuration of the device: MOS grid connections (Face 2 of the piezoelectric bridge: red), Source connections (Face 1 of the piezoelectric bridge: green)**



Let  $S_{MOS}$  be the surface of the gates of the MOS of switch circuits 1 and 2. The mobile charges, for example positive  $Q_{mp2}$ , located on the surface  $S_{p2}$  of face 2 going to the gate of a MOSNE enriched transistor in the ratio  $Q_{mp2MOS} = Q_{mp2} * S_{MOS} / S_{p2}$ , then produce a positive voltage  $V_G = Q_{mp2MOS} / C_{OX}$  on the gate of the MOS transistors, with  $C_{ox}$  the gate capacitance of the MOS transistors.

Depending on the sign of these mobile charges on the gates of the MOSNE or MOSPE transistors, they can turn one of them ON, if they are sufficient to induce a voltage  $V_G$  greater than their threshold voltage  $V_{TE}$ , positive for the MOSNE transistor and negative on the MOSPE transistor in parallel.

The nature of these charges depends on the initial polarization of the deposited piezoelectric parallelepiped and on the direction of the deformation imposed by the Casimir force. The sign of these mobile charges on the surfaces  $S_{p1}$  and  $S_{p2}$  depending on the real polarization obtained during the realization of the piezoelectric material of this bridge, it is the reverse which occurs if the mobile charges are negative on  $S_{p2}$ , hence the parallel setting of switches! (See figure 5)

As long as this voltage on face 2 of the bridge, for example positive, is less than the threshold voltage  $V_{TNE}$  of this MOSNE transistor, the latter remains blocked!. Consequently, the mobile charges  $Q_{mn1} = -Q_{mp2}$  located on the other face  $S_{p1}$  of the deformed piezoelectric device (connected by a metal block to  $S_{s2}$ ) and connected to the sources of the MOSNE and MOSPE remain on these surfaces and do not propagate on the surface of the return electrode. The MOS switches N and P depleted in series from the switch circuit 2 are then on and connect this return electrode to ground (FIG. 5).

On the other hand, if this voltage  $V_G$  becomes greater than the threshold voltage  $V_{TNE}$  of the enriched MOSNE, it becomes conducting, and circuit 2 is then blocked, so the mobile charges  $Q_{mn1}$ , located on  $S_{p1}$  and the metal block can cross the MOSNE to homogenize the charge density on all the return electrodes. These electric charges pass through the self- $L_{IN}$  in series, (figure 5).

When one of the two MOSNE or MOSPE enriched transistors of circuit 1 turns on, then the depleted MOS N and P switches of circuit 2 are blocked. The return electrode, no longer connected to ground, therefore does not discharge these mobile electrical charges and is isolated (Figure 5).

Let  $S_{p1} = S_{p2} = l_p * b_p$  be the surface area of the faces of the piezoelectric bridge,  $S_{bloc}$  = the surface of the metal block of the Casimir reflector (figure 5). Let  $S_r = S_{p2} = S_{p1}$  be the surface of the return electrode facing the metallized face  $S_{p2}$  of the piezoelectric bridge.

The mobile charges for example negative  $Q_{mn1} = -Q_{mp2}$  which was initially distributed on the metallic surfaces  $S_{p1}$  are distributed, after the closing of the MOSNE switch, on the surfaces  $S_{p1} + S_r$ . They induce between the faces  $S_{p2}$  and  $S_r$ , electric charges of opposite sign, an attractive force of Coulomb, parallel and opposite to the attractive force of Casimir,

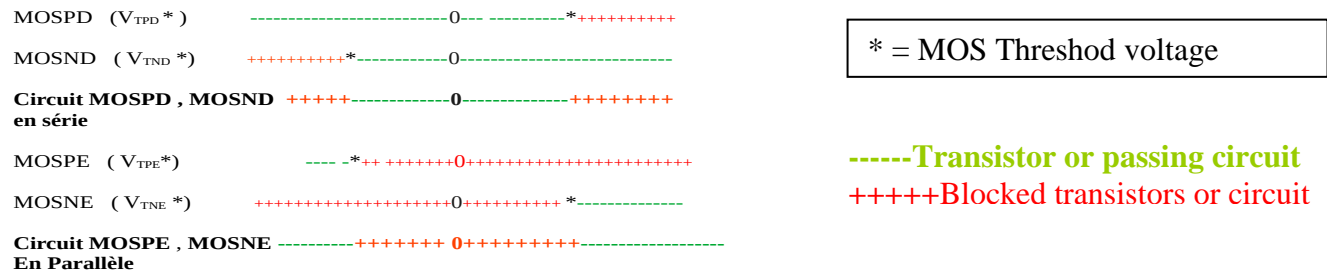
These same electrical charges opposite on the surfaces  $S_{p2}$  and  $S_r$  become after distribution

$$Q_{mn1f} = Q_{mn1} * \frac{S_{p1}}{S_{p1} + S_r} \approx \frac{Q_{mn1}}{2} \quad \text{as } S_{p1} = S_r$$

This charge  $Q_{mn1f}$  remains on the return electrode because circuit 2 is blocked (see figures 5 and 6)

If the threshold voltages of the transistors are positioned according to  $V_{TND} \cong V_{TPE} < 0 < V_{TNE} \cong V_{TPD}$ , then we have the following configurations depending on the value of the voltage  $V_G$

**Figure 6: distribution of the threshold voltages of enriched and depleted N and P MOS switches.**



As a result, when circuit 1 is blocked, there is no Coulomb electrostatic attraction between  $S_{p2}$  and  $S_r$  because the metal return electrode  $S_r$  is grounded and therefore free of charges! However, when circuit 1 is on, circuit 2 is then blocked, so as the metallic return electrode  $S_r$  is isolated, the charges of opposite sign and present on the electrodes  $S_{p2}$  and  $S_r$  induce an attractive Coulomb electrostatic force!

This attractive Coulomb force as a first approximation is written (4):

$$F_{co} = \frac{Q_f^2}{4\pi\epsilon_0\epsilon_r} \left( \frac{1}{(z_r+z^0-z_s)^2} - \frac{1}{(z_r)^2} \right) = \left( \frac{d_{31}l_p F_{CA}}{2a_p} \right)^2 \frac{1}{4\pi\epsilon_0\epsilon_r} \left( \frac{1}{(z_r+z^0-z_s)^2} - \frac{1}{(z_r)^2} \right) = \left| S_s * \frac{\pi^2 \hbar c}{240} * \frac{d_{31}l_p}{a_p} \right|^2 * \frac{1}{16\pi\epsilon_0\epsilon_r} * \frac{1}{z_s} \left( \frac{1}{(z_r+z^0-z_s)^2} - \frac{1}{(z_r)^2} \right) \quad (4)$$

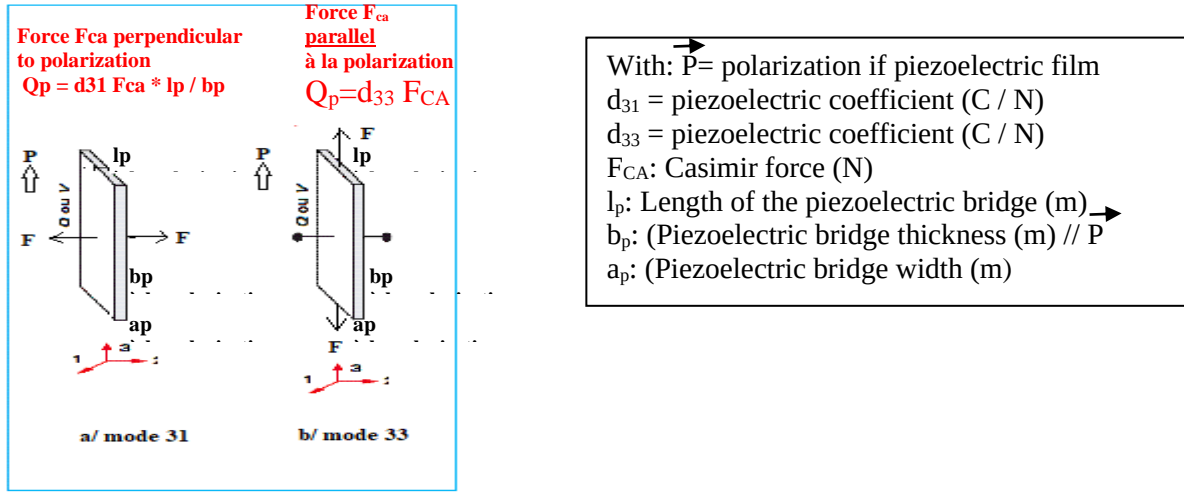
This attractive force triggered by an input of mobile electric charges of opposite sign on the surfaces  $S_{p2}$  and  $S_r$  is exerted only when the Casimir force between the two reflectors reaches a defined value, dependent on the threshold voltage of the MOSNE transistor. It will therefore be necessary to adjust the threshold voltage of all these MOSs adequately.

Initially, when the piezoelectric beam is not deformed, the electric charges on the faces  $S_{p1}$ ,  $S_{p2}$ ,  $S_{s2}$  and  $S_{s3}$  of the Casimir reflector are zero! The face  $S_{s2}$  of the Casimir sole plate, distant from  $z_0$  from the face  $S_{s3}$  is then attracted against the fixed face  $S_{s3}$ , only by the force of Casimir. This force is communicated via the connecting finger at the center of the face  $S_{p1}$  of the piezoelectric bridge and then deforms it. (See figures 3, 4, 5)

In the case of a deformation perpendicular to the polarization of the piezoelectric bridge subjected to the  $F_{CA}$  force (mode 31), this piezoelectric bridge deforming horizontally, generates fixed charges  $Q_{fp} = -Q_{mn1}$  and  $Q_{fn} = -Q_{mn2}$  on its

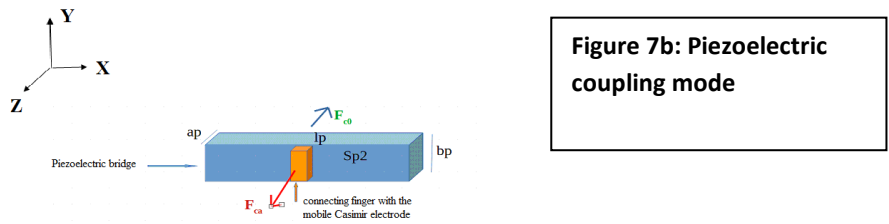


two faces according to the formula  $Q_F = \frac{d_{31} F_{CA} l_p}{a_p}$  (3) [5]: where  $d_{31}$  (C/ N) is one of the coefficients of the piezoelectric material of the piezoelectric bridge,  $l_p$  and  $a_p$  respectively the length and thickness of this bridge (see figure 7 and [5]) In the case of a deformation parallel to the polarization (mode 33), this load becomes:  $Q_{fp} = - Q_{mn} = d_{33} * F_{CA}$  where  $d_{33}$  (C/N) is another coefficient of the piezoelectric material of the bridge (see reference no. 4.5])



Modes de couplage piézoélectrique **Figure 7: Polarization, applied force and load on a piezoelectric block.**

We will admit in the remainder of this presentation that we are in the case of mode 31 and that when the piezoelectric bridge undergoes a deformation then the fixed electric charges of the piezoelectric bridge attract negative mobile charges on the electrode Sp1 from the mass and positive mobiles on the other Sp2 electrode. If, the threshold voltage of the MOSNE is adjusted so that the Coulomb force is triggered only when  $F_{CO} = p F_{CA}$  with  $p$  proportionality factor  $\geq 2$ , then the total repulsion force Ft variable in time and applied to the piezoelectric bridge becomes (figure 7, 8)



$$\vec{F}_T = + \vec{F}_{CA} - \vec{F}_{CO} = (1-p)\vec{F}_{CA} \Rightarrow \vec{F}_T < 0$$

Becoming repulsive, this force Ft (dependent on time) induces a deformation of the piezoelectric bridge in the other opposite direction, and the piezoelectric bridge returns or slightly exceeds (because of inertia) its neutral position, without initial deformation, therefore towards its position without any electrical charge.

The variation in time of these mobile charges follows, as a first approximation, a law of distribution of the charges on a short-circuited capacitor. Indeed, the fixed electrode Sr initially at zero potential since at ground, is now isolated by switch circuit 2 which is open and isolates it from ground! This temporal variation of the charges is given by the well-known exponential form of discharge of a capacitor according to the formula:

This variation in mobile charges stops when these electrical charges  $Q_{mn}$   $Q_{mn} = Q_{mn2} * \text{Exp}(-\frac{t}{R_m * C_s})$  are uniformly distributed over the two electrodes Sp2 and Sr and are equal to

$Q_{mn2} / 2 = - Q_{mn1} / 2$  on the two electrodes, therefore at time  $t_e$   $t_e = R_m * C_s * \ln(2)$  (5),  $t_e$  being the time to reach equilibrium,  $R_m$  the ohmic resistance of the metal track and of the coil  $L_{in}$ ,  $C_s$  the capacitance formed by the electrodes Sp2 and Sr and the input capacitances of the electronics (fig. .43).

This homogenization of electric charges within a metallic conductor:

- 1 / occurs when the gate voltage of the MOSs constituting circuits 1 and 2 exceeds their threshold voltage.
- 2 / induces an attraction of the piezoelectric structure in the direction opposite to that of Casimir
- 3 / decreases the deformation of the piezoelectric bridge and brings the gate voltage back below the threshold voltage.
- 4 / The transistor MOS only turns off after the charges are homogenized during the short time  $t_e$ .

We therefore obtain a current peak during this homogenization with a duration  $t_e$  of the order of a nanosecond!  
This current peak  $I_{IN}$  circulating for the duration of time  $t_e$  is:

$$I_{IN} = d(Q_{mn})/dt \quad (6) \quad I_{IN} = - \frac{Q_{mn2}}{R_m * C_s} * \left| \text{Exp} \left( - \frac{t}{R_m * C_s} \right) \right|$$

We therefore obtain a current peak during this homogenization with a duration  $t_e$  of the order of a nanosecond!  
A current peak is obtained at time  $t = 0$ . With  $Q_{mn2} / 2$  the charge which is distributed uniformly over the two electrodes  $S_{p2}$  and  $S_r$ .

Time  $t$  is counted from the closing of one of the transistors of circuit 1 and the opening of the switches of circuit 2.  
This current peak  $I_{IN}$  crossing a self  $L_{IN}$  during the time  $t_e$ , induces a voltage  $U_{IN}$  at the terminals of this self  $L_{IN}$  as a function of time according to the usual formula:

$$U_{IN} = L_{IN} * d(I_{IN})/dt = U_{IN} = \frac{L_{IN} * Q_{mn2}}{(R_m * C_s)^2} * \left| \text{Exp} \left( - \frac{t}{R_m * C_s} \right) \right| = \frac{L_{IN} * Q_{mn2} * \ln(2)}{(R_m * C_s * t_e)} * \left| \text{Exp} \left( - \frac{t}{R_m * C_s} \right) \right| = L_{IN} * I_{IN} * \ln(2) / t_e \quad (7)$$

There is therefore a voltage peak across the coil and the electronics appearing without power supply at time  $t = 0$  !

As the deformations of the piezoelectric bridge cancel each other out during its "rise", the mobile charges on the surfaces  $S_{p1}$  as well as  $S_{p2}$  also cancel each other out! As a result, the gate voltage on circuit 1 and 2 MOSs drops below the threshold voltages and circuit 1 blocks. Circuit n°2 turns on again and connects face 2 of return electrode to ground, so the electrical charges on the bridge and the  $S_r$  electrode cancel each other out! (See figure 5).

The force of Casimir  $F_{CA}$ , still present, again attracts the metallic surface  $S_{S2}$  against  $S_{S3}$  and the events described above are repeated. Casimir's force deforms this bridge again and it seems that all starts all over again!

The consequence is that the structure made up of the piezoelectric bridge, the connecting finger, the metal block forming the mobile Casimir electrode starts to vibrate, with a frequency dependent:

- of the Casimir restoring force, and of the return electrode therefore of the starting  $z_0$  and  $z_r$  separation interface
- geometric dimensions of the different electrodes,
- properties of the piezoelectric bridge,
- the choice of threshold voltages of the different MOS transistors
- the choice of conductive metal!

As we will see, this frequency is lower than that of the first resonant frequency of the mobile structure if the initial interface  $z_0$  is not weak enough ( $< 150 \text{ A}^\circ$ ) to induce a sufficient Casimir force (see chapter V and X)!

An AC voltage peak  $U_{IN}$  is therefore automatically recovered at the terminals of the solenoid  $L_{IN}$ . This AC voltage peak can then be rectified to a DC voltage of a few volts, by suitable electronics operating without power supply (see amplification electronics without VI power supply).

Before moving on to theoretical calculations and mathematical simulations of the structure we wish to emphasize that the alternating signal  $U_{IN}$  is obtained without the input of any external energy!

Indeed, it is the Casimir force due to fluctuations in vacuum energy that induces a displacement of the mobile electrode  $S_{S2}$  of the Casimir reflector and then naturally causes a deformation of the piezoelectric bridge. This deformation by nature generates fixed electric charges in the structure of this piezoelectric bridge which is insulating.



These fixed charges then attract from the mass, opposing mobile charges on the metal electrodes  $S_{p1}$  and  $S_{p2}$  of this bridge. These mobile electric charges also go to the gates and the sources of enriched transistors of circuits 1 and 2 (FIG. 5). When the voltage developed by these mobile charges on the gates of the MOS transistors exceeds their threshold voltages, then circuit n°1 naturally turns on and circuit n° 2 is blocked.

Depending on the value of the threshold voltages of the enriched MOS transistors of circuit n°1, the mobile charges  $Q_{mn}$  of face n°1 can then flow and reach the other fixed return electrode  $S_r$  via an inductor  $L_{IN}$  and the input of the electronics. As this  $S_r$  electrode is then electrically isolated by the automatic opening of circuit n°2, this mobile electric charges are distributed uniformly over the two metal surfaces  $S_{p2}$  and  $S_r$  of the Casimir reflector. The charges on the  $S_{s2}$  and  $S_r$  electrodes being of opposite sign induce, without external energy input, a Coulomb force which can be large ( $> 2$  times) and opposite to the Casimir force.

This force moves away the mobile electrode  $S_{s2}$  of the Casimir reflector from  $S_{s3}$ , and by this movement naturally cancels the deformation and therefore the charges present on the piezoelectric bridge. The Coulomb force vanishes, and the ever-present Casimir force then re-attracts the  $S_{s2}$  electrode and.... everything restarts.

The structure consisting of the piezoelectric bridge, the connecting finger and the mobile part of the Casimir reflector then vibrates at a frequency depending on the geometric and physical characteristics of the Casimir reflector and the piezoelectric bridge and this a priori without any energy input from our world!

In conclusions it seems (except errors) that all the electro-physical phenomena leading to a vibration of the structure and to the production of a voltage modulation are only the consequence of a first phenomenon which is at the origin of the Force of Casimir induced by fluctuations in vacuum energy.

They occur naturally and automatically without the input of any external energy except that of a vacuum ...!

We can then hope that this complete device extracts its operating energy from the Casimir force due to isotropic fluctuations in vacuum and works without contradicting Noether's theorem....

But we know that the devil is hiding in the details!!

### III / CALCULATION OF THE CURRENT GENERATED BY THE CASIMIR STRUCTURE

If the initial separation interface  $z_0$  is greater than  $150 \text{ \AA}$ , the forces present are too weak to induce a vibration frequency of the device corresponding to its first resonant frequency (see chapter V).

We sought the numerical solutions of the differential equations obtained and unfortunately insoluble analytically when the device does not vibrate at its first resonant frequency!

#### III.1 / calculation of the frequency of vibration of the Casimir structure.

In order to verify whether the structure of figure 5 can enter into resonance at its first frequency (see Appendix) or vibrate at another frequency under the action of the forces of Casimir and Coulomb, let us calculate the evolution in time of the force of Casimir which is applied between the two electrodes separated by an initial distance  $z_0$ .

Let us take again the diagram of figure 3 and apply the theorem of angular momentum to this vibrating structure.

The angular momentum of the device is;  $\sigma_{A,x,y,z}^S(Structure) = \bar{I}_{A,x,y,z}^S \bar{\Omega}_A^S$  (8)

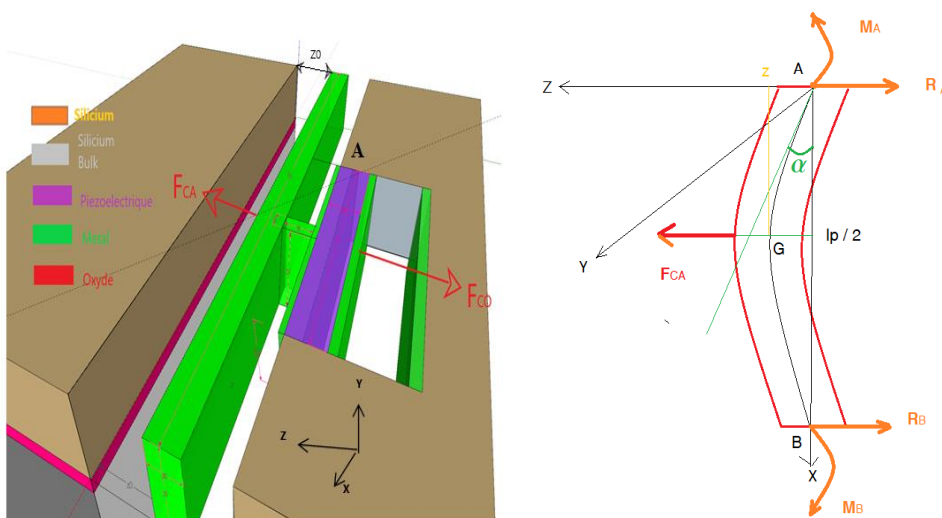


**Figure 8:**  
Piezoelectric  
bridge Cutting  
Reactions and  
Bending Moment,  
Deflection Angle

With  $\vec{\sigma}_{A,x,y,z}^S$  the angular momentum vector of the structure, the inertia matrix of the structure with respect to the reference (A, x, y, z) and  $\bar{\Omega}_A^S$  the rotation vector of the piezoelectric bridge with respect to the axis Ay with  $\alpha$  the low angle of rotation along the y axis of the piezoelectric bridge. We have:

$$\sin(\alpha) = \sin\left(\frac{z}{l_p}\right) = \sin\left(\frac{2^*z}{l_p}\right) \approx \frac{2^*z}{l_p} \Rightarrow \bar{\Omega}_A^S = \begin{pmatrix} 0 \\ \frac{d\alpha}{dt} \\ 0 \end{pmatrix} \text{avec } \frac{d\alpha}{dt} \approx \frac{2^*}{l_p} \frac{dz}{dt}$$

Let  $(G_p, x, y, z)$ ,  $(G_i, x, y, z)$ ,  $(G_s, x, y, z)$  be the barycentric points respectively of the piezoelectric bridge, of the metal connecting finger and of the metal block constituting the sole mobile of the Casimir reflector. We have (fig 5):

$$AG_{P,x,y,z}^{\vec{}} \text{ a pour coordonnées } \frac{1}{2} \begin{pmatrix} l_p \\ b_p \\ a_p \end{pmatrix}; \quad AG_{I,x,y,z}^{\vec{}} \text{ a pour coordonnées } \frac{1}{2} \begin{pmatrix} l_p + l_i \\ b_p + b_i \\ a_p + a_i \end{pmatrix}; \quad AG_{S,x,y,z}^{\vec{}} \text{ a pour coordonnées } \frac{1}{2} \begin{pmatrix} l_p + l_i + l_s \\ b_p + b_i + b_s \\ a_p + a_i + a_s \end{pmatrix}$$

The inertia matrix of the bridge in the frame of reference  $(G_p, x, y, z)$  is:

$$\bar{I}_{G_p}^p = \frac{m_p}{12} * \begin{pmatrix} a_p^2 + b_p^2 & 0 & 0 \\ 0 & l_p^2 + b_p^2 & 0 \\ 0 & 0 & l_p^2 + a_p^2 \end{pmatrix}$$

Taking Huygens' theorem into account, this inertia matrix becomes:

$$I_{A,x,y,z}^p = m_p * \begin{pmatrix} a_p^2 + b_p^2 & 0 & 0 \\ 0 & l_p^2 + a_p^2 & 0 \\ 0 & 0 & l_p^2 + b_p^2 \end{pmatrix} + m_p * \begin{pmatrix} \frac{b_p^2 + a_p^2}{4} & \frac{-l_p * b_p}{4} & \frac{-l_p * a_p}{4} \\ \frac{-l_p * b_p}{4} & \frac{l_p^2 + a_p^2}{4} & \frac{-b_p * a_p}{4} \\ \frac{-l_p * a_p}{4} & \frac{-b_p * a_p}{4} & \frac{l_p^2 + b_p^2}{4} \end{pmatrix} = m_p * \begin{pmatrix} \frac{b_p^2 + a_p^2}{3} & \frac{-l_p * b_p}{4} & \frac{-l_p * a_p}{4} \\ \frac{-l_p * b_p}{4} & \frac{l_p^2 + a_p^2}{3} & \frac{-b_p * a_p}{4} \\ \frac{-l_p * a_p}{4} & \frac{-b_p * a_p}{4} & \frac{l_p^2 + b_p^2}{3} \end{pmatrix} \quad (9)$$

The inertia matrix of the connecting finger is in the frame of reference (Gi, x, y, z):

$$I_{Gi}^l = m_i * \begin{pmatrix} a_i^2 + b_i^2 & 0 & 0 \\ 0 & l_i^2 + a_i^2 & 0 \\ 0 & 0 & l_i^2 + b_i^2 \end{pmatrix}$$

Taking Huygens' theorem into account, this inertia matrix becomes:

$$I_{A,x,y,z}^m = m_i * \begin{pmatrix} a_i^2 + b_i^2 & 0 & 0 \\ 0 & l_i^2 + a_i^2 & 0 \\ 0 & 0 & l_i^2 + b_i^2 \end{pmatrix} + m_i * \begin{pmatrix} \frac{(b_p + b_i)^2 + (a_p + a_i)^2}{4} & \frac{-(l_p + l_i) * (b_p + b_i)}{4} & \frac{-(l_p + l_i) * (a_p + a_i)}{4} \\ \frac{-(l_p + l_i) * (b_p + b_i)}{4} & \frac{(l_p + l_i)^2 + (a_p + a_i)^2}{4} & \frac{-(a_p + a_i) * (b_p + b_i)}{4} \\ \frac{-(l_p + l_i) * (a_p + a_i)}{4} & \frac{-(a_p + a_i) * (b_p + b_i)}{4} & \frac{(b_p + b_i)^2 + (l_p + l_i)^2}{4} \end{pmatrix} \quad (10)$$

The inertia matrix of the connecting finger is in the frame of reference (Gs, x, y, z):

$$I_{Gs}^m = m_s * \begin{pmatrix} a_s^2 + b_s^2 & 0 & 0 \\ 0 & l_s^2 + a_s^2 & 0 \\ 0 & 0 & l_s^2 + b_s^2 \end{pmatrix}$$

Taking Huygens' theorem into account, this inertia matrix becomes:

$$I_{A,x,y,z}^c = m_s * \begin{pmatrix} a_s^2 + b_s^2 & 0 & 0 \\ 0 & l_s^2 + a_s^2 & 0 \\ 0 & 0 & l_s^2 + b_s^2 \end{pmatrix} + m_s * \begin{pmatrix} \frac{(b_p + b_i + b_s)^2 + (a_p + a_i + a_s)^2}{4} & \frac{-(l_p + l_i + l_s) * (b_p + b_i + b_s)}{4} & \frac{-(l_p + l_i + l_s) * (a_p + a_i + a_s)}{4} \\ \frac{-(l_p + l_i + l_s) * (b_p + b_i + b_s)}{4} & \frac{(l_p + l_i + l_s)^2 + (a_p + a_i + a_s)^2}{4} & \frac{-(a_p + a_i + a_s) * (b_p + b_i + b_s)}{4} \\ \frac{-(l_p + l_i + l_s) * (a_p + a_i + a_s)}{4} & \frac{-(a_p + a_i + a_s) * (b_p + b_i + b_s)}{4} & \frac{(b_p + b_i + b_s)^2 + (l_p + l_i + l_s)^2}{4} \end{pmatrix} \quad (11)$$

The total inertia of the structure becomes in the reference (A, x, y, z),  $I_{A,x,y,z}^p = I_{A,x,y,z}^m + I_{A,x,y,z}^l + I_{A,x,y,z}^c$  with A at the edge of the embedded piezoelectric bridge.

The angular momentum theorem applied to the whole structure gives:

$$\frac{d(\vec{\sigma}_{Axyz})}{dt} = \vec{I}_{Axyz} \frac{d\vec{\Omega}_s}{dt} \Rightarrow \vec{I}_{Axyz} * \frac{2}{l_p} * \begin{bmatrix} 0 \\ \frac{d^2 z}{dt^2} \\ 0 \end{bmatrix} = \sum_i \text{Moment appliqués à la structure} = \vec{M}_{Az} + \vec{M}_{Bz} + \vec{F}_{CA} \wedge \begin{pmatrix} \frac{2}{l_p} \\ 0 \\ 0 \end{pmatrix} \text{ avec } \vec{F}_{CA} = \begin{bmatrix} 0 \\ 0 \\ F_{CA} \end{bmatrix} \quad (12)$$

Now we know (see X) that according to the axis of Az:  $M_{AY} = M_{BY} = -F_{CA} l_p / 8$ , therefore  $\Sigma \text{ Moments} / Ay = 1/4 * l_p * F_{CA}$ .

Any calculation done that gives:  $I_Y^S \frac{2}{l_p} * \frac{d^2 z}{dt^2} = \frac{l_p}{4} * F_{CA} = \frac{l_p}{4} * S_s \left( \frac{\pi^2 \hbar c}{240} \right) * \frac{1}{z^4}$  (11) with:

$$I_Y^S = \rho_p * \left( (a_p * b_p * l_p) * \left( \frac{l_p^2 + a_p^2}{12} \right) + \left( \frac{l_p^2 + a_p^2}{4} \right) \right) \\ + \rho_i * (a_i * b_i * l_i) * \left( \frac{l_i^2 + a_i^2}{12} \right) + \left( \frac{(l_p + l_i)^2 + (a_p + a_i)^2}{4} \right) \\ + \rho_s * (a_s * b_s * l_s) * \left( \frac{l_s^2 + a_s^2}{12} \right) + \left( \frac{(l_p + l_i + l_s)^2 + (a_p + a_i + a_s)^2}{4} \right) \quad (13)$$

with  $\rho_p$ ,  $\rho_i$ ,  $\rho_s$  respectively the densities of the piezoelectric bridge, of the intermediate finger and of the mobile electrode of the Casimir reflector.

We then obtain the differential equation which makes it possible to calculate the interval between the two electrodes of the Casimir reflector as a function of time during the "descent" phase when the Coulomb forces are not present.

$$\frac{d^2 z}{dt^2} = \frac{l_p^2}{8 * I_Y^S} * S_s \left( \frac{\pi^2 \hbar c}{240} \right) \frac{1}{z^4} = \frac{B}{z^4} \text{ avec } B = \frac{l_p^2}{8 * I_Y^S} * S_s \left( \frac{\pi^2 \hbar c}{240} \right) \quad (14)$$

Coulomb forces do not intervene yet because the MOS switches in parallel of circuit 1 - before the self Lin - are open and the MOS switches in series of circuit 2 - after the self Lin - being closed the return Coulomb electrode is to earth. The fixed Casimir electrode is always to earth (see figures 5 and 6).

Coulomb forces will intervene when the gate voltage  $V_G = Q_{mp2\text{MOS}} / C_{OX}$  on the MOSs of circuit n°1 exceeds the threshold voltage of one of them and when circuit n° 2 of the depleted N and P MOSs in series will be open (figure 5 and 6)! Then the switches of the circuit of the parallel MOS transistors will close. The switches of the series MOS circuit will open and the charge  $Q_{mn1}$  initially present exclusively on the electrode of the bridge and of the metallic block will be distributed uniformly over the second part of coulomb electrodes according to:

$$Q_{mn1f} = Q_{mn1} * \frac{S_p}{S_p + S_r} \approx \frac{Q_{mn1}}{2} \quad \text{Because } S_r = S_{p1}$$

Just at the moment of closing circuit n°1 and opening circuit n° 2 (figure 5) we have  $F_{CO} = -p F_{CA}$  with p a coefficient of proportionality  $\geq 2$  defined by the threshold voltages of the MOS interrupters.

The total force  $F_T$  exerted in the middle of the piezoelectric bridge just at the start of the charge transfer becomes  $F_T = F_{CA} - F_{CO} = F_{CA} - p * F_{CA} = F_{CA} (1-p)$

The "descent" time of the free Casimir electrode will therefore stop when  $F_{CO} = -p F_{CA}$ .

However, we know that:

$$F_{CA} \approx S_s \left( \frac{\pi^2 \hbar c}{240 z_s^4} \right) \quad (2)$$

1 / The Casimir force variable in time =

2 / The mobile charge on the Casimir electrodes (3) variable in time =  $Q_{mn2} \approx \frac{Q_{mn}}{2} = \frac{d_{31} F_{CA} l_P}{2 a_P}$

3 / The Coulomb force (4), variable over time, acting in opposition to the Casimir force

$$F_{CO} = \left| l_s b_s \frac{\pi^2 \hbar c}{240} * \frac{d_{31} l_P}{a_P} \right|^2 * \frac{1}{16 \pi \epsilon_0 \epsilon_r} \frac{1}{z_s^8} \left( \frac{1}{(z_r + z_0 - z_s)^2} - \frac{1}{(z_r)^2} \right)$$

This differential equation (13) unfortunately does not have a literal solution and we programmed on MATLAB the solution of this differential equation "descent" and calculated the duration of this "descent" of the free Casimir electrode.

This duration of the "descent" depending on the desired value of the coefficient of proportionality p, is regulated by the values of the threshold voltages of the MOS transistors defined during the manufacture of the device.

$$\text{We have then: } F_{CO} = p F_{CA} \Rightarrow \left| S_s \frac{\pi^2 \hbar c}{240} * \frac{d_{31} l_P}{a_P} \right|^2 * \frac{1}{16 \pi \epsilon_0 \epsilon_r} \frac{1}{z_s^8} \left( \frac{1}{(z_r + z_0 - z_s)^2} - \frac{1}{(z_r)^2} \right) = p * S_s \frac{\pi^2 \hbar c}{240 z_s^4}$$

The "descent" of the free Casimir electrode stops when the inter electrode interface  $z_s$  is such that:

$$\frac{1}{z_s^8} \left( \frac{1}{(z_r + z_0 - z_s)^2} - \frac{1}{(z_r)^2} \right) = p * \frac{3840 \pi \epsilon_0 \epsilon_r}{\pi \hbar c S_s} \left( \frac{a_P}{d_{31} l_P} \right)^2 \quad (15)$$

This programmable equation shows that the time of the "descent" depends on the coefficient of proportionality p, is calculable and will stop when the inter-electrode interface  $z_s$  has a value  $z_{sm}$  satisfying equation (15)

At the instant of the appearance of the Coulomb force, the total force is therefore:

$$F_T = (1-p) F_{CA} = (1-p) S_s \left( \frac{\pi^2 \hbar c}{240 z_{sm}^4} \right) < 0 \text{ si } p > 1$$

4 / The total force, variable over time and exerted at the center of the piezoelectric bridge, becomes:

$$F_T = F_{CA} - F_{CO} = S_s \left( \frac{\pi^2 \hbar c}{240} \right) \left| \frac{1}{z_s^4} - S_s \frac{\pi^2 \hbar c}{240} \left( \frac{d_{31} l_P}{a_P} \right)^2 \right| * \frac{1}{16 \pi \epsilon_0 \epsilon_r} \frac{1}{z_s^8} \left( \frac{1}{(z_r + z_0 - z_s)^2} - \frac{1}{(z_r)^2} \right)$$

The piezoelectric bridge subjected to this force then rises towards its neutral position. The Casimir interelectrode interval increases causing the Casimir force to decrease!

As the deformations of the piezoelectric bridge decrease, the electric charge present on the piezoelectric faces decreases, which consequently leads to a drop in the Coulomb Force. The  $F_T$  force therefore rapidly approaches the starting  $F_{CA}$  force, during the "ascent" of the Casimir electrodes.

Let us calculate the duration of this "rise" of the mobile electrode of the Casimir reflector triggered when

$$F_{CO} = p * F_{CA}.$$

To know the time taken by the structure to "go back" to its neutral position we must solve the following differential equation:

$$\frac{d^2 z}{dt^2} = \left(\frac{l_p^2}{8 I_Y}\right) (F_{CA} - F_{CO}) = \left(\frac{l_p^2}{8 I_Y}\right) l_s b_s \left| \frac{\pi^2 h c}{240} \right| \left| \frac{1}{z_s} - l_s b_s \frac{\pi^2 h c}{240} \left| \frac{d_{31} l_p}{a_p} \right|^2 * \frac{1}{16 \pi \epsilon_0 \epsilon_r} \frac{1}{z_s} \left( \frac{1}{(z_r + z_0 - z_s)^2} - \frac{1}{(z_r)^2} \right) \right| \quad (16)$$

By then posing  $A1 = l_s b_s \left| \frac{\pi^2 h c}{240} \right|$  the differential equation (16) concerning the "ascent" of the bridge is written:

$$\frac{d^2 z}{dt^2} = \left(\frac{l_p^2}{8 I_Y}\right) (F_{CA} - F_{CO}) = \left(\frac{l_p^2}{8 I_Y}\right) A1 \left| \frac{1}{z_s} - A1 \left| \frac{d_{31} l_p}{a_p} \right|^2 * \frac{1}{16 \pi \epsilon_0 \epsilon_r} \frac{1}{z_s} \left( \frac{1}{(z_r + z_0 - z_s)^2} - \frac{1}{(z_r)^2} \right) \right| \quad (17)$$

This differential equation has no analytical solution and can only be solved numerically. We programmed it on MATLAB with the inter-electrode distance  $z_s$  belonging to the interval  $[z_{sm}, z_0]$ .

The properties and dimensions of the different materials used in this simulation are as follows (figure 9) The metal used for the Casimir reflector block is Aluminum with a density of  $2.7 \text{ gcm}^{-3}$

**figure 9: Table of characteristics used for MATLAB and ANSYS simulations**

	PZT	AlN	LiNbO3	PMN-PT : (1-x)Pb(Mg1/3- Nb1/3)O3-xPbTiO3
Young Modulus ( $\text{kg} \cdot \text{m} \cdot \text{s}^{-2} / \text{m}^2$ )	$E_p = 8.9 \cdot 10^{10}$	$E_p = 32 \cdot 10^{10}$	$E_p = 2.45 \cdot 10^9$	$E_p = 150 \cdot 10^9$
Volumic mass ( $\text{kg m}^{-3}$ )	$d_p = 7600$	$d_p = 3255$	$d_p = 4700$	$d_p = 7920$
Piezoelectric coefficient $d_{31}$ of the beam ( $\text{C} / (\text{kg} \cdot \text{m} \cdot \text{s}^{-2})$ )	$d_{31} = 200 \cdot 10^{-12}$	$d_{31} = 2.400 \cdot 10^{-12}$	$d_{31} = 6 \cdot 10^{-12}$	$d_{31} = 1450 \cdot 10^{-12}$
Length piezoelectric beam $l_p$ (m)	$50 \cdot 10^{-6}$	$50 \cdot 10^{-6}$	$50 \cdot 10^{-6}$	$50 \cdot 10^{-6}$
Width piézoélectrique beam $b_p$ (m)	$150 \cdot 10^{-6}$	$150 \cdot 10^{-6}$	$150 \cdot 10^{-6}$	$150 \cdot 10^{-6}$
Thickness piézoélectrique $a_p$ (m)	$10 \cdot 10^{-6}$	$10 \cdot 10^{-6}$	$10 \cdot 10^{-6}$	$10 \cdot 10^{-6}$
Longueur doigt raccordement $l_i$ (m)	$10 \cdot 10^{-6}$	$10 \cdot 10^{-6}$	$10 \cdot 10^{-6}$	$10 \cdot 10^{-6}$
Width finger connection $b_i$ (m)	$150 \cdot 10^{-6}$	$150 \cdot 10^{-6}$	$150 \cdot 10^{-6}$	$150 \cdot 10^{-6}$
Thickness finger connection $a_i$ (m)	$10 \cdot 10^{-6}$	$10 \cdot 10^{-6}$	$10 \cdot 10^{-6}$	$10 \cdot 10^{-6}$
Mobile Casimir electrode block length $l_s$ (m)	$500 \cdot 10^{-6}$	$500 \cdot 10^{-6}$	$500 \cdot 10^{-6}$	$500 \cdot 10^{-6}$
Mobile Casimir electrode block width $b_s$ (m)	$150 \cdot 10^{-6}$	$150 \cdot 10^{-6}$	$150 \cdot 10^{-6}$	$150 \cdot 10^{-6}$
Casimir mobile electrode block thickness $a_s$ (m)	$10 \cdot 10^{-6}$	$10 \cdot 10^{-6}$	$10 \cdot 10^{-6}$	$10 \cdot 10^{-6}$

In these MATLAB calculations we considered that the metal of the electrodes and of the metal block was oxidized over a thickness allowing to have an interface between Casimir electrodes of  $200 \text{ \AA}$  (see chapter 5) which modifies the mass and the inertia of the vibrating structure.

It turns out that the choice of aluminum as the metal deposited on these electrodes is preferable given:

1 / the ratios between the thickness of the metal oxide obtained and that of the metal attacked by the growth of this oxide during its thermal oxidation (see chapter V)

2 / with a view to increasing and optimizing the vibration frequency of the structure by minimizing the inertia of the parallelepipedal block for transferring the Casimir force to the piezoelectric bridge and that the density of the aluminum is weak.

The mass M of the vibrating structure is then:

$$M = d_{pm} * (a_s * b_s * l_s + a_i * b_i * l_i) + d_{om} * 2 * z_{of} * (a_{so} * b_{so} + b_{so} * l_{so} + a_{so} * l_{so}) + d_p * (a_p * b_p * l_p);$$

With  $d_{pm}$  the density of the metal,  $a_s, b_s, l_s$  the geometries of the final metal part of the Casimir electrode sole,  $d_{om}$  the density of the metal oxide,  $a_{so}, b_{so}, l_{so}$  the geometries of the oxidized parts around the 6 faces of the metal block,  $d_p$  the density of the piezoelectric parallelepiped (see figure 10):

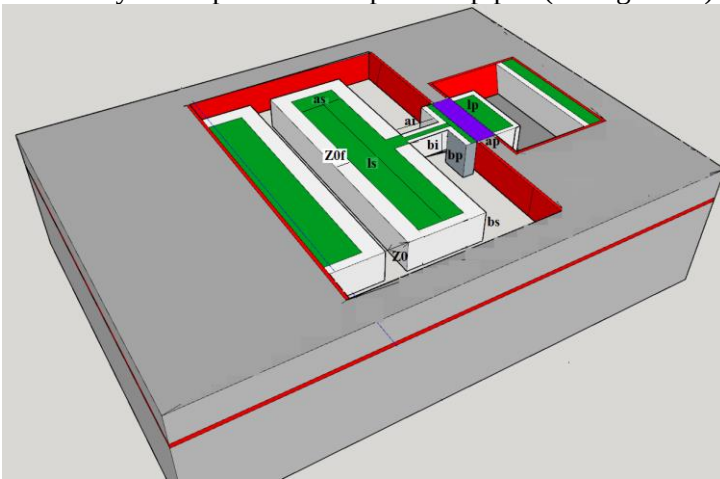


**Figure 10: Final structure with the metal oxides surrounding the metal electrodes.**

### III .2 / Calculation of the current peak

Let us estimate the duration of the current peak linked to the circulation and homogenization on the return electrodes of the mobile charges.

Let  $R_m$  be the ohmic resistance of the metals used for the surface electrodes  $S_{p1}$  + the  $L_{IN}$  solenoid + the  $S_r$  electrode (see figure 5) and  $C_s$  the capacitance formed by the gap between the return electrodes  $S_{p2}$  and  $S_r$ .

Then the current peak circulating during the transition of the mobile loads between  $S_{p1}$  to  $S_r$  via circuit n°1 and the  $L_{IN}$  solenoid is as we have already seen

$$I_{IN} = - \frac{Q_{mn2}}{R_m * C_s} * \left| \text{Exp} \left( - \frac{t}{R_m * C_s} \right) \right|$$

The time  $t$  being counted from the closing of the MOSNE switch.

The duration of this current peak is estimated at  $t_e = R_m * C_s * \text{Log} (2)$  when the charges on each electrode will be  $Q_{mn2} / 2$ . In this expression:

- $R_m \approx \rho_m * l_m / S_m$ , with  $\rho_m$  the resistivity of the metallic conductor in the circuit between electrodes (the solenoid + the electrodes themselves),
- $l_m$  its total length of this conductor,  $S_m$  its section
- $C_s = \epsilon_0 * \epsilon_{om} * l_p * b_p / z_r$ , the inter-electrode return capacitance, with  $\epsilon_0$  the permittivity of vacuum,  $\epsilon_{om}$  the relative permittivity of the metal oxide,  $l_p$  and  $b_p$  the geometries of the return electrode.

A calculation of the duration of the homogenization of the electric charges and therefore of the duration of the current peak (based on an estimate to propagate in a  $L_{IN}$  coil of about  $10^{-5}$  Henri) gives  $t_e \approx 10^{-9}$  s.

This current peak passing through a  $L_{IN}$  solenoid develops a voltage peak  $U_{IN} = L_{IN} I_{INP} / t_e = L_{IN} * Q_{mn2} / (2.t_e * R_m. C_s)$  which will be exploited by an integrated electronics without any power supply described in chapter IV.

We present below the results of the MATLAB simulations carried out by numerically calculating the differential equations (13) and (17). These numerical calculations give the vibration frequency of the structure which, as we will see, vibrates at a frequency lower than its first resonant frequency (IV)

This vibration frequency depends on the characteristics of the structure (Nature of the piezoelectric material, nature of the metallic conductors, initial interface  $z_0$  and  $z_r$  between Casimir electrodes and return electrodes, geometric dimensions of the Casimir reflectors, coefficient of proportionality  $p = F_{CO} / F_{CA} \dots$ ). (See IV and Annex)

#### IV/ SIMULATION OF DEVICES WITH DIFFERENTS PIEZOELECTRIC BRIDGE

We will see that this device vibrates at a frequency lower than its first resonant frequency and that its vibration frequency depends on the characteristics of the structure (Nature of the piezoelectric material, nature of the metallic conductors, starting interface  $z_0$  and  $z_r$  between Casimir electrodes and return Coulomb electrodes, dimensions of the Casimir reflectors, coefficient of proportionality  $p = F_{CO} / F_{CA} \dots$ ).

Except precision the interface  $z_r$  between the coulombs electrode is the same that those of Casimir reflector  $z_0$

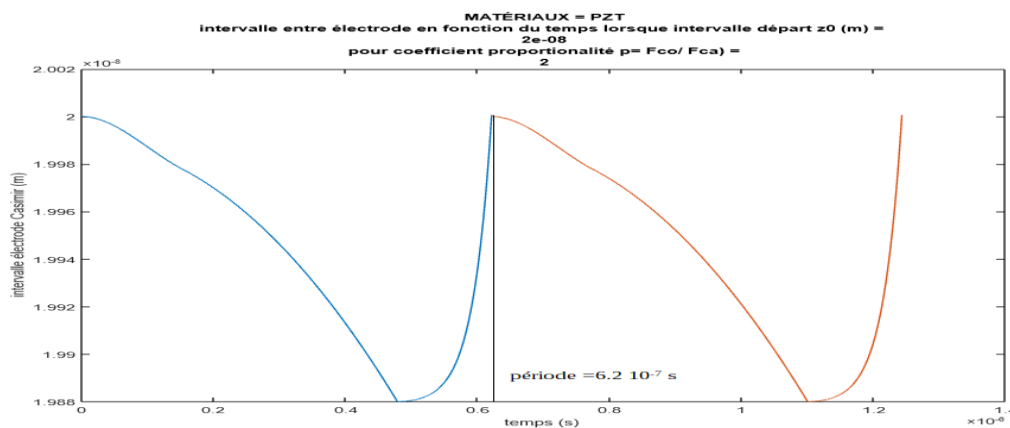
#### IV- 1 / PIEZOELECTRIC MATERIALS = PZT (Lead Zirconia Titanium)

##### **IV-1-1 / interface between Casimir electrodes as a function of time for different trigger values of MOS transistors**

For a starting interface between Casimir electrode of  $z_0 = 200 * 10^{-10}$  (m) and a coefficient of proportionality  $p = F_{CO} / F_{CA} = 2$ , we obtain the following evolution in time of the Casimir interface:

Curves concerning the phases of descent and rise of the mobile Casimir electrode: vibration frequency.

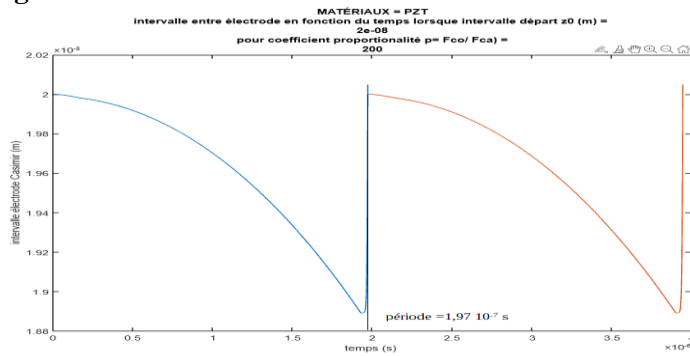
**Figure 11: Interval between Casimir electrodes as a function of time for a proportionality coefficient  $F_{CO} / F_{CA} = 2$ : PZT**



We notice a phase of rise of the Casimir electrode faster than that of descent. The period of vibrations is  $6.18 \cdot 10^{-7}$  s therefore with a vibration frequency of  $1.613 \cdot 10^6$  Hertz while the first resonant frequency of the same structure is  $6.54 \cdot 10^6$  hertz. The moving electrode drops to  $z_s = 198.8$  Angstroms from the fixed electrode  $S_{S3}$ . The current peak for this coefficient of proportionality  $p = 2$  is  $2.58 \cdot 10^{-8}$  A. This current is obtained by adjusting the threshold voltage of the enriched and depleted MOS transistors to a value  $V_t = 0.6553V$  for a length  $L = \text{width} = W = 4 \cdot 10^{-6}$  m and with a grid oxide thickness  $\text{SiO}_2 = t_{ox}$  of  $250 \cdot 10^{-10}$  m (See figure 18)!

Let us simply change the coefficient  $p = F_{CO} / F_{CA}$  of proportionality to  $p = 200$ , then we get (See figure 12):

**Figure 12: Vibrations of the structure for a coefficient of proportionality  $p = F_{CO} / F_{CA} = 200$ : PZT**



Because of the inertia, this mobile electrode rises very slightly at 201 A ° from the fixed electrode, therefore exceeds its neutral starting position of 1 A °. The peak current for this coefficient of proportionality  $p = 200$  is  $1.7910^{-7}$  A

We notice for the ratio  $p = F_{CA} / F_{CO} = 200$  (figure 12), a phase of "rise" of the Casimir electrode also much faster than that of "descent" but also more dynamic than for the ratio of previous  $p = 2$ . The vibration frequency of the device of  $5.07 \cdot 10^5$  hertz, while the first resonant frequency of the structure is still  $6.54 \cdot 10^6$  hertz! The moving electrode is now approaching  $z_s = 188.9 \text{ \AA}$  to the fixed electrode  $S_{S3}$ , so the vibration amplitude of the structure is  $200 - 188.9 = 11.1$  Angstroms!

This current is obtained by adjusting the threshold voltage of the enriched and depleted MOS transistors to a value  $V_t = 6.89$  V for the same geometries as above (see figure 27).

We must therefore adjust the threshold voltages to precisely adjust the ratio  $p = F_{CO} / F_{CA}$  for which the Coulomb force is triggered. This is a point that can be easily obtained technologically (see the technological part of this report)

In conclusion, as the vibration frequency of the structure depends, among other things, on the coefficient of proportionality  $p$  and therefore on the current that one wishes to obtain, **the structure does not vibrate at its first resonant frequency.**

**IV-1-2 / Spatial and temporal evolution of the Coulomb and Casimir force during an entire period**

Figure 13 illustrates for the same device the values of the force of Casimir and that of Coulomb for an evolution of the interface between the Casimir electrodes from  $189.5 \text{ \AA}$  to  $200 \text{ \AA}$  during a complete cycle "descent + rise" of the movable electrode.

Figure 14 shows the evolution over time of the Casimir and Coulomb forces. Note that the Coulomb force is canceled out when the structure returns to its starting position at time  $t = 1.95 \cdot 10^{-6}$  seconde.

**Figure 13: Casimir force and Coulomb force during a complete cycle  $f$  (interface between electrodes of the Casimir resonator) and for a coefficient of proportionality  $p = F_{CO} / F_{CA} = 200$**

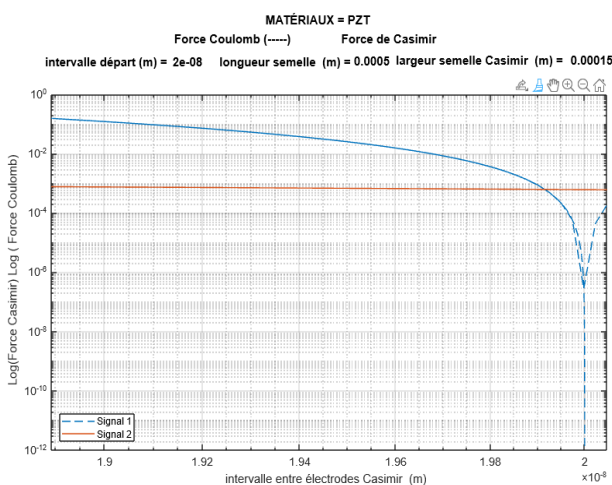


**Figure 14: Casimir force and Coulomb force during a complete cycle  $f$  (time) and for a coefficient of proportionality  $p = F_{CO} / F_{CA} = 200$**

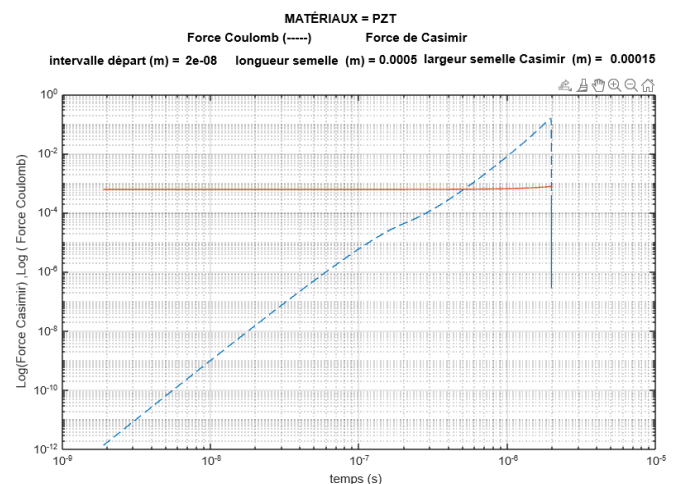




Figure 15 shows the ratio  $p = F_{CO} / F_{CA} = f(\text{time})$  during a complete structural vibration cycle and with a choice of maximum ratio = 200

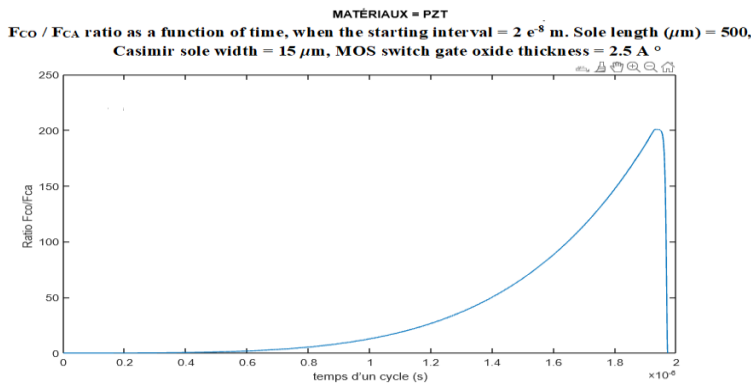
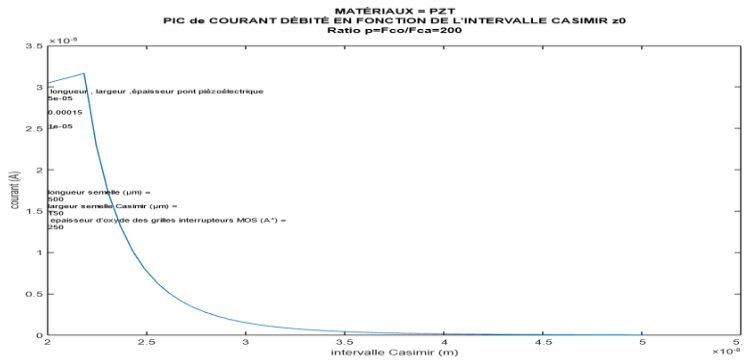


Figure 15 shows the ratio  $p = F_{CO} / F_{CA}$  between the Coulomb force and that of Casimir during a complete structural vibration cycle. We notice that this ratio reaches the chosen ratio of 200 at time  $1.95 \times 10^{-6}$  seconds then plunges to zero during the "rise" of the structure.

IV-1-3 / Variation of the starting interface  $z_0$  between Casimir electrodes: PZT

Figure 16: Maximum Peak CURRENT = f (starting interface  $z_0$ ), Maximum selected  $F_{CO} / F_{CA}$  p ratio = 200



Note that to have a significant current it is necessary to use starting interfaces between Casimir electrodes of low values and less than 300 Angstroms. This weak interface is difficult to obtain but remains possible with a technology that we offer (see technology chapter).

If  $Q_p =$  charge on the piezoelectric bridge just before the triggering of the MOS switches and  $t_e = R_m * C_s * \ln(2) \cong 10^{-9}$  the transition period of these charges during their homogenization on the 2 return electrodes, then the peak of current is approximated with  $I_s = \Delta Q_p / (2 * t_e)$ . This current peak is present even if the transistors may close some time after its existence because the mobile charges have already propagated.

We notice (Figure 17) that the vibration frequency of the structure drops as the initial space between the Casimir electrodes increases, which is related to a decrease in the Casimir Force and therefore makes sense. The vibration frequency depends on the chosen  $F_{CO} / F_{CA}$  ratio. This frequency drops and stabilizes around 2.6 MHz as the electrode interface increases by a ratio of 200. It is much lower than the first resonant frequency of the structure which is 6.85 Megahertz (for this structure). The vibration frequency approaches that of first resonance if the starting  $z_0$  interface is less than 200 Angstroms.

We chose an initial interface of  $200 \text{ \AA}$  for reasons of technological feasibility (see VI)!

Figure 17: Structure vibration frequency = f (starting interface  $z_0$ ):  $F_{CO} / F_{CA}$  chosen = 200: PZT

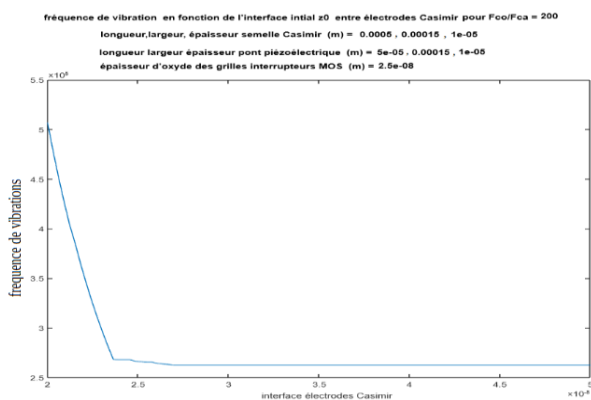
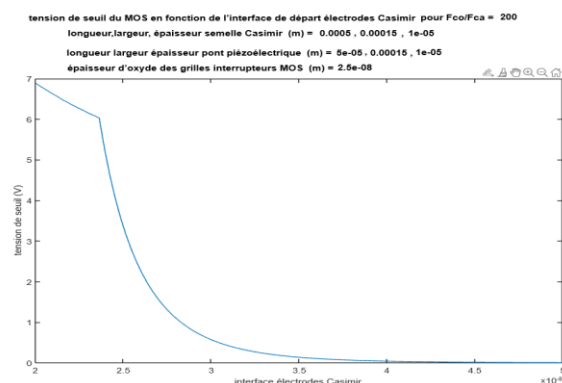


Figure 18: MOS threshold voltage = f (starting interface  $z_0$ ):  $F_{CO} / F_{CA}$  chosen = 200: PZT



We also notice (Figure 18) that the threshold voltage of the Enriched and Depleted MOS transistors increases with a decrease in the starting interface between Casimir electrodes. This seems logical, since the Casimir force increasing, the deflection of the bridge and therefore the charges generated on its faces do the same. It is therefore necessary that the threshold voltage of the MOS transistors be greater so that the voltage  $V_G$  on the gates of the MOS does not trigger them!!

**IV-1-4 / variation of the length  $l_s$  of the Casimir electrode: PZT**

We obtain (figure 19) a small decrease in current with the increase in the length of this electrode and a significant increase in the threshold voltage (figure 20), which is understandable since the inertia of the structure increases.

**figure 19: maximum current = f (length of the Casimir electrode  $l_s$ ), starting interface = 200 A °, selected coefficient of proportionality =  $p = F_{co} / F_{ca} = 2$**

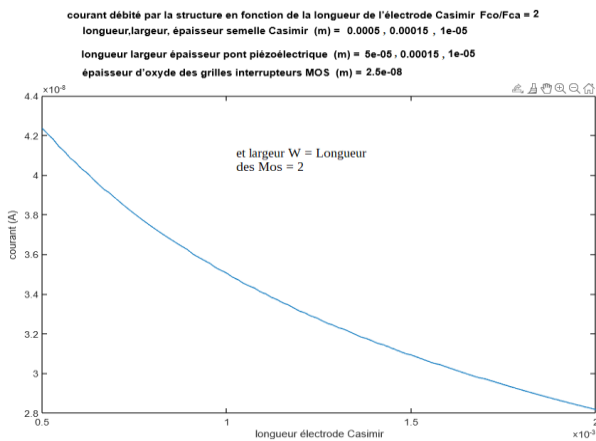
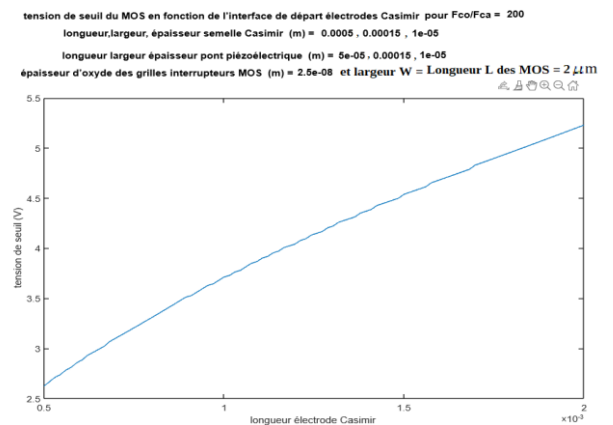


**figure 20: Threshold Voltage = f (length of the Casimir electrode  $l_s$ ), starting interface = 200 A °, selected coefficient of proportionality =  $p = F_{co} / F_{ca} = 2$**



**IV-1-5 / variation of the width  $b_p$  of the piezoelectric bridge: PZT**

We now vary the width  $b_p$  of the piezoelectric bridge. We obtain an increase in the threshold voltage of the MOS by increasing the width  $b_p$  of the piezoelectric bridge, however the current delivered by the structure varies little with the width of the piezoelectric bridge (figure 21 and 22).

*For reasons of technological convenience, it will be preferable to choose a thickness of around 20  $\mu$ m!*

**figure 21: threshold voltage of the MOS = f (width of the Casimir electrode  $l_s$ ), starting interface = 200 A °, selected coefficient of proportionality =  $p = F_{co} / F_{ca} = 10$**

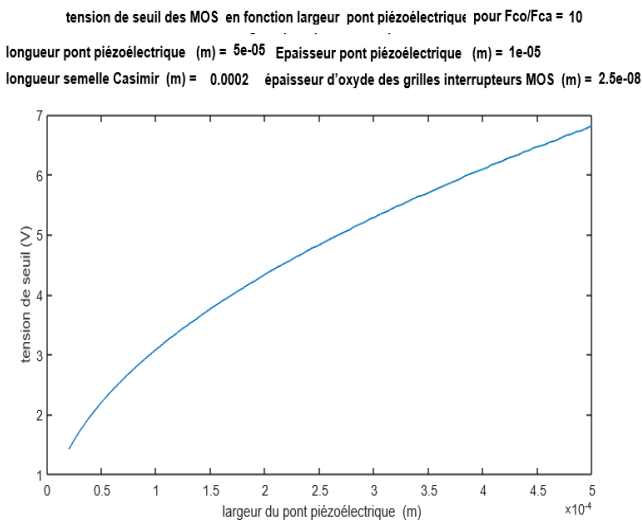
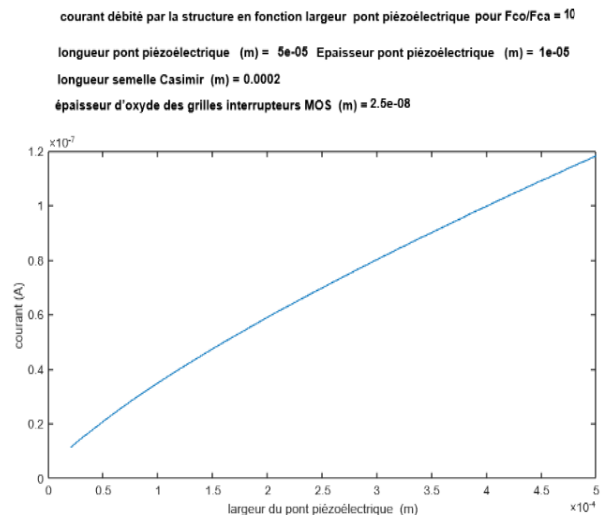


**figure 22: Maximum current = f (width of the Casimir electrode  $l_s$ ), starting interface = 200 A °, selected coefficient of proportionality =  $p = F_{co} / F_{ca} = 10$**



**IV-1-6 / variation of the thickness ap of the piezoelectric bridge: PZT**

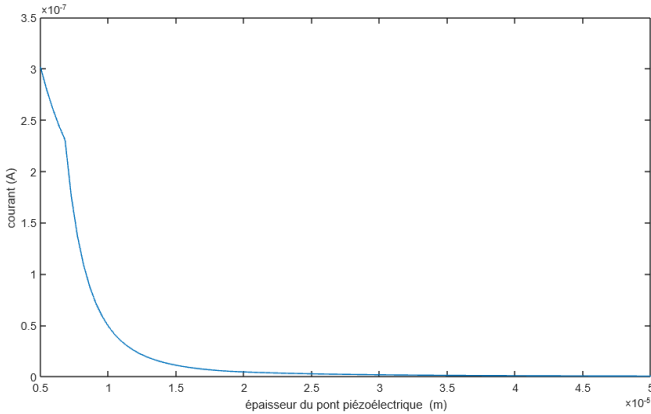
If we increase the thickness  $a_p$  of the piezoelectric bridge, we obtain a decrease in the current (figure 23) and the threshold voltage of the MOS (figure 24) but an increase in the vibration frequency (figure 25)

**Figure 23 ; courant of the MOS = f( Thickness of piezoelectric film ), start Interface = 200 A° with a choice  $F_{CO}/F_{CA} = 10$**

**Figure 24 ; Threshold of the MOS = f( Thickness of piezoelectric film ), start Interface = 200 A° with a choice  $F_{CO}/F_{CA} = 10$**

courant débité par la structure en fonction l'épaisseur pont piézoélectrique pour  $F_{CO}/F_{CA} = 10$

longueur pont piézoélectrique (m) =  $5e-05$  Epaisseur pont piézoélectrique (m) =  $1e-05$   
 longueur semelle Casimir (m) = 0.0002 épaisseur d'oxyde des grilles interrupteurs MOS (m) =  $2.5e-08$   
 épaisseur d'oxyde des grilles interrupteurs MOS (m) =  $2.5e-08$



tension de seuil des MOS en fonction épaisseur du pont piézoélectrique pour  $F_{CO}/F_{CA} = 10$

longueur pont piézoélectrique (m) =  $5e-05$  Epaisseur pont piézoélectrique (m) =  $1e-05$   
 longueur semelle Casimir (m) = 0.0002 épaisseur d'oxyde des grilles interrupteurs MOS (m) =  $2.5e-08$   
 épaisseur d'oxyde des grilles interrupteurs MOS (m) =  $2.5e-08$

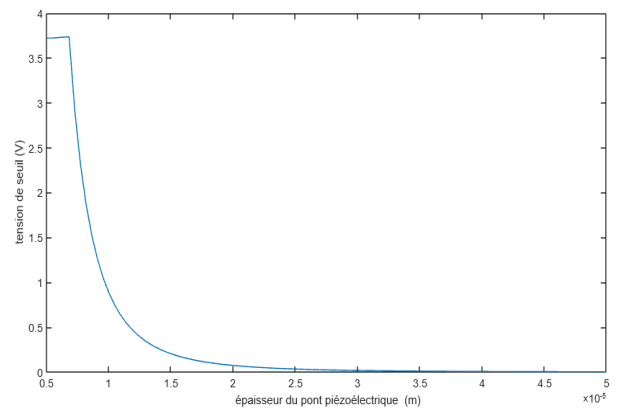
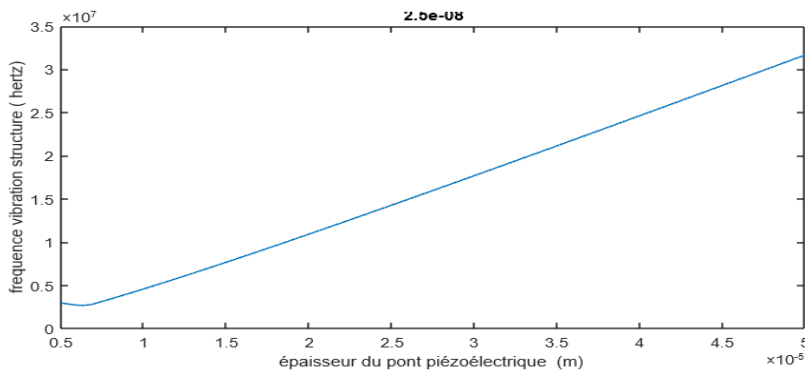


**Figure 25: Structure vibration frequency as a function of the thickness ap of the piezoelectric bridge, starting interface  $z_0$  to 200 A°, Ratio  $p = F_{CO} / F_{CA} = 10$**

fréquence vibration structure en fonction épaisseur pont piézoélectrique pour  $F_{CO}/F_{CA} = 10$

longueur pont piézoélectrique (m) =  $5e-05$  Epaisseur pont piézoélectrique (m) =  $1e-05$   
 longueur semelle Casimir (m) = 0.0002 épaisseur d'oxyde des grilles interrupteurs MOS (m) =  $2.5e-08$   
 épaisseur d'oxyde des grilles interrupteurs MOS (m) =  $2.5e-08$



**IV-1-7 / variation of the proportionality ratio  $p = F_{CO} / F_{CA}$ : PZT**

In a non-intuitive way, the current simply increases linearly by a factor of 40 (figure 26) if we increase the proportionality ratio  $p = F_{CO} / F_{CA}$  by a factor of 500. On the other hand, the threshold voltage of the MOS switches increases by a factor 8 for the same variation of the interface (figure 27). The MOS N or P switch transistors enriched in parallel have the following geometries: Width  $W = 4 \mu\text{m}$  and length  $L = 4 \mu\text{m}$

**Figure 26 ; current of the MOS = f( ratio = Fco/Fca ), start Interface = 200 A° piezoelectric material = PZT**

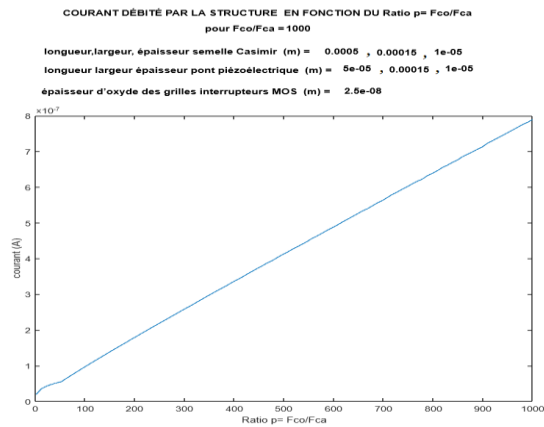
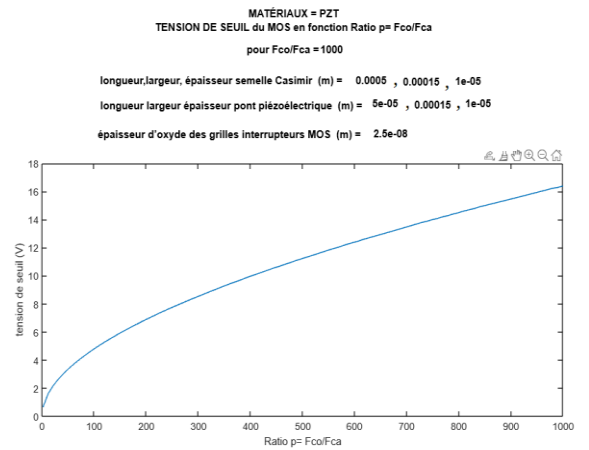


**Figure 27 ; Threshold voltage of the MOS = f( ratio = Fco/Fca ), start Interface = 200 A° piezoelectric material = PZT**



**IV-2 / USE OF OTHER PIEZOELECTRIC MATERIALS**

In the presentation above we used PZT but , in order to increase the density of electric charges at the terminals of the piezoelectric bridge, piezoelectric material PMN-PT can be used which can be deposited by RF-magnetron sputtering and of composition , for example : PMN-PT= (1-x) Pb (Mg1 / 3 - Nb1 / 3) O3-xPbTiO3;  $d_{31} = 1450 * 10^{-12} C / (kg * m * s^{-2})$  and a Young's modulus of  $E_p = 150 * 10^9$  (Figure 9).

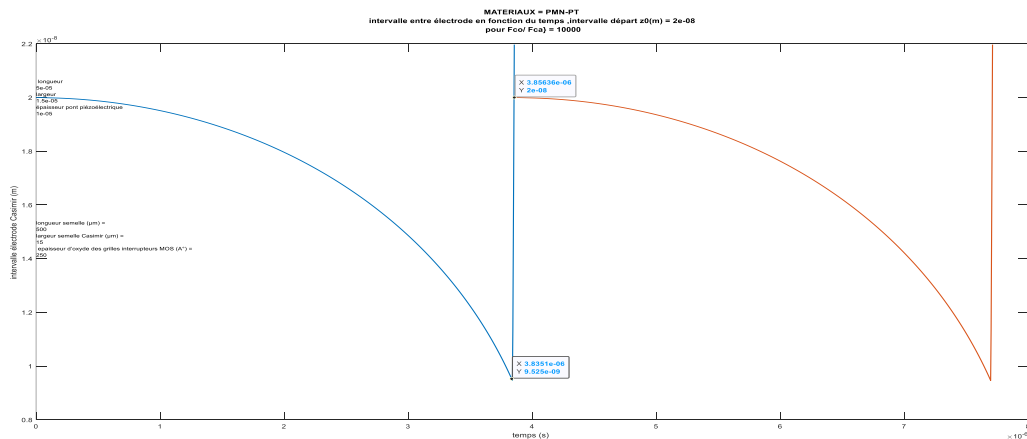
We will also simulate the results obtained with AlN (Aluminum nitride), another piezoelectric material or AlN widely used in microelectronics because it is easily removable and lead-free!

**IV-2-1 / Piezoelectric material = PMN-PT**

With the MATLAB simulation of a structure using PMN-Pt we obtain the evolution over time of the Casimir and Coulomb forces as well as the  $F_{CO} / F_{CA}$  ratio of figures 28 to 41 below. For a ratio of 1000, the maximum current delivered by the vibrating structure , the threshold voltage of the MOSE and MOSD and the vibration frequency of the structure are respectively:  $1.2 * 10^{-4} A$ ,  $V_t = 3.2 V$  and 957000 Hertz

**IV-2-1-1 / Evolution of the Casimir interface as a function of time during two periods: PMN-PT**

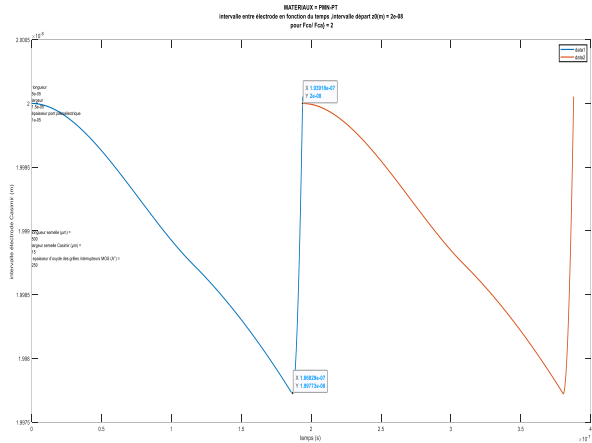
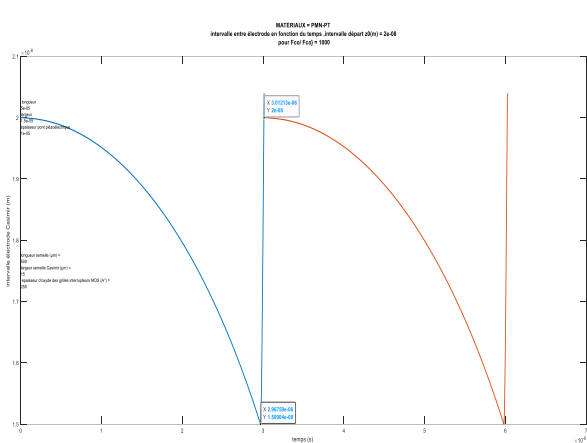
**Figure 28: plot of the evolution of the Casimir inter-electrode interval as a function of time over two periods and an Fco / Fca Ratio = 10000: Casimir inter-electrode interface = 200 A°**



The  $F_{CO} / F_{CA}$  ratio = 10000 induces a period of  $3.85 \cdot 10^{-6}$  s and a rise time of  $21.3 \cdot 10^{-9}$  s with a deflection of the bridge of  $105 \text{ A}^\circ$ . The structure vibrates at 259.7 kHz. At the rise sequence, the structure exceeds the initial  $200 \text{ A}^\circ$  by  $20 \text{ A}^\circ$  due to inertia (Fig 28).

**Figure 29: plot of the evolution of the Casimir inter-electrode interval as a function of time over two periods and an  $F_{CO} / F_{CA}$  Ratio = 1000: Casimir inter-electrode interface =  $200 \text{ A}^\circ$**

**Figure 30: plot of the evolution of the Casimir inter-electrode interval as a function of time over two periods and a Ratio  $F_{CO} / F_{CA} = 2$ . Casimir inter-electrode interface =  $200 \text{ A}^\circ$**



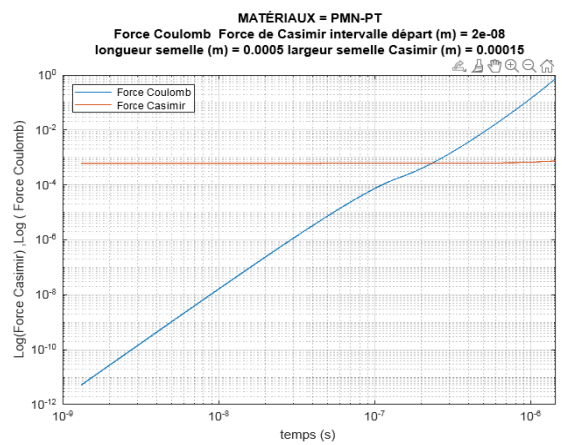
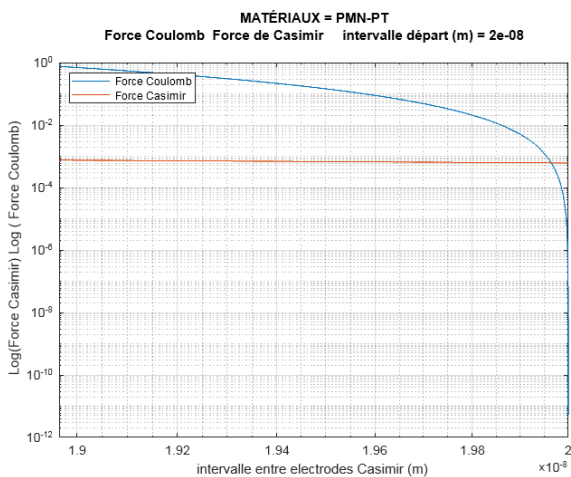
For  $p=1000$ , we notice a vibration amplitude of  $50 \text{ A}^\circ$  with a period of  $2.96 \cdot 10^{-6}$  s, with faster rise of the mobile electrode producing a slight rebound of  $5 \text{ A}^\circ$ , because of the inertia of the structure (Figure 29). For the ratio  $F_{CO} / F_{CA} = 2$  (figure 30) a vibration amplitude of just  $0.27 \text{ A}^\circ$  and a period of  $1.86 \cdot 10^{-7}$  s is obtained

This low deformation of the PMN-PT piezoelectric bridge is mainly due to the extremely high piezoelectric coefficient  $d_{31}$  of 1450 (pC/N) of PMN-PT compared to 120 (pC/N) for PZT (figures 9). It is also observed that weak overshoot of the initial interface ( $200 \text{ A}^\circ$ ) for the mobile electrode increases with the ratio ( $F_{CO} / F_{CA}$ )

**IV-2-1-2 / Evolution of the forces of Casimir and Coulomb: PMN-PT**

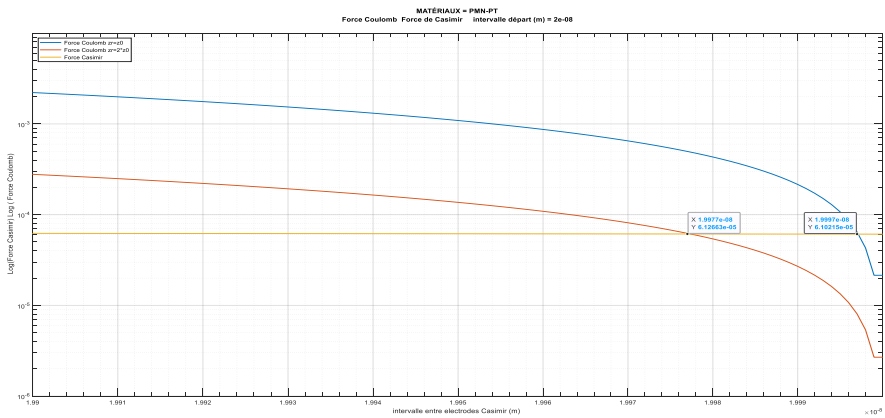
**Figure 31: Materials = PMN-PT: Coulomb and Casimir force as a function of the inter-electrode interface. Starting interface =  $200 \text{ A}^\circ$**

**Figure 32: Materials = PMN-PT: Coulomb and Casimir force as a function of time. Starting interface =  $200 \text{ A}^\circ$**



We obtain the evolution of the Casimir and Coulomb forces as a function of the inter-electrode interface (figure 31) and over time (figure 32) as well as the  $F_{CO} / F_{CA}$  ratio as a function of time for an entire period (figures 33)

Figure 32 b: Materials = PMN-PT: Coulomb force for  $z_r = 200 \text{ \AA}$  and  $z_r = 400 \text{ \AA}$  and Casimir force ( $z_0=200 \text{ \AA}$ ) as a function of the inter-electrode interface. Starting interface =  $200 \text{ \AA}$



$Z_0 = 200$  Angstroms (Blue)  
 $Z_r = 400$  Angstroms (red)

We observe (Figure 32 b) that the Coulomb return force becomes more important than the Casimir force even if the interval  $z_r = 400$  Angstroms between return electrodes is 2 times that between Casimir electrode  $z_0 = 200$  Angstroms.

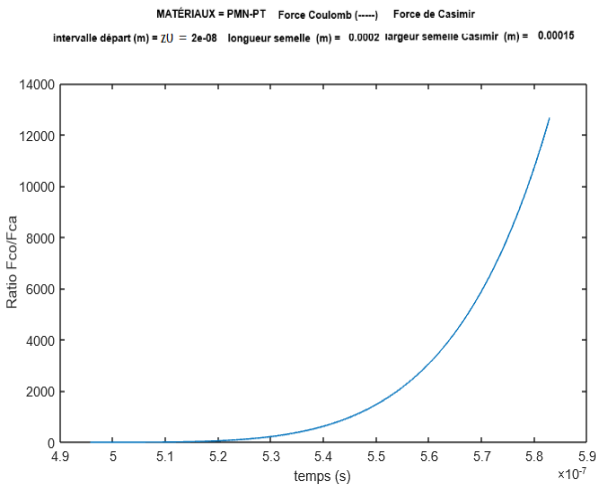


Figure 33: Materials = PMN-PT: Ratio  $p = F_{CO}/F_{CA}$  as a function of time. Starting interface =  $200 \text{ \AA}$

We observe the extremely rapid evolution towards a strong ratio above 10000.

IV-2-1-3 / Ratio as a function of Casimir interval and current peak as a function of the ratio: PMN-PT

Figure 34: Materials = PMN-PT: Coulomb Force / Casimir Force ratio as a function of the Casimir inter-electrode interface. Starting interface =  $200 \text{ \AA}$

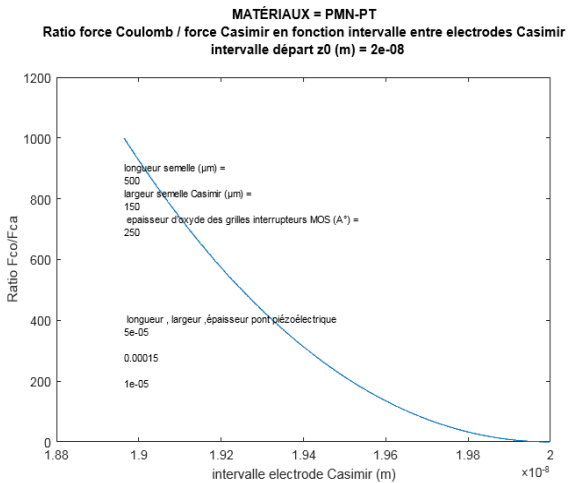
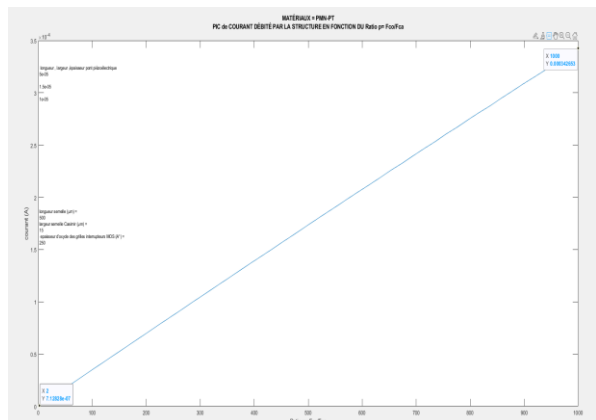


Figure 35: Materials = PMN-PT: Peak Current delivered by the structure as a function of the  $F_{CO} / F_{CA}$  Ratio. Starting interface =  $200 \text{ \AA}$



We observe (Fig 34 and 35) that for PMN-PT a deflection of  $10 \text{ A}^\circ$  and a length of the piezoelectric bridge of  $150 \mu\text{m}$  of the mobile Casimir electrode is sufficient to have an  $F_{co} / F_{ca} = 1000$ . A Ratio of 2 gives a peak current of  $7 \cdot 10^{-7} \text{ A}$ , while a ratio of 1000 produces a peak current of about  $3.5 \cdot 10^{-4} \text{ A}$  (Fig 35) for the same period of homogenization of the charges of about  $10^{-9} \text{ s}$ !

**IV-2-1-4 / peak current as a function of time and peak voltage across the coil for 2 periods: PMN-PT**

The following figures illustrate the current peak generated by the automatic vibrating structure with an inserted magnification showing the shape of this peak as a function of time (figure 36) and its exponentially decrease during about  $10^{-9} \text{ s}$ . This current of about  $3.5 \cdot 10^{-4} \text{ A}$  flowing through an inductor  $L_{IN}$  of  $4 \cdot 10^{-5} \text{ Henri}$  naturally generates a voltage of 4 Volts (figure 37)

**Figure 36: Materials = PMN-PT: Current peak as a function of time obtained over 2 cycles. Starting interface =  $200 \text{ A}^\circ$  Ratio  $p=F_{co} / F_{ca}=1000$**

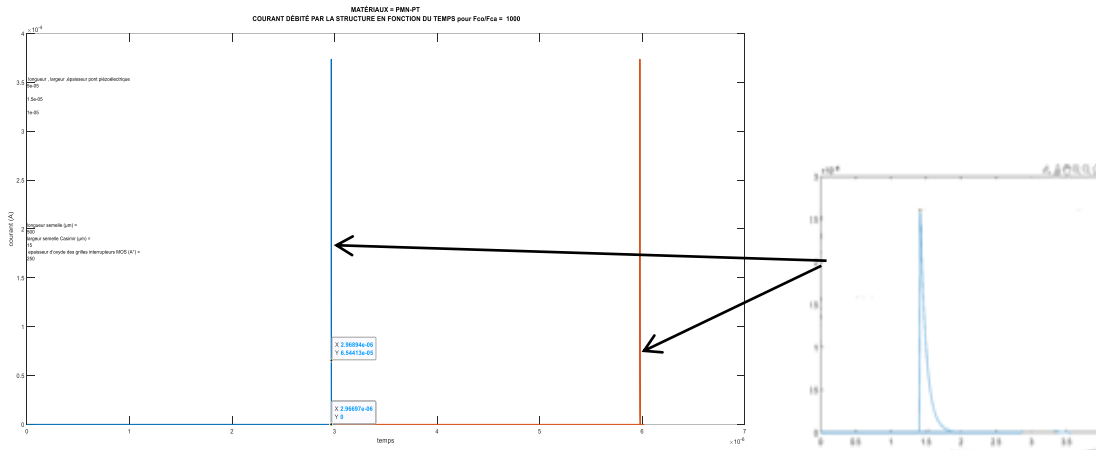
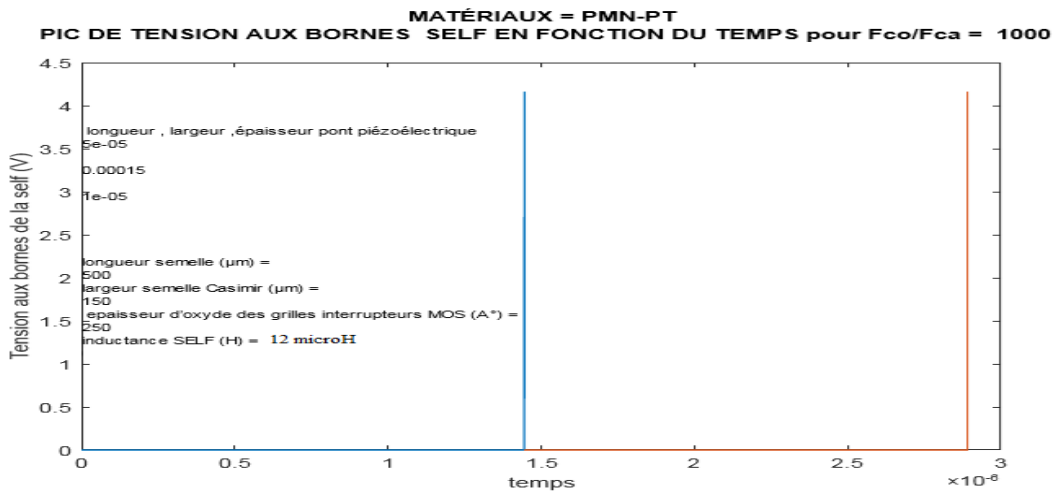


**Figure 37: Materials = PMN-PT: Voltage peak across the  $4 \cdot 10^{-5} \text{ H}$  solenoid as a function of the time obtained over 2 cycles. Starting interface =  $200 \text{ A}^\circ$ , Ratio  $p=F_{co} / F_{ca}=1000$**



The current peak that appears with each cycle of vibration is due to the homogenization of the electrical charges on the two parts of the return electrode. This current peak follows the equation

$$I_{IN} = -\frac{Q_{mn2}}{R_m * C_s} * \left| \text{Exp}\left(-\frac{t}{R_m * C_s}\right) \right|$$

with  $Q_{mn2} = d_{31} \cdot l_p \cdot F_{CA} / (2 * a_p)$ .

This charge transferred from the electrode on face 1 of the piezoelectric bridge to the return electrode which is initially grounded does not depend on the common width  $b_p = b_s = b_i$  of the structures.



This point is important and facilitates the technological realization of these structures since it limits the difficulties of a deep and straight engraving of the different structures.

On the other hand, the intensity of this current peak depends linearly on the lengths  $l_p$  and  $l_s$  of the structures. However, the duration  $t_e = R_m * C_s * \ln(2)$  of the exponential peak is independent of the geometries of the

structure, these only intervening in the frequency of vibration of the structure and in the intensity of the peak.

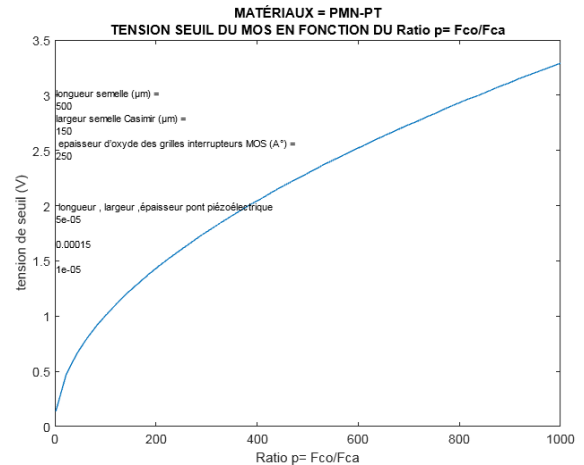
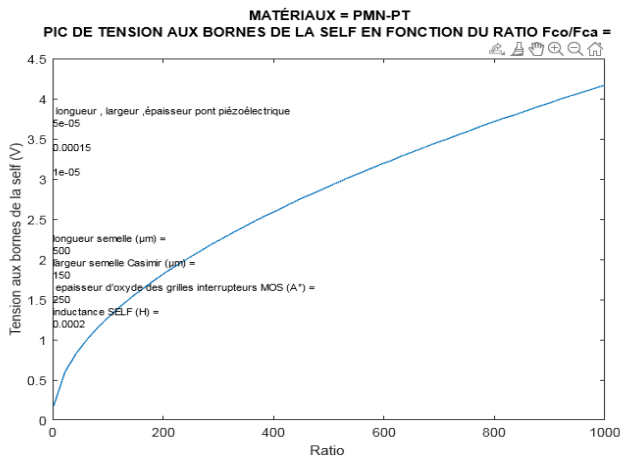
As this current peak cross an inductor it induces by itself a voltage peak  $U_{IN} = L_{IN} \frac{d(I_{IN})}{dt} = \frac{L_{IN}}{dt} (Q_{ms2})^2$

Note in Figure 36 the exponential form of the current peak of a duration appearing in each period. It is the same for the voltage peaks at the terminals of the coil (fig 37)

**IV-2-1-5 / peak voltage across the self and threshold voltage according to the desired FCO / FCA Ratio: PMN-PT**

**Figure 38: Materials = PMN-PT: Voltage peak across the  $4 * 10^{-5}$  H solenoid as a function of the  $F_{CO} / F_{CA}$  Ratio. Starting interface = 200A °**

**Figure 39: Materials = PMN-PT: Threshold voltage of the Enriched or Depleted MOTs according to the  $F_{CO} / F_{CA}$  Ratio. Start interface = 200A °**

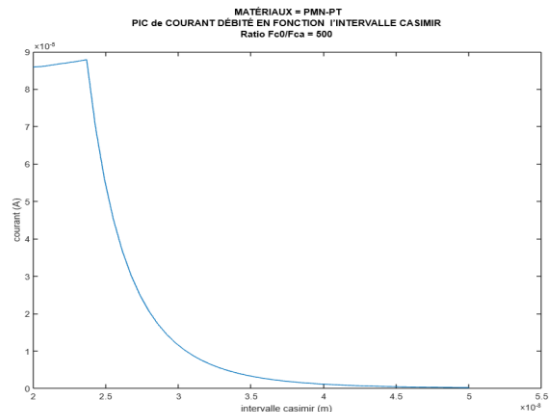
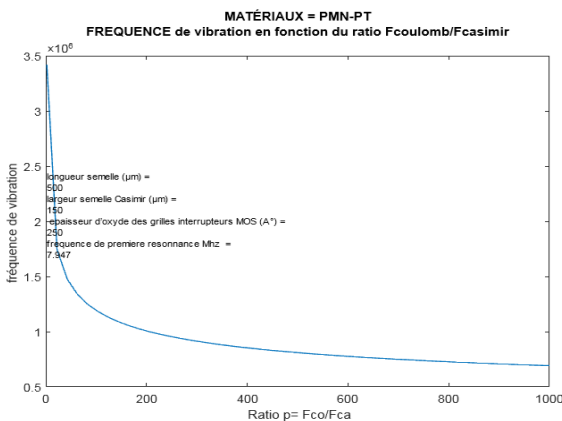


We observe (Fig 38) that the voltage peak obtained automatically and without any energy expenditure increases by a factor of 16 and goes from 0.25 V to 4 V when the ratio  $p = F_{CA} / F_{CO}$  increases from 2 to 1000. Likewise, the threshold voltage MOSE and MOSD authorizing these ratios increases from 0.2 V to 3.2 V (Fig 39).

**IV-2-1-6 / Vibration frequency as a function of the  $F_{CO} / F_{CA}$  ratio and peak current as a function of the initial Casimir interval chosen: PMN-PT.**

**Figure 40: Materials = PMN-PT: Vibration frequency as a function of the  $F_{CO} / F_{CA}$  Ratio. Starting interface = 200A °**

**Figure 41: Materials = PMN-PT: Current peak across the  $2 * 10^{-4}$  H choke as a function of the starting interval between Casimir electrodes. Starting interface = 200A °**





Note that (fig 40), for an initial interface  $z_0 = 200 \text{ \AA}$ , the maximum vibration frequency of the structure is 3.50 MHz for a ratio  $F_{CO} / F_{CA} = 2$  and that it fall to 750 kHz for a ratio of 1000. These frequencies remain lower than that of the first resonance of the structure which is the order of 7.94 Megahertz!

For an  $F_{CO} / F_{CA}$  ratio = 500, the maximum current delivered by the structure drops as a function of the initial Casimir interval (Fig 41).

This vibration frequency of the Casimir structure approaches that of the first resonance for weaker interfaces and less than  $200 \text{ \AA}$ . We are then unfortunately confronted with the technological possibility of mastering such a weak interface.

It seems that the piezoelectric material PMN-PT coupled with a conductor like aluminum is an interesting couple for our vacuum energy extraction structure!

### IV-2-2 / Piezoelectric material = AlN

With the MATLAB simulation of the behavior of the structure for piezoelectric Aluminum Nitride (AlN), we obtain the evolution with the time of the Casimir and Coulomb forces as well as the  $F_{CO} / F_{CA}$  ratio of figures 42 and 43 below. For a ratio  $F_{CO}/F_{CA}$  of 10, the maximum current delivered by the vibrating structure, the threshold voltage of the MOS and the vibration frequency of the structure is respectively  $1.85 \cdot 10^{-7} \text{ A}$ ,  $V_t = 3.7 \text{ V}$  and 667000 Hertz.

**Figure 42: Piezoelectric Material = AlN**  
Casimir , Coulomb Force = f( Time ) starts Interface =  $200 \text{ \AA}$

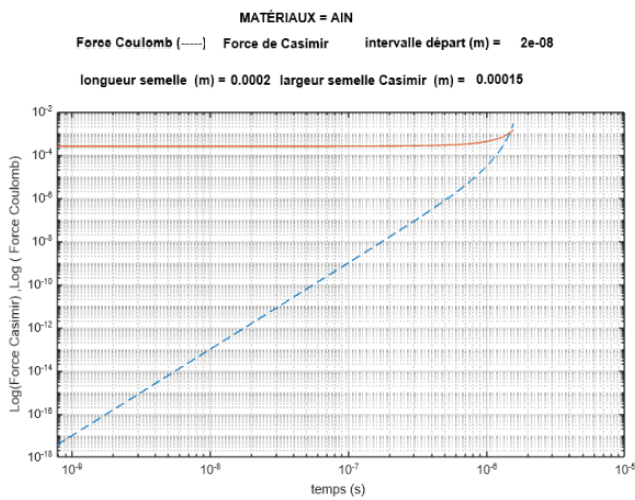


**Figure 43: Piezoelectric Material = AlN**  
Ratio  $F_{CO} / F_{CA} = f( \text{Time} )$  starts Interface =  $200 \text{ \AA}$

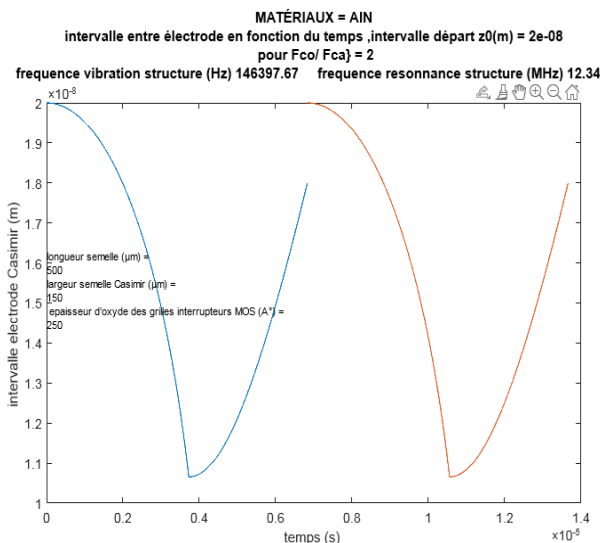
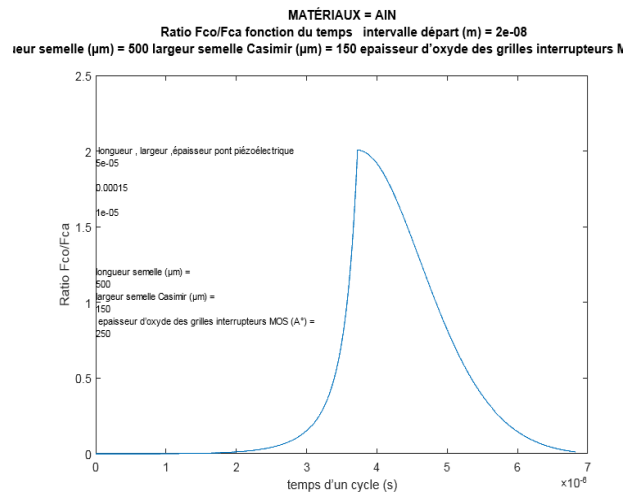


**Figure 44: Material = AlN Interval between Casimir electrodes = f( time) during two complete cycles: Interface between starting electrodes =  $200 \text{ \AA}$**

We observe (figure 42) that the ratio  $p = F_{CO} / F_{CA}$  barely equals 2 and that the time of "rise" of the mobile Casimir electrode is relatively slow (figure 44), a consequence of the low value of the piezoelectric coefficient  $d_{31}$  of AlN.

In conclusion, the use of AlN does not seem suitable for this vacuum energy extraction application.

### IV-3 / CONCLUSIONS

*It seems that for the piezoelectric material we used, the most suitable piezoelectric material for this vacuum energy extraction device is PMN-PT with a peak current of  $350\mu A$ , at least for the materials we used for the previous simulations (figures 28 to 41) .*

In order to convert these alternating current peaks into an alternating voltage without input of energy, this current passes through a  $L_{IN}$  inductor coil which converts these current peaks without input of external energy into voltage peaks of several volts and of a duration of the order of the nanosecond.

Inductors  $L_{IN}$  for printed circuits of the order of  $100\mu H$  or less are conventional and are commercially available.

The next chapter proposes to convert these peaks of alternating voltage, to amplify them to obtain a direct voltage of several volts without any external power supply!

### V / TRANSFORMATION AND AMPLIFICATION ELECTRONICS WITHOUT EXTERNAL SUPPLY OF A PERIODIC SIGNAL OF A FEW MILLIVOLTS IN A CONTINUOUS VOLTAGE OF A FEW VOLTS

Consider the diagram in Figure 5 which shows the location and configuration of the electronic circuits for collecting the current generated during a small fraction of the period of hypothetically self-sustaining vibrations of the structure.

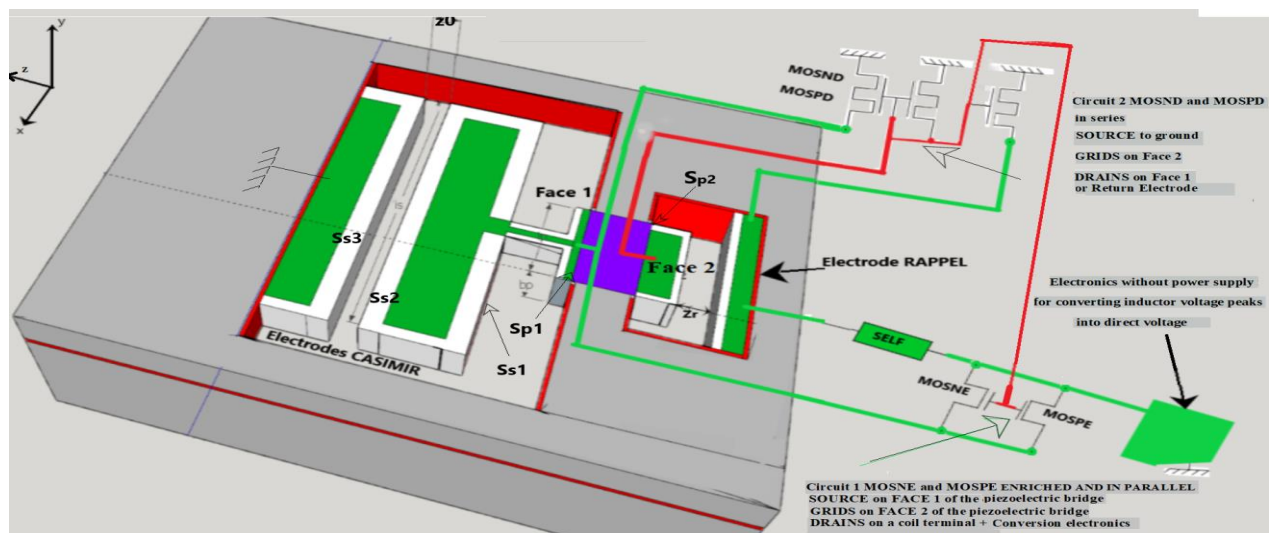


**Figure 5: Location of electronics and MOS in series and in parallel for shaping the signal deriving from a modulation of the mobile loads induced by the CASIMIR effect.**

The mobile charges  $Q_{mn}$  at the terminals of the electrode  $S_{S2}$  are variable over time since they vary cyclically from nul to  $Q_{mn} / 2$ . A part of these electrical charges , in the ratio of the input impedance between the inductor  $L_{IN}$  and that of the transformer electronics of this signal, generate during the short durations of their homogenization time , a peak of current which go inside this inductor and create between the two terminals of this solenoid , a voltage peak.

$$u = L_{IN} \frac{dI_{IN}}{dt} = L_{IN} \frac{d^2 Q_{MN}}{dt^2}$$

In figure 5, the gray and red surfaces are stationary, the others are free to move.

The green metallic connector connects face n°1 of the piezoelectric bridge  $Sp_2$  to the return electrode. The red metallic connector connects face n° 2 of the piezoelectric bridge to the MOS gates.

For circuit n° 1: The MOSE sources in // are connected to the metal electrode on face n°1 of the piezoelectric bridge. The MOSE drains are connected to the electronics without an external power supply for transforming the AC signal, and to a terminal of the  $L_{IN}$  solenoid . The other terminal of the self- $L_{IN}$  is connected to the return electrode or to ground via circuits n°2 if it is conductive. If the MOSD of circuit n°2 are blocked the fixed Casimir electrode is then non connected!

The enriched MOSNE and MOSPE of circuit n°1 then connect face 1 to the return electrode via the self  $L_{IN}$ , and this when their gates have a voltage making one of them ON. During this period the circuit composed of MOSND and MOSPD of circuit n°2 is then blocked.

Likewise, when circuit n°1 is blocked, then circuit n°2 is conducting and connects the return electrode to ground, which eliminates the charges present on this electrode and then prevents any electrostatic attraction.

We will describe these electronics designed and successfully tested at ESIEE with SPICE when I was studying abandoned sensors. This electronic gave very encouraging SPICE simulation results and was presented succinctly in various conferences but was never produced ... for lack of financial means!

In these SPICE simulations, the micro transformer was assimilated to a voltage source delivering a power  $U * I$  limited to a few nW (voltages of a few mV and current much lower than the microampere).

The  $L_{IN}$  self plays the same role as this micro transformer since it delivers a voltage during current variation generated during vibrations!

Now retired and no longer having sufficient means of simulations, I am simply describing the results of the SPICE simulations obtained in 2008. Because it seems that these electronics would correspond quite well to the modification without external energy of the alternating and small signals in an exploitable direct voltage.

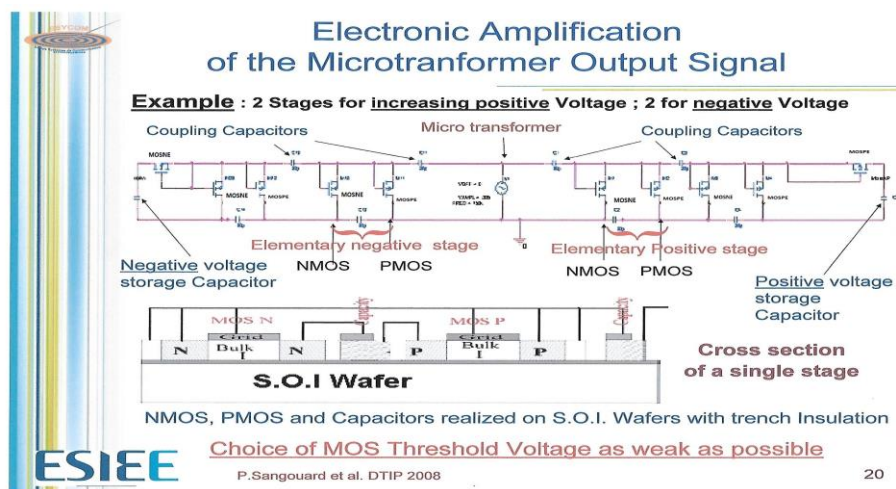
The principle used to amplify and transform a weak signal without power supply derives from that well known of the diode bridge rectifier of Graetz or the doubler of Schenkel and Marius Latour

The crippling problem with this type of rectifier is that the diodes of these rectifiers are conductive only with a minimum voltage of around 0.6 V at their terminals.

As the alternating signal from the vacuum energy extraction device can be weaker, it is necessary to have switches that are triggered with a lower control voltage and ideally zero.

The principle diagram of this electronics is presented in figure (45)

**figure 45 Principle of electronics for amplifying and rectifying a weak AC signal**



The MOSE N and P transistors of this rectifier circuit must have a technologically defined threshold voltage at **a value as close as possible to zero.**

The precision of nullity of these threshold voltages will depend on the values of alternating voltages at the terminals of the inductor  $L_{IN}$ , therefore on the second derivative of the temporal variations of the charges appearing on  $S_{p2}$  during the time of their homogenization which is of the order of  $t_e = R_m \cdot C_s \cdot \text{Log}(2)$

In this circuit of figure 45 the self  $L_{IN}$  was replaced by a micro transformer, but this self  $L_{IN}$  plays the same role as this micro transformer since it delivers a limited power  $U \cdot I$

The left part of the micro-transformer takes care of the negative voltages of the input signal, while the right part takes care of the positive voltages. The circuit is composed of several stages without no power supply which rectify and amplify, on the one hand the negative parts of the weak input signal and on the other hand the positive parts .

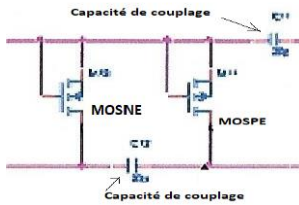


Figure 46 : Elementary stage for obtaining a negative voltage from the negative part of the alternative signal of the transformer ( coil)

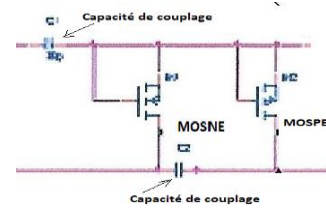
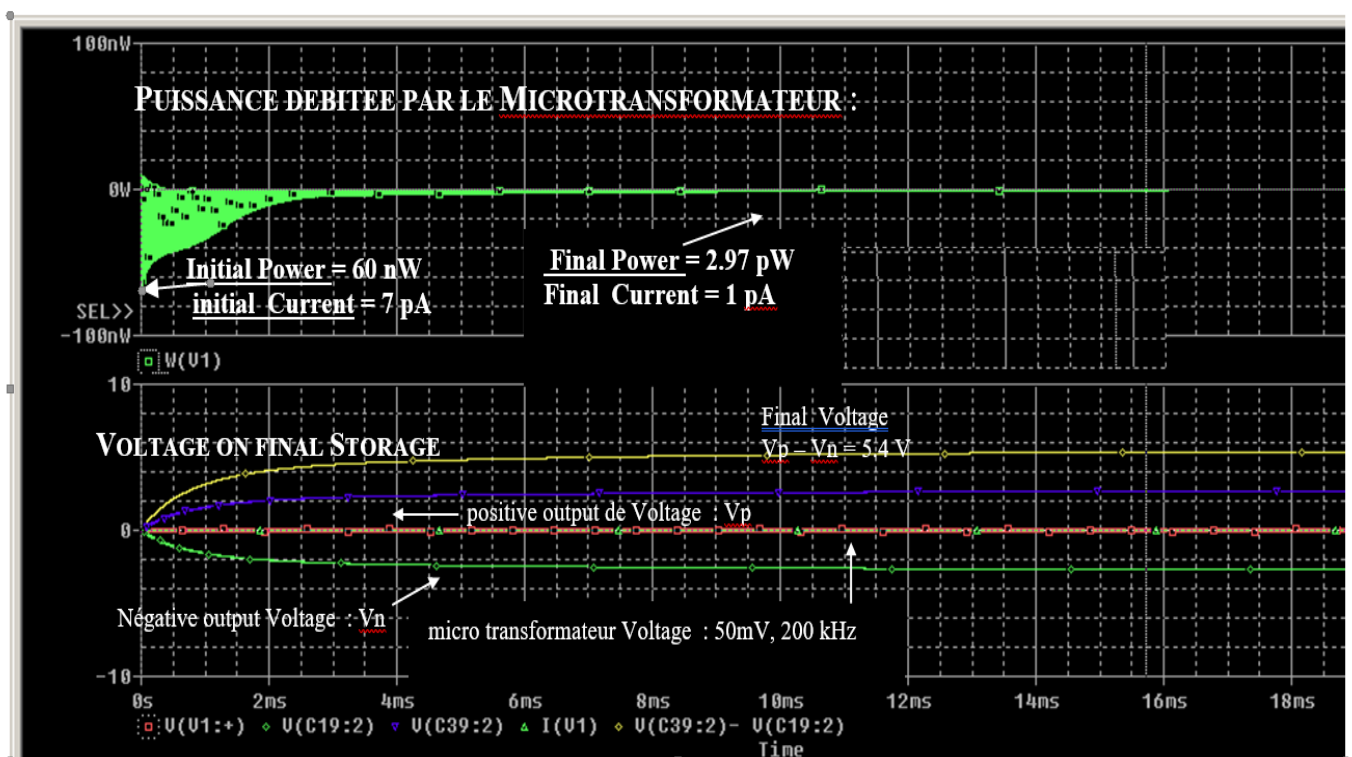


Figure 47 : Elementary stage for obtaining a positive voltage from the positive part of the alternative signal of the transformer ( coil)

The number of elementary stages depends on the desired DC voltage, but it saturates with the number of stages in series (figure 50). The results obtained from SPICE simulation are shown in figure 48.

Figure 48: SPICE simulations of voltages, current, power of the transformation electronics into a direct voltage (5.4 V) of an alternating input signal of 50 mV



In these SPICE simulations, the input signal is 50 mV at a frequency of 200 kHz, the number of stages is 14 (Fig. 48) for each positive or negative part.

The coupling and storage capacitances are 20 pF, and 2 nF.

The DC output voltage obtained is 5.4 V in less than 8 milliseconds!

We notice the extremely low power and current delivered by the power source (Micro transformer), as well as the fast stabilization of the outputs (on infinite impedances) since it takes less than 1 ms ! .

Initial current =  $7 \cdot 10^{-12} \text{ A}$ ,

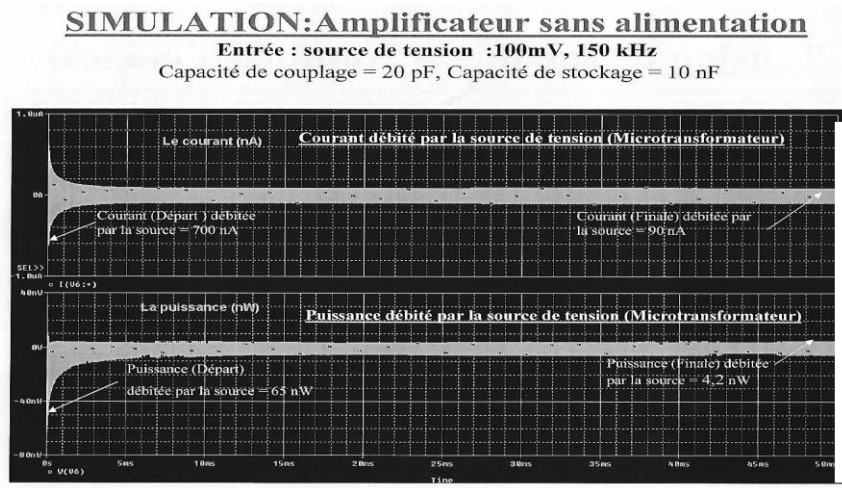
Final current = 1 pA

Initial power = 60 nWatt,

Final power = 2.97 pW



Figure 49: SPICE simulations of the currents drawn by the transformer and the power consumed by this transformer.



In these SPICE simulations, the input signal is 100 mV (Fig. 49) at a frequency of 150 kHz, the number of stages is 30 for each positive or negative part. The coupling and storage capacities are 20 pF and 10nF. The DC output voltage = 7.8 V is obtained in less than 7 milliseconds! Initial Current = 700 nA, Final current = 90nA Initial Power =65 nW , Final Power = 4.2 nW

An important point is (figure 48 and 49) the very low power and current consumption on the source since they are:

1 / in figure 46 respectively at the start of 60 nW and ends with a power delivered by the source of 2.97 pW for a current of input current of 7 pA and a final current of 1pA with an input signal of 50 mV at 150 KHz. The negative component of the alternating signal is transformed in 10 ns into a negative direct voltage of  $V_n = -2.7 V$ . Likewise the positive component transforms the positive alternating part into a positive direct voltage of  $V_p = 2.7 V$ . We obtain therefore a direct voltage  $V_p - V_n = V_t = 5.4 V$ .

2 / in figure 47 respectively at the start of 65 nW with a current consumption of 700 nA to end with a power consumed on the transformer of 4.2 nW with a current of 90 nA. The negative component of the alternating signal is transformed into 18 ms into a negative direct voltage of  $V_n = -3.9 V$ . Similarly, the positive component transforms the positive alternating part into a positive direct voltage of  $V_p = 3.9 V$ . We therefore obtain a direct voltage  $V_p - V_n = V_t = 7.8 V$ .

Another important point is the need to have a high circuit output impedance of several  $10^7$  ohms, so typically the input impedance of an operational amplifier.

The DC voltage obtained depends on the number of stages constituting these electronics for transforming an AC signal of a few millivolts into a DC signal of a few volts. However, this transformation saturates with the number of floors, as shown in figure 50.

Figure 50: DC output voltages as a function of the number of elementary stages for AC input voltages of 20 mV and the other of 100 mV

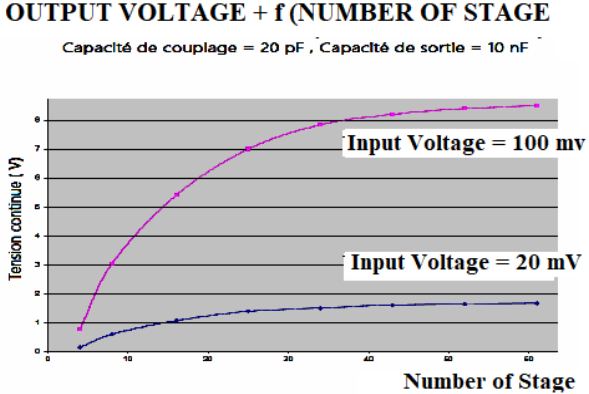
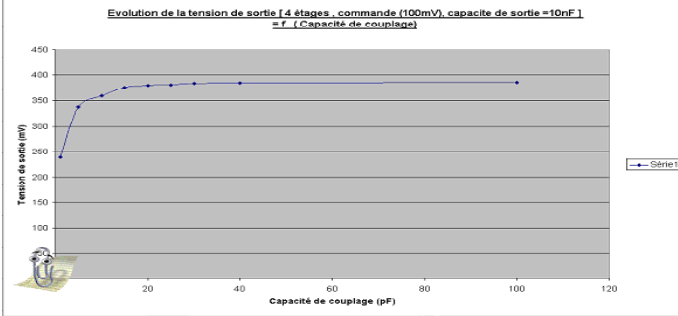


Figure 50: DC output voltages as a function of the number of elementary stages for AC input voltages of 20 mV and the other of 100 mV.

Note in Figure 50 that the DC output voltage saturates with the number of elementary stages and that the optimal number of stages is of the order of 40.

We also looked at the influence of the coupling capacitance on the amplification of an input signal of 100mV with a storage capacity of 10nF. This amplification saturates and a coupling capacity of 20 pF which seems to be optimal signal (figure 51)

**figure 51: influence of the coupling capacitance on the amplification of the input signal**

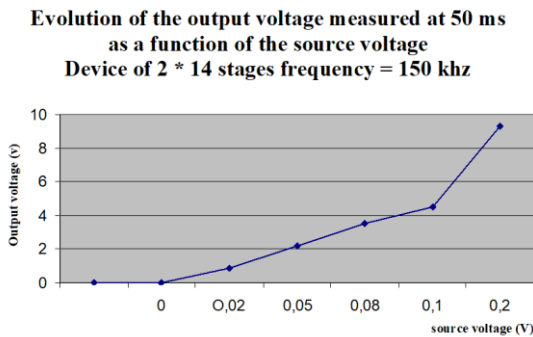


The following figure 51 shows the influence of the value of the coupling capacitance on the DC voltage obtained at the output of a 2 \* 4 stage device and an AC input voltage of 100 mV.

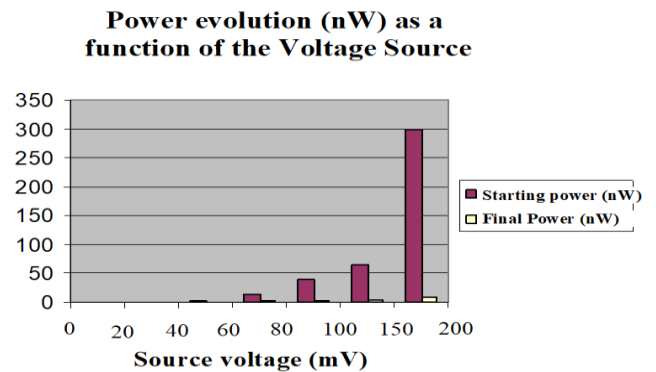
The following figure 52 shows the influence of the value of the input AC voltage, with a frequency of 150 kHz, on the DC voltage obtained at the output of a 2 \* 14 stage device.

Figure 53 shows the power in nW delivered by the source at the start of the amplification and at the end of this amplification.

**Figure 52 / Evolution of the DC output voltage as a function of the amplitude of the AC input signal for a frequency of 150 kHz**



**Figure 53 / Evolution of the power supplied in nW by the source as a function of the amplitude of the voltage supplied in mV.**



A summary of the performance of this low “voltage doubler” device is shown in Figure 54 below.

**CHARACTERISTICS OF OUTPUT VOLTAGES (V), POWERS (nW) CURRENTS (nA) AS A FUNCTION OF THE NUMBER OF STAGES INPUT SIGNAL FREQUENCY = 150 kHz OUTPUT VOLTAGE MEASUREMENT FOR t = 50 ms**

number of stages	Vg=50mV					Vg=100mV				
	Output Voltage	Current (nA) start	Current (nA) end	Power (nW) start	Power (nW) end	Output Voltage	Current (nA) start	Current (nA) end	Power (nW) start	Power (nW) end
2 *3	550mV	300nA	26nA	15nW	1.3nW	1.1v	800nA	46nA	75nW	5nW
2 *6	1	300nA	29nA	13nW	1.3nW	2V	700nA	67nA	60nW	6.5nW
2 *14	2.2v	300nA	40nA	14nW	2.6nW	4.5v	700nA	50nA	65nW	4.8nW
2 *21	2.8v	250nA	38nA	13nW	860pw	6v	600nA	80nA	60nW	2.7nW
2 *30	3.3	250nA	43nA	12nW	1.2nW	6.5V	750nA	85nA	61nW	4nW
2 *39	3.5v	250nA	45nA	12nW	900pW	7.5V	750nA	95nA	64nW	3.5nW
2 *48	3.6v	250nA	46nA	12nW	1nW	7.6V	750nA	100nA	60nW	4.2nW
2 *60	3.8	270nA	47nA	12nW	1.1 nW	7.9V	700nA	90nA	65nW	4.2nW
2 *61	3.8	270nA	48nA	12.1nW	1.3nW	8V	700nA	90nA	65nW	4.2nW

**Figure 54: Summary of the characteristics of the circuit for transforming a voltage of a few millivolts into a direct voltage of a few volts and without any power supply circuit.**

The interesting points for the presented electronic's device are:

- 1 / the low alternative input voltages required to obtain a continuous voltage of several volts at the output
- 2 / the low power and current consumed by this conversion and amplification circuit on the source which in this case is only an inductor supplied by the current peaks generated by the autonomous vibrations.
- 3 / the rapid time to reach the DC voltage (a few tens of milliseconds)

The technology used to fabricate the MOSNE and MOSPE transistors with the lowest possible threshold voltages is CMOS on intrinsic S.O.I. and wafer technology where the elements are isolated from each other on independent islands. This technology, represented in the following figure 55, strongly limits the leakage currents.

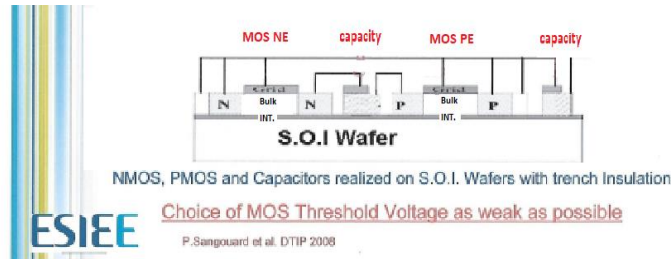


**Figure 55: S.O.I technology for making the elements of the “doubler”**

We note that the coupling capacities the order of 20 pF of this electronic, like that of storage of the order of 10 nF, have relatively high values which will require a square surface of 120  $\mu\text{m}$  for a thickness of 250  $\text{\AA}$ , if the use silicon oxides  $\text{SiO}_2$  with its relative permittivity of order of 4, which is a lot! Alumina  $\text{Al}_2\text{O}_3$  obtained by oxidizing aluminum has only a relative permittivity of the order of 9 and would require alumina squares of 79  $\mu\text{m}$ .

On the other hand, if one uses as insulator of the titanium dioxide which has a relative permittivity of the order of 100 and is one of the most important for a metal oxide then the size of the capacity passes to 23  $\mu\text{m}$  for a thickness of  $\text{TiO}_2 = 500 \text{\AA}$ , which is more reasonable!

## **VI / TECHNOLOGY OF REALIZATION OF THE CURRENT EXTRACTOR DEVICE USING THE FORCES OF CASIMIR IN A VACUUM**

It can be seen in Figures 21 and 22 that if PZT is used as the piezoelectric material, then the peak current output goes from  $2 \cdot 10^{-8} \text{A}$  to  $6 \cdot 10^{-8} \text{A}$ , when the width of the piezoelectric layer  $b_p$  changes from 50  $\mu\text{m}$  to 150  $\mu\text{m}$  and this for a length of the piezoelectric layer  $l_p = 50 \mu\text{m}$ , thickness  $a_p = 10 \mu\text{m}$ , a length of the Casimir sole  $l_s = 200 \mu\text{m}$ , starting interface  $z_0 = 200 \text{\AA}$  and a Ratio of  $F_{CO} / F_{CA} = 10$

As a result, it will be necessary, using micro-technology techniques on S.O.I silicon, to machine devices with a high thickness while maintaining exceedingly small spaces between structures Casimir. The microelectronics laboratory of the ESIEE has acquired a great experience in the plasma etching of deep submicron structures by etching remarkably parallel layers of silicon of 100  $\mu\text{m}$  separated by intervals of 0.8  $\mu\text{m}$  and well parallel [6, 7] and figure 56

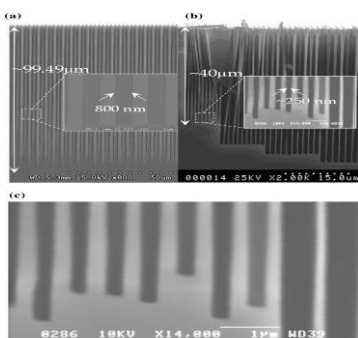


**Figure 56 extract de [7]**

High aspect ratio (HAR) structures manufactured using the Bosch process: (a) 800 nm-wide trenches with a depth of 99.5  $\mu\text{m}$  (aspect ratio 124:1) and (b) 250 nm-wide trenches with a depth of 40  $\mu\text{m}$  (aspect ratio 160:1).

Some of the walls collapsed during the dicing procedure.

© Is a magnified view of the inset shown in (b)

However, for the structures presented above, the space between the two surfaces of the reflectors must be of the order of  $200 \text{ \AA}$ , almost 4000 times less wide.... which is not technologically feasible by engraving!

*On the other hand, it seems possible, to be able to be obtained that this parallel space of the order of  $200 \text{ \AA}$  between Casimir reflectors, not by etching layers but by making them thermally grow!*

Indeed, the  $S_{S3}$  and  $S_{S2}$  surfaces of the Casimir reflector must on the one hand be metallic to conduct the mobile charges and on the other hand also insulating as stipulated by the expression of Casimir's law who established for surfaces without charges!

This should be possible if we grow an insulator on the z direction of the structure, for example  $\text{Al}_2\text{O}_3$  or  $\text{TiO}_2$  or another oxide metal which is previously deposited and in considering the differences in molar mass between the oxides and the original materials (see figure 31)!!

For example, silicon has a molar mass of  $28 \text{ g/mol}$  and silicon dioxide  $\text{SiO}_2$  has a molar mass of  $60 \text{ g/mol}$ . However, it is well known that when we grow a silicon dioxide  $\text{SiO}_2$  of one unit we "attack" a silicon depth of the order of  $28/60 = 46.6\%$  (figure 57)

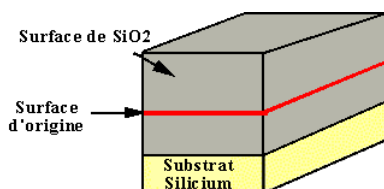


**Figure 57: Growth of  $\text{SiO}_2$  oxide on silicon**

The initial silicon layer reacts with the oxidizing element to form  $\text{SiO}_2$ . We will thus "consume" Silicon. The Si/ $\text{SiO}_2$  interface will therefore end up "below" the initial surface.

A simple calculation shows that the fraction of oxide thickness "below" the initial surface is 46% of the total oxide thickness; the fraction "above" therefore represents 54% according to S.M. Sze. We therefore moved the original silicon surface by 46%.

The same must happen, for example for thermal growth of alumina. As the molecular masses of Alumina and Aluminum are  $M_{\text{Al}_2\text{O}_3} = 102 \text{ g/mole}$  and  $M_{\text{Al}} = 27 \text{ g/mole}$ , we obtain an aluminum attack ratio of  $27/102 = 26\%$ , which implies that the original surface of this metal has shifted by 26% so that 74% of the alumina has grown out of the initial surface of the aluminum....

Likewise, if titanium is used for thermal growth of  $\text{TiO}_2$ , the molar mass ratio being  $M_{\text{TiO}_2} = 79.9 \text{ g/mole}$  and  $M_{\text{Ti}} = 47.8 \text{ g/mole}$  we obtain a titanium attack ratio of 59.8% which implies that the original surface has moved by 59.8%.

So, this growth covers up the initial interface and it can be finely controlled! As a result, it should be possible to define finely the interface between the two Casimir reflectors using the oxidative growth conditions of a metal such as titanium or aluminum.

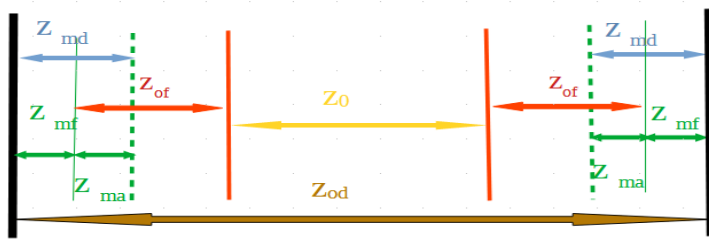
As regards the technological manufacture of electronics and structure, it therefore seems preferable:

1 / for electronics to choose Titanium Oxide because of its high relative permittivity  $\epsilon_r$  ( $80 < \epsilon_r < 160$ ) allowing to minimize the geometries required for the different capacities

2 / For the Casimir structure, the choice of aluminum seems preferable, because its low density increases the resonant frequency of the structure and 74% of the Alumina is outside the metal

A quite simple calculation shows for example that for aluminum shows that:





**Metal Thickness at the start** =  $z_{md}$   
**Final Oxide Thickness** =  $z_{of}$   
**Final Metal Thickness** =  $z_{mf}$   
**Attacked Final Metal** =  $z_{ma}$   
**Final interface between electrodes** =  $z_0$   
**Start Opening Interval** =  $z_{od}$

**Figure 58 DISTRIBUTION OF THICKNESSES**

We obtain:  $z_{od} = 2 * (z_{md} + z_{of} - z_{ma}) + z_0 = 2 * (z_{md} + z_{of} (1 - 0.26)) + z_0$

For example, if we start from an opening  $z_{od} = 3 \mu m$  and deposit a metal layer of aluminum that is etched leaving a width  $z_{md} = 1 \mu m$  on each side of the reflector. Then an Alumina  $Al_2O_3$  can grow, the thickness of which is precisely adjusted, simply by considerations of time, temperature, and pressure to increase a necessary thickness in order to have a desired interface  $z_0$ !

For example, if  $z_0 = 200 \text{ \AA}$ ,  $z_{od} = 3 \mu m$ ,  $z_{md} = 1 \mu m$ , then  $z_{of} = (z_{od} - z_0 - 2 * z_{md}) / (2 * (1 - 0.26)) = 0.662 \mu m$ . So, we obtain a Casimir interface of  $200 \text{ \AA}$ , the final remaining metal thickness will be  $x_{mf} = 1 - 0.662 = 0.338 \mu m$  and will act as a conductor under the aluminum oxide.

Obviously, the growth of this metal oxide between the electrodes of the Casimir reflector modifies the composition of the dielectric present between these electrodes, therefore of the mean relative permittivity of the dielectric.

Let:  $\epsilon_0$  be the permittivity of vacuum and  $\epsilon_0 \cdot \epsilon_r$  the one of the metal oxides ( $\epsilon_r$  = relative permittivity = 8 in the case of  $Al_2O_3$ ),  $z_{of}$  the final oxide thickness on one of the electrodes and  $z$  the thickness of the vacuum present between electrode, (initially we want  $z = z_0$ ).

Métal	$z_{of}, \epsilon_r$ metal Oxide	$z, \epsilon_0$ Vacuum	$z_{of}, \epsilon_r$ Metal oxide	Métal
-------	--	---------------------------	--	-------

Then the average permittivity  $\epsilon_{0m}$  of the dielectric is:  
 $\epsilon_{0m} = (z_{of} \cdot \epsilon_0 \cdot \epsilon_r + z \cdot \epsilon_0 + z_{of} \cdot \epsilon_0 \cdot \epsilon_r) / (2 \cdot z_{of} + z)$   
 $\epsilon_{0m} = \epsilon_0 \cdot (2 \cdot z_{of} \cdot \epsilon_r + z) / (2 \cdot z_{of} + z) \approx \epsilon_0 \cdot \epsilon_r$  because  $z$  is  $\ll z_{of}$ !!

For example,  $z_{of} = 6620 \text{ \AA}$  is large compared to  $z \leq 200 \text{ \AA}$  therefore  $\epsilon_{0m} \approx 8 * \epsilon_0$  in the case of  $Al_2O_3$ .

We have taken this change in permittivity into account in the preceding simulations.

## VII / STEPS FOR THE REALIZATION OF THE STRUCTURE AND ITS ELECTRONICS

We start by the voltage “doubler”. These electronics are produced using CMOS technology with 8 ion implantations on an S.O.I wafer with an intrinsic silicon layer above the oxide:

- 1 / To make the drains, sources of the MOSNE, MOSND of the "doubler" circuits, of the MOSNE and MOSND of the Coulomb force trigger circuit and of the grounding switches of the  $S_{S3}$  electrode of the Casimir reflector
- 2 / To make the source drains of the MOSPE, MOSPD of the "doubler" circuits, of the MOSPEs and MOSPDs of the Coulomb force trigger circuit and the grounding switches of the  $S_{S3}$  electrode of the Casimir reflector
- 3 / To best adjust the zero-threshold voltage of the MOSNE of the "doubler" circuit

4 / To best adjust the zero-threshold voltage of the MOSPE of the "doubler" circuit

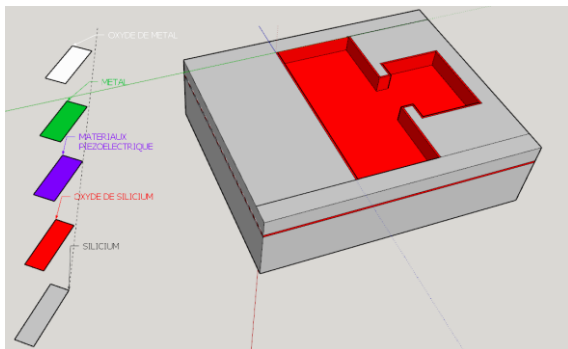
5 / To define the threshold voltage of the MOSNE of the parallel circuit triggering the Coulomb force

6 / To define the threshold voltage of the MOSPE of the parallel circuit triggering the Coulomb force

7 / To define the threshold voltage of the MOSND of the series circuit for grounding the  $S_{S3}$  electrode of the Casimir reflector

8 / to define the MOSPD threshold voltage of the series circuit for grounding the  $S_{S3}$  electrode of the Casimir reflector.

Once this electronics is done, we are interested in the realization of the structure of CASIMIR with the following technology proposal:



9 / Burn the S.O.I. silicon to the oxide to define the location of the Casimir structures (figure 59)

**Figure 59: etching of S.O.I silicon**

10/ Place and engrave a protective metal film on the rear faces of the S.O.I wafer (figure 60)

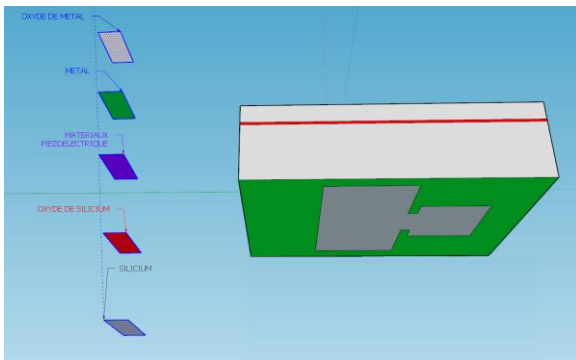


**Figure 60: Engraving of the protective metal rear face of the S.O.I.**

11 / Deposit and engrave the piezoelectric layer (figure 61)

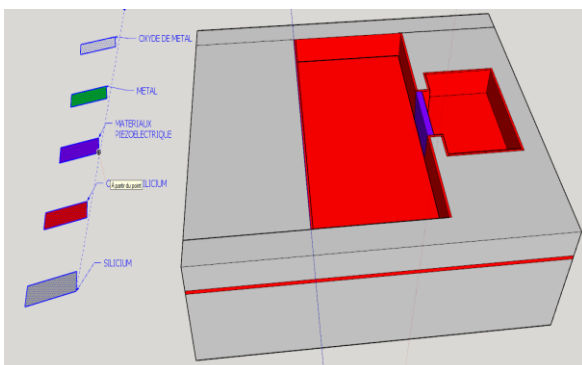
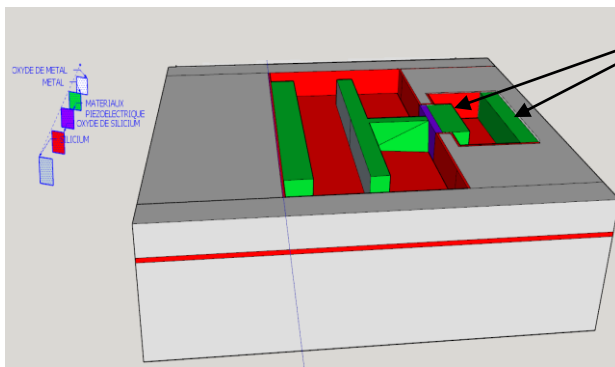


**Figure 61 deposition and etching of the piezoelectric layer**

12/ Depose and etch the metal layer of aluminum (figure 62) .



Coulomb Return electrodes

**Figure 62: Metal deposit, Metal engraving**

13 / Plasma etching on the rear side the silicon of the Bulk and the oxide of the S.O.I wafer protected by the metal film to free the Casimir structure then very finely clean both sides (figure 63)

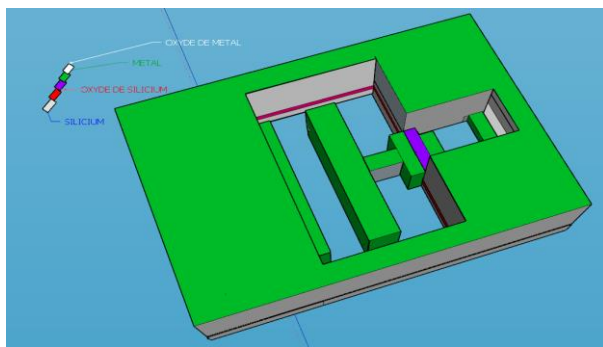


**Figure 63: view of the Casimir device on the rear face, engraving on the rear face of the structures.**

14 / Place the structure in a hermetic integrated circuit support box and carry out all the bonding necessary for the structure to function.

15 / Carry out the thermal growth of aluminum oxide  $Al_2O_3$  with a measurement and control of the circuit under a box which should generate a signal when the interface between the Casimir electrodes becomes weak enough for the device to vibrate ... and then stop the oxidation. (Figure 64)

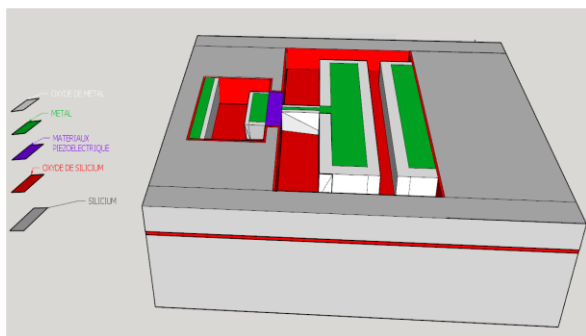


**Figure 64: Adjusted growth of metal oxide under the electronic control, front view of the Casimir device**

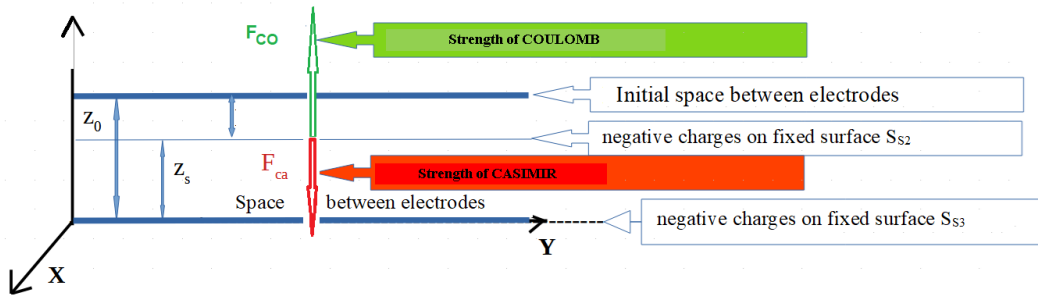
16 / Create a vacuum in the hermetic box

In the case where the 2 metal electrodes of Casimir which are separated by a very weak interface of the order of  $200 \text{ \AA}$  adhere to one another, then these two surfaces can be separated by the application of a electrical voltage on the electrodes on the other side of the piezoelectric bridge (see Fig 82) !

## VIII/ ENERGY BALANCE

Perform an energy balance during a vibration cycle

Figure 15: Axis, Force, CASIMIR reflector electrodes.



$$F_{ca} = S \left( \frac{\pi^2 \hbar c}{240 z_s^4} \right) \quad (1)$$

The force of Casimir related to the vacuum is:

This force attracts the mobile electrode which deforms a piezoelectric bridge, thus naturally creating fixed charges QF within this structure. These fixed charges change according to equation (5)

$$Q_F = \frac{d_{31} E_{CALP}}{a_P}$$

These fixed charges attract moving charges from the mass which trigger MOSE and MOSD switches. Passing through the source drain space of one of the MOSE transistors, they are distributed uniformly over the two Casimir S<sub>S2</sub> and S<sub>S3</sub> electrodes which therefore each have a mobile charge Q<sub>mn</sub> / 2.

A Coulomb force then appears between these two electrodes.

$$F_{CO} = \left| l_s b_s \frac{\pi^2 \hbar c}{240} * \frac{d_{31} l_P}{a_P} \right|^2 * \frac{1}{16 \pi \epsilon_0 \epsilon_r} \frac{1}{z_s} \left( \frac{1}{(z_r + z_0 - z_s)^2} - \frac{1}{(z_r)^2} \right)$$

The position z<sub>e</sub> of appearance of this force is such that F<sub>CO</sub> = p F<sub>CA</sub>, so if we choose z<sub>r</sub> = z<sub>0</sub>

Then, the z<sub>e</sub> position of appearance of this force is: 
$$\left| l_s b_s \frac{\pi^2 \hbar c}{240} * \frac{d_{31} l_P}{a_P} \right|^2 * \frac{1}{16 \pi \epsilon_0 \epsilon_r} \frac{1}{z_e} \left( \frac{1}{(2z_0 - z_e)^2} - \frac{1}{(z_0)^2} \right) = p * l_s b_s \frac{\pi^2 \hbar c}{240} \frac{1}{z_e} \quad (18)$$

This position z<sub>e</sub> is illustrated in the following figures 65 and 66

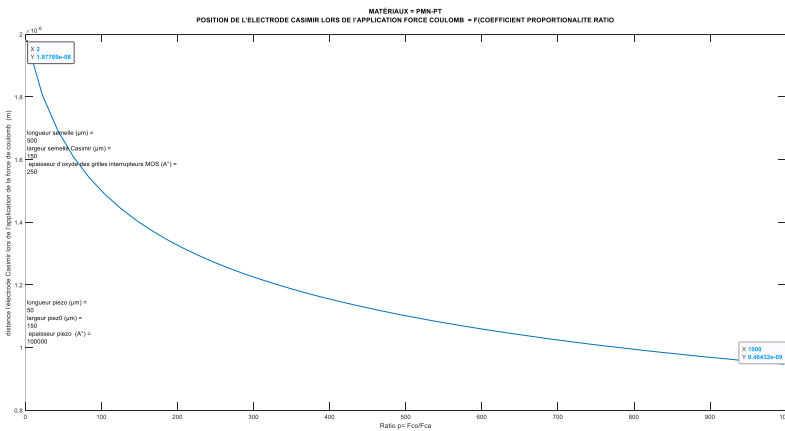


**Fig. 65: Position of the mobile Casimir electrode when the Coulomb force occurs**  $l_s = 500 \mu\text{m}$   $b_s = 150 \mu\text{m}$   $l_p = 50 \mu\text{m}$   $b_p = 150 \mu\text{m}$   $a_p = 10 \mu\text{m}$

As a result, the movement of the movable electrode shown in Figure 65

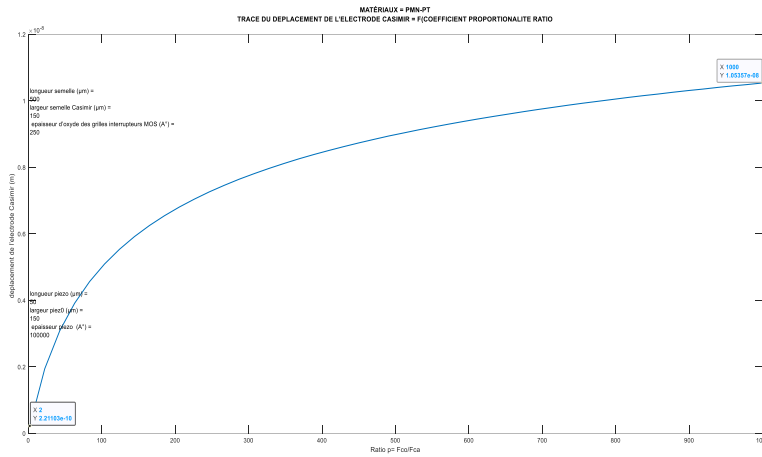


**Fig 66: Displacement of the mobile Casimir electrode during the appearance of the Coulomb force**  $l_s = 500 \mu\text{m}$   $b_s = 150 \mu\text{m}$   $l_p = 50 \mu\text{m}$   $b_p = 150 \mu\text{m}$   $a_p = 10 \mu\text{m}$

Note that the displacement of this mobile Casimir electrode is extremely small since it goes from  $2 \text{ A}^\circ$  for an  $F_{CO} / F_{CA}$  ratio = 2 to  $105 \text{ A}^\circ$  for a ratio of 1000.

When moving "went" of the position (1), to the position (2)  $z_e$ , the energy associated with this movement is provided by the Casimir force, it is the only active:

$$E_{12} = \int_{z_0}^{z_e} F_{CA} dz = l_s * b_s * \left( \frac{\pi^2 \hbar c}{720} \right) * \left( \frac{1}{z_e^3} - \frac{1}{z_0^3} \right)$$

As we have seen previously, this energy linked to the Casimir force makes it possible to infer vibrations of the structure but also current peaks  $I_{IN}$  which in turn induce voltage peaks  $U_{IN}$  at the terminals of an inductor.

We have;

$$t_e = R_m * C_s * \ln(2) \quad (4) \quad \text{= duration of current and voltage peaks}$$

$$I_{IN} = -\frac{Q_{mn2}}{R_m * C_s} * \left[ \text{Exp}\left(-\frac{t}{R_m * C_s}\right) \right] \quad (5) = \text{Current peak}$$

$$U_{IN} = \frac{L_{IN} Q_{mn2}}{(R_m C_s)^2} \exp\left(\frac{-t}{R_m C_s}\right) = \frac{L_{IN} Q_{mn2} \ln^2(2)}{(t_e)^2} \exp\left(\frac{-t \ln(2)}{t_e}\right) \quad (6) = \text{voltage peaks at the terminals of the LIN coil}$$

The Energy associated with these current and voltage peaks is therefore:

$$dW_{electric} = I_{IN} U_{IN} dt \Rightarrow W_{electric} = Abs\left(\int_0^{t_e} I_{IN} U_{IN} d(t)\right) = L_{IN} \left(\frac{d_{31} F_{Ca} L_P}{2 a_P}\right)^2 \left(\frac{\ln(2)}{t_e}\right)^3 \int_0^{t_e} \exp\left(\frac{-2 \ln(2) t}{t_e}\right) d(t) \text{ then}$$

$$W_{electric} = \frac{L_{IN}}{2} \left(\frac{d_{31} F_{Ca} L_P}{a_P}\right)^2 \left(\frac{\ln(2)}{t_e}\right)^2 \left[1 - \exp(-2 * \ln(2))\right] \quad (19)$$

When "returning" from position (2) to position (1), if we choose  $z_r = z_0$ , the energy associated with the Coulomb force is then:

$$E_{Coulomb} = E_{Coulomb} = \left| l_s b_s \frac{\pi^2 \hbar c}{240} \frac{d_{31} L_P}{a_P} \right|^2 \frac{1}{16 \pi \epsilon_0 \epsilon_r} \int_0^{z_e} \frac{1}{z} \left[ \frac{1}{(2z_0 - z)^2} - \frac{1}{(z_0)^2} \right] d(z)$$

Integrating this equation gives  $E_{12} + E_{21} = E_{Coulomb}$

$$E_{Coulomb} = \left| l_s b_s \frac{\pi^2 \hbar c}{240} \frac{d_{31} L_P}{a_P} \right|^2 * \frac{1}{16 \pi \epsilon_0 \epsilon_r} * \left[ \frac{1}{64 z_0} \ln\left(\left|\frac{z}{2z_0 - z}\right|\right) - \frac{105 z^6 (z - z_0) - 70 z^2 z^4 (z - z_0) - 84 z^4 z^3 - 112 z^5 z^2 - 640 z^6 z + 720 z^0}{3360 z^0 z (z - 2z_0)} \right]_{z_0}^{z_e} \quad (20)$$

For example for  $z_0 = 200 \text{ A}^\circ$ , dimensions of the Casimir electrodes (length =  $500 \mu\text{m}$ , width =  $15 \mu\text{m}$ , thickness =  $10 \mu\text{m}$ ), dimensions of the piezoelectric bridge in PMN-PT (length =  $50 \mu\text{m}$ , width =  $15 \mu\text{m}$ , thickness =  $10 \mu\text{m}$ ), a proportionality factor  $p = F_{CO} / F_{CA} = 1000$ , a coil  $L_{IN} = 1 * 10^{-6} \text{ H}$ , we obtain:

- $Z_e = 9.46 \cdot 10^{-09}$  (m) i.e., a displacement of the mobile Casimir electrode of about  $105\text{\AA}$  (fig 64)
- $E_{12} = E_{\text{Casimir}} = 3.4 \cdot 10^{-11}$  (Joule) = Energy of Casimir expended by the vacuum.
- $E_{12} + E_{21} = E_{\text{Coulomb}} = 1.49\text{e-}8$  (Joule) = Energy of the Coulomb force.
- Peak current =  $350 \cdot 10^{-6}$  A
- Voltage peak across the coil = 1.2 V
- Structure vibration frequency = 750 kHz
- $W_{\text{electric}} = 2.7 \cdot 10^{-11}$  (Joule) = Usable energy associated with current and voltage peaks.

This energy is not brought by an external electrical source but is caused by the omnipresent and perpetual force of Casimir, itself controlled by a Coulomb force of opposite direction.

This Coulomb force appears by the automatic switching of MOS transistors when its intensity is greater than a predetermined value and opposite to that of the Casimir force.

This technologically programmable switching of the MOS switches induces the spontaneous appearance of current peaks of a few nanoseconds, themselves inducing voltage peaks at the terminals of an inductor. When the system returns to its starting position, the Coulomb force disappears, leaving the Casimir force to deform the structure again! The system then spontaneously enters into vibrations!

We observe that the usable energy =  $W_{\text{electric}}$  is less than  $E_{\text{Casimir}}$ . The energy balance of a cycle therefore seems to satisfy Emmy NOTHER's theorem!

## IX / CONCLUSIONS

1 / the proposal to use isotropic and perpetual energy of Casimir called Energy of the vacuum, to obtain a variation of electric charges of a piezoelectric bridge which generates current peaks at the frequency of self-sustaining vibrations of the structure, usable without no energy input

2 / the system which should allow the conversion of this vacuum energy into alternating current peaks at the vibration frequency of the system. This current passes through an inductor which converts these alternating current peaks into alternating voltage peaks.

3 / The current and the voltage at the terminals of this choke feed electronics which rectifies and amplifies, without any external power supply, these voltage peaks in a direct voltage of a few usable volts.

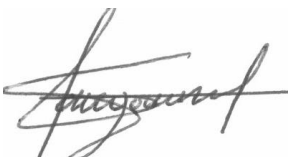
4 / a proposal for micro and nano electronic technology giving hope for a possible realization of this set.

According to this study, it would seem that **unless we are mistaken** we can extract energy from the vacuum by the use of the Casimir force thwarted at the appropriate time by a temporary Coulomb force which makes the system return to its initial position and makes enter into vibrations the structure!!

I am fully aware that this concept may sound like a crazy idea, but it **does not seem to contradict Emmy Noether's theorem** and, mathematical calculations and simulations give encouraging results and merit further study of this concept by a thesis.

I am looking for a microelectronics laboratory with sufficient technological and design resources for a doctoral student to confirm or deny this idea of a retired dreamer.

The dreamer would be, with pleasure, the thesis supervisor of this concept. Dr Patrick SANGOUARD



7 Allée Guillaume Apollinaire 21000 Dijon

Tel : 06 86 50 78 44

Email : [patrick.ps.patrick@gmail.com](mailto:patrick.ps.patrick@gmail.com)

## **BIBLIOGRAPHIE**

[1] Fluctuations du vide quantique : Serge Reynaud Astrid Lambrecht( a) , Marc Thierry Jaekel ( b)

a / Laboratoire Kastler Brossel UPMC case Jussieu F Paris Cedex 05

b / Laboratoire de Physique Théorique de l'ENS 24 rue Lhomond F 75231 Paris Cedex 05 , Juin 2001

[2] H.B.G. Casimir, *Proc. Kon. Nederl. Akad. Wet.* 51 793 (1948)

[3] B.V. Deriagin and I.I. Abrikosova, *Soviet Physics JETP* 3 819 (1957)

[4] E.M. Lifshitz, *Sov. Phys. JETP* 2 73 (1956); E.M. Lifshitz and L.P. Pitaevskii, *Landau and Lifshitz Course of Theoretical Physics: Statistical Physics Part 2* ch VIII (Butterworth-Heinemann, 1980)

[5] Techniques de l'Ingénieur : l'expertise technique et scientifique de référence

« Applications des éléments piézoélectriques en électronique de puissance » Dejan VASIC: *Maître de conférences à l'université de Cergy-Pontoise, Chercheur au laboratoire SATIE ENS Cachan*, François COSTA: Professeur à l'université de Paris Est Créteil, Chercheur au laboratoire SATIE ENS Cachan

[6] 1. Wachel, J. C., and Bates, C. L., "Techniques for controlling piping vibration failures", ASME Paper, 76-Pet-18, 1976.

[7] Jayalakshmi Parasuraman, Anand Summanwar · Frédéric Marty · Philippe Basset · Dan E. Angelescu · Tarik Bourouina « Deep reactive ion etching of sub-micrometer trenches with ultra-high aspect ratio Microelectronic Engineering » Volume 113, January 2014, Pages 35-39

[8] F. Marty, L. Rousseau, B. Saadanya, B. Mercier, O. Français, Y. Mitab, T. Bourouina, «Advanced etching of silicon based on deep reactive ion etching for silicon high aspect ratio microstructures and three-dimensional micro- and nanostructure» *Microelectronics Journal* 36 (2005) 673–677

[9] Semiconductor Devices S. M. Sze Physics and Technology

APPENDICES

X / A FEW REMINDERS FROM RDM

X.1 / Calculation of the deflection of a bridge embedded at its 2 ends

Note: We take the case of pure bending, the shear force  $T$  is such that  $T = -\frac{dM}{dx}$  With  $M$  the bending moment applied to the piezoelectric bridge. The Casimir force in the  $z$  axis is applied in  $l_p / 2$  at the center of the bridge. (Figure 67)

Figure 67: general appearance of the device studied, forces and applied moments

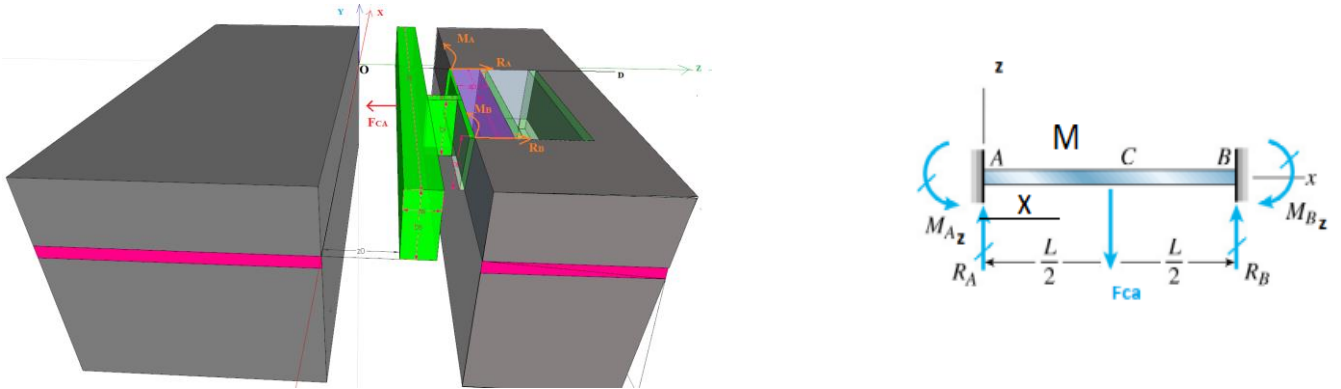
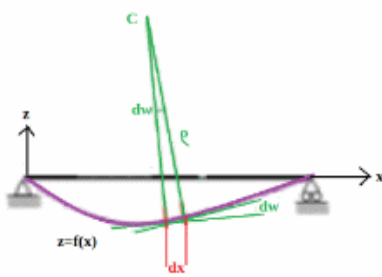


Figure 68 : view of the deformed bridge



Recall that the neutral axis  $G(x)$ , is the place where the normal bending stress is zero.  $G$  is a point of this neutral axis which in the case of a symmetrical bridge is also on the median line of the center of gravity of the bridge

Let's name:

- $M_z(x)$  = Bending moment depending on the position  $x$  on the bridge,
- $Gz$  a point of the neutral axis,  $z = f(x)$  the deformation of the bridge
- $I_p(x)$  the bending moment of inertia of the bridge section
- $E_p$  the Young's modulus of the piezoelectric material
- $\rho$  = the radius of curvature of the deformation  $z = f(x)$  the deformation of this bridge.

We will assume that the strains of the bridge subjected to the weak Casimir force are themselves small, so the induced strain angles  $d(\omega)$  are also small. Thus:

$$\tan(d\omega) = \frac{dx}{\rho} \approx d\omega \Rightarrow \frac{1}{\rho} \approx \frac{d\omega}{dx}$$

Then as it is stipulated in all the works of RDM we can assimilate the radius of curvature  $\rho$  with

$$\frac{1}{\rho} = \frac{\frac{d^2f(x)}{dx^2}}{\left(1 + \frac{df(x)}{dx}\right)^{3/2}} \approx \frac{d^2f(x)}{dx^2} \approx \frac{d\omega}{dx} = \frac{M_z(x)}{E_p I_p(x)} \quad (21)$$

Indeed  $\frac{1}{\rho} = \frac{d\omega}{dx} = \frac{M_z(x)}{E_p I_p(x)} \quad (22)$



Since the bridge is parallelepiped in shape, the bending moment of inertia along the z axis of the section of this bridge is:  $I_{Cz} = \frac{b^p a^p}{12} = Cte$  (23)

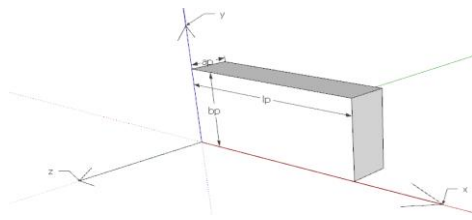


Figure 69 : width , length , thickness of the bridge

So:  $\frac{d^2(f(x))}{dx^2} \approx \frac{d\omega}{dx} = -\frac{Mz(x)}{E_P I_P(x)} \Rightarrow f(x) = -\iint \frac{Mz(x)}{E_P I_P(x)} d(x) = -12 \iint \frac{Mz(x)}{E_P b^p a^p} d(x)$  (24)

In the case of a beam embedded at both ends, we have a hyperstatic system. However, we then know (see works on Resistance of Materials) that the generalized stresses in a given section of the deformed bridge are equal to the torsor of the external actions to the right of the section, or, contrariwise to the torsor of the actions external to left.

At equilibrium, the sum at all points of the forces and bending moments is zero. Because of the symmetry of the system, we therefore have  $R_{AZ} = R_{BZ}$  and  $M_{BZ} = M_{AZ}$  and the calculation reasoning for the deformed equation is identical for  $0 \leq x \leq l^p/2$  or  $l^p/2 \leq x \leq l^p$  (see figure 67) so.

So, for the forces:  $\vec{R}_A + \vec{R}_B + \vec{F}_{CA} = \vec{0} \Rightarrow R_{AZ} + R_{BZ} + F_{CA} = 0 \Rightarrow R_{AZ} = R_{BZ} = \frac{F_{CA}}{2}$

And for bending Moments :

$Mz(x) = -E_P I_P \frac{d^2 z}{dx^2} = \frac{F_{CA}}{2} x - M_{AZ}$   
 $\Rightarrow -E_P I_P \frac{d^2 z(x)}{dx^2} = \frac{F_{CA}}{2} x - M_{AZ} x + C_1$  (25)  
 $\Rightarrow E_P I_P z(x) = -\left(\frac{F_{CA}}{12} x^3 - M_{AZ} \frac{x^2}{2} + C_1 x + C_2\right)$

$M_x$  = the bending moment at a point  $x < l^p/2$   
 $M_{AZ}$  = the bending moment in A  
 $F_{CA}$  = the force of Casimir applied in  $l^p/2$  see (9)

So for  $0 \leq x \leq \frac{l^p}{2}$   
 $z(x) = -\frac{\left(\frac{F_{CA}}{12} x^3 - M_{AZ} \frac{x^2}{2} + C_1 x + C_2\right)}{E_P I_P}$

However, we have the boundary conditions which impose:

In  $x=0 \Rightarrow z(0)=0$  et  $\left(\frac{dz}{dx}\right)_{x=0}=0 \Rightarrow C_1 = C_2 = 0$   
 In  $x = \frac{l^p}{2} \Rightarrow \left(\frac{dz}{dx}\right)_{x=l^p/2} = 0 \Rightarrow (M_x)_{x=l^p/2} = \frac{F_{CA} \cdot l^p}{8} \Rightarrow (M_x)_{x=0} = -\frac{F_{CA} \cdot l^p}{8}$   
 $\Rightarrow z = -\frac{\left(\frac{F_{CA} x^3}{12} - \frac{F_{CA} l^p x^2}{16}\right)}{E_P \cdot I_P} = \frac{F_{CA} x^2}{16 E_P \cdot I_P} \cdot \left(l^p - \frac{4x}{3}\right)$  pour  $(0 \leq x \leq \frac{l^p}{2})$

The maximum deflection is in  $x = l^p/2$  which gives an arrow:  
 $z_{max} = \frac{F_{CA} l^3}{192 E_P I_P}$  en  $x = \frac{l^p}{2}$   
 (26)

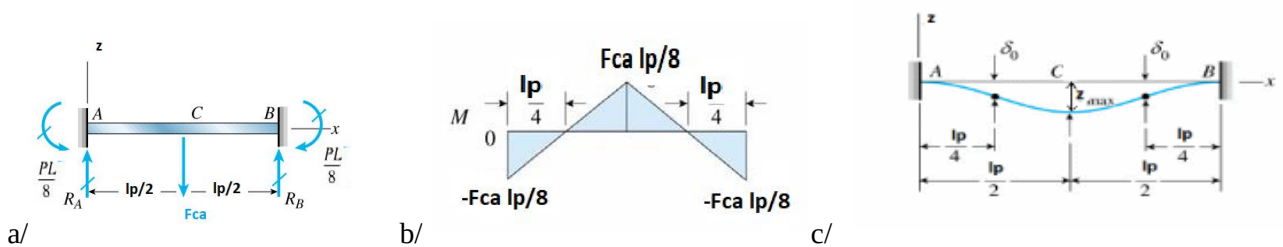


Figure 70: a / Forces, shear forces and Moments applied on the bridge. b / Variation of bending moment. c / Shape and arrow of the bridge embedded at both ends. With:  $\delta_0$  = inflection points,  $z_{max}$  = arrow of the bridge

## X.2 / Calculation of the resonant frequency of the piezoelectric bridge

We have seen that the differential equation of the deformation of the bridge reduces to:  $\frac{d^2 f(x)}{dx^2} = \frac{d^2 z}{dx^2} = -\frac{M_z(x)}{E I_{xx}(x)}$

The minus sign comes from the fact that the deformation  $z(x)$  is in the reference frame  $x, y, z$  while the moment of bending  $M(x)$  is defined in the Frenet trihedron: tangent  $t$ , normal  $n$  and bi normal  $r$ . (figure 71)

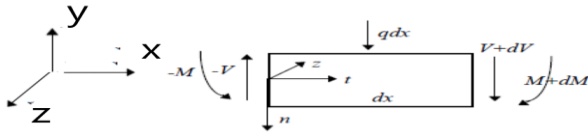


Figure 71; Section, Frenet trihedron

Let us calculate the differential equation of the deformation in terms of linear loading  $q(x) = dV/dx$  (N/m). In the Frenet trihedron, we write then the mechanical equilibrium of the beam section of length  $dx$  subjected to the linear loading  $q(x)$ .

The balance of forces (nullity of the resultant) is written:  $-V + q dx + V + dV = 0$ . So,  $q(x) = -dV/dx$ .

The balance of moments with respect to the origin of the trihedron is written:  $-\bar{M} + (\bar{V} + d\bar{V}) \wedge \bar{t} + \bar{M} + d\bar{M} = \vec{0}$

In projection on the  $z$  axis:  $-M + (V + dV) dx + M + dM = 0$ . Hence, neglecting the second order term  $dV dx$ : we obtain  $V(x) = -dM/dx \Rightarrow q(x) = dV/dx = -d^2 M/dx^2$

By differentiating twice, the differential equation  $E_p I_p \frac{d^2 z}{dx^2} = -M_z$  of the deformation written in terms of bending moment  $M_z$  and considering the two preceding relations, this equation is finally written in terms of linear loading:

$$E_p I_p \frac{d^4 z}{dx^4} = q(x) \quad (27)$$

### X.2.1 / Differential equation of a vibrating beam and determination of the eigen modes

We consider a rectangular beam (figure 67, 69) of thickness  $a_p$ , width  $b_p$  and length  $l_p$ . Let  $S$  ( $m^2$ ) be the section,  $\rho$  the density ( $Kg/m^3$ ),  $E_p$  the Young modulus with the inertia of the cross section of the beam in the width direction  $b_p$ .

$I_{cz} = \frac{b_p a_p^3}{12} = Cte$  It is demonstrated (see for example: *Vibrations of continuous media Jean-Louis Guyader*

(*Hermès*)) that the amplitude  $z(x, t)$  of the transverse displacement of a cross section of the beam is given by the

partial differential equation:  $\frac{\delta^4 z}{\delta x^4} + \frac{\rho S}{E_p I_p} \frac{\delta^2 z}{\delta t^2} = 0$ , if one neglects the internal damping!

The linear mass  $m(x)$  being equal to  $\rho S$  ( $Kg/m$ ), the linear inertia force  $F(x)$  induced by the vibration will be

$F(x) = -m(x) \gamma(x) = -\rho S d^2 z(x) / dt^2$  with  $\gamma(x) = d^2 z(x) / dt^2 =$  acceleration induced by vibration, hence the differential equation of free vibrations deduced is:

$\frac{\delta^4 z}{\delta x^4} = -\frac{\rho S}{E_p I_p} \frac{\delta^2 z}{\delta t^2}$  (28) Considering the weak bending assumptions, the solution of this equation will be acceptable only insofar the amplitude of the vibrations  $a_z$  remains small compared to the thickness  $a_p$ :  $a_z \ll a_p$ .

By setting:  $z(x, t) = Z(x) \exp(i\omega t)$  with ( $i$  = pure imaginary), and by separating the temporal  $Z(x)$  and spatial parts  $\exp(i\omega t)$ , the equation differential (28) expressing the amplitude  $Z(x)$  of the deformation at the pulsation  $\omega$  gives:

$$\frac{\delta^4 Z}{\delta x^4} + k^4 Z = 0 \quad \text{With} \quad k^4 = \frac{\rho S \omega^2}{E_p I_p} \Rightarrow k = \left( \frac{\rho S \omega^2}{E_p I_p} \right)^{1/4}$$

The solution of this differential equation is written in the general form:  
 $Z(x) = A_1 \exp(kx) + A_2 \exp(-kx) + A_3 \exp(ikx) + A_4 \exp(-ikx)$

It is also written in the more convenient form:  $Z(x) = a \cdot \sin(kx) + b \cdot \cos(kx) + c \cdot \text{sh}(kx) + d \cdot \text{ch}(kx)$  (29)

### X.2.2 / Eigen modes and frequencies

In this part, we will assume that the moving part of the structure (fig. 9) vibrates at its resonant frequency. This hypothesis will only be verified if the interface  $z_0$  between Casimir electrodes is weak enough so that the forces involved are sufficient to induce a vibration at a frequency close to the first resonant frequency (chapter 5). This simplifying assumption will allow us to analytically calculate the equation of the current derived from the vibrations of the Casimir structure but independent of the interface of Casimir electrode  $z_0$ .

The admissible values of the quantity  $k$  will be given by the roots  $k_i L = \alpha_i$  of the from the previous equation  $f(kL) = 0$ . The function  $f(kL)$  is itself defined by the four boundary conditions necessary to determine the relations between the four integration constants  $a, b, c, d$ .

It results from it, that only a series of discrete pulsations  $\omega_i$  (proper pulsations of vibration) will be authorized, these pulsations being obtained in the general form:  $\omega_{pi} = \left| \frac{\alpha_i}{l_p} \right|^2 \sqrt{\frac{E_p}{\rho}} \sqrt{\frac{I_p}{S}} \Rightarrow f_{pi} = \frac{1}{2\pi} \left| \frac{\alpha_i}{l_p} \right|^2 \sqrt{\frac{E_p}{\rho}} \sqrt{\frac{I_p}{S}}$  (30) with:

$\omega_{pi}$  = resonance pulsation and therefore  $f_{pi}$  = resonant frequency. Each of these resonance frequencies  $f_{pi}$  will be associated with a profile of deformed amplitude vibrations  $Z(\omega_i, x) = Z_i(x)$  called eigenmode of vibration. The natural frequencies (resonant frequencies) therefore result in this model from the competition between inertial forces and elastic restoring forces.

This vibration equation does not contain any term that could limit the amplitude of the oscillations, so that the amplitude solution will be defined only to an arbitrary multiplicative constant. (In this preliminary model, the viscous damping inside the bridge is neglected, it will also be placed in a vacuum,).

Eigen frequencies are the combination of a term  $\sqrt{\frac{E_p}{\rho}}$  characterizing the intrinsic properties of the material (elasticity  $E_p$ , density  $\rho$ ) which can be identified as the speed of sound propagation in the beam and a geometric term  $\sqrt{\frac{I_p}{S}}$  which characterizes the geometry of the structure.

### X.2.3 / Boundary conditions:

In our situation we have a recessed-recessed bridge.  $Z(x) = a \cdot \sin(kx) + b \cdot \cos(kx) + c \cdot \text{sh}(kx) + d \cdot \text{ch}(kx)$  (22)

In this case for  $x = 0$  and for  $x = l_p$ , we have  $z(x) = 0$  and  $dz/dx = 0$  (zero elongations and slopes). Let:

For:  $x = 0$ : 1:  $a + c = 0 \Rightarrow a = -c$       2:  $b + d = 0 \Rightarrow b = -d$

For  $x = l_p$ : 3:  $a \sin(kl_p) + b \cos(kl_p) + c \text{sh}(kl_p) + d \text{ch}(kl_p) = 0$ ; 4:  $a \cos(kl_p) - b \sin(kl_p) + c \text{ch}(kl_p) + d \text{sh}(kl_p) = 0$

We deduce from the preceding equations (1, 2, 3, 4) that:

$c \cdot (\text{sh}(kl_p) - \sin(kl_p)) + d \cdot (\text{ch}(kl_p) - \cos(kl_p)) = 0$ ; and  $c \cdot (\text{ch}(kl_p) - \cos(kl_p)) + d \cdot (\text{sh}(kl_p) + \sin(kl_p)) = 0$

These last 2 equations lead to a transcendental equation in  $kl_p$ : so, the determinant of this system is zero!  
 $[\text{sh}(kl_p)^2 - \sin(kl_p)^2] - [\text{ch}(kl_p) - \cos(kl_p)]^2 = 0 \Rightarrow \cos(kl_p) \text{ch}(kl_p) = 1 \Rightarrow \cos(kl_p) = 1/\text{ch}(kl_p)$

The solutions of this equation can be solved graphically or numerically.

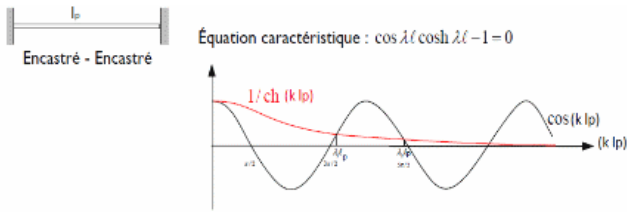


**Figure 72: Numerical solution of equation 18**

The numerical resolution (for example by the dichotomy method in figure 72 of this equation gives for the first 5 solutions:  $\alpha_1 = 4.7300$ ;  $\alpha_2 = 7.8532$ ;  $\alpha_3 = 10.9956$ ;  $\alpha_4 = 14.1317$ ;  $\alpha_5 = 17.2787$

So, the first resonant frequency of the piezoelectric bridge is

$$\omega_{p1} = (4.73)^2 \sqrt{\frac{E_p I_p}{M_s l_p}} \Rightarrow f_{p1} = \frac{1}{2\pi} (4.73)^2 \sqrt{\frac{E_p I_p}{M_s l_p}} \quad (31)$$

For example, for a bridge embedded at both ends with the following characteristics,

For geometries:  $l_p = 50 \cdot 10^{-6} \text{ m}$ ,  $b_p = 150 \cdot 10^{-6} \text{ m}$ ,  $a_p = 10 \cdot 10^{-6} \text{ m}$ ;  $S_p = 1,5 \cdot 10^{-9} \text{ m}^2$ ,  $I_p = b_p \cdot a_p^3 / 12 = 1.25 \cdot 10^{-20} \text{ m}^4$

$l_i = 10 \cdot 10^{-6} \text{ m}$ ;  $b_i = 150 \cdot 10^{-6} \text{ m}$ ;  $a_i = 10 \cdot 10^{-6} \text{ m}$ ;  $l_s = 1000 \cdot 10^{-6} \text{ m}$ ;  $b_s = 150 \cdot 10^{-6} \text{ m}$ ;  $a_s = 10 \cdot 10^{-6} \text{ m}$

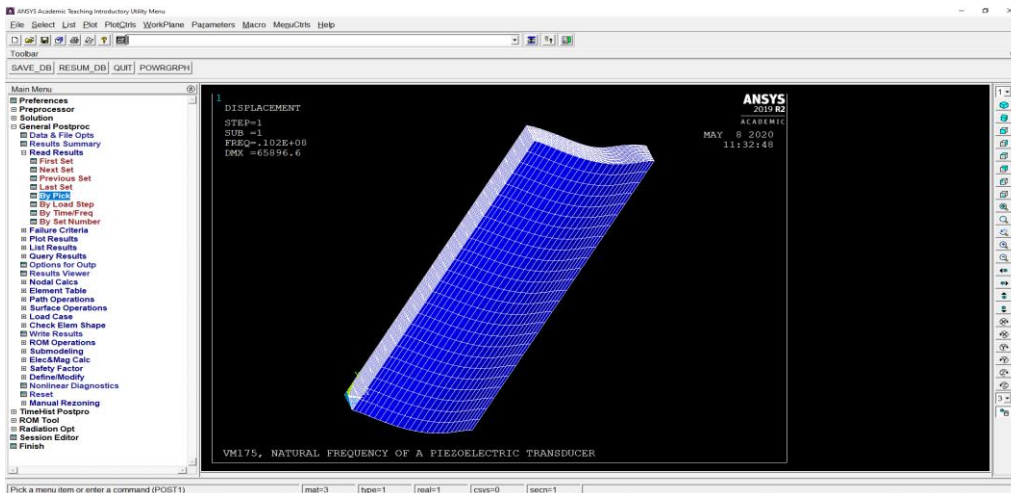
For the material: PZT: density  $\rho = 7600 \text{ (kg/m}^3\text{)}$ , Young's modulus  $E_p = 6 \cdot 10^{10} \text{ (Pa)}$  ( $\text{Kg m s}^{-2}$ )

For the section inertia:  $I_p = b_p \cdot a_p^3 / 12 = 1.25 \cdot 10^{-20} \text{ (m}^4\text{)}$

Then the calculated first resonance frequency is for the PZT material:  $f_{p1} = 1.1553 \cdot 10^7 \text{ hertz}$ .

For this embedded bridge, an ANSYS simulation (figure 73) gives a resonant frequency of  $f_1 = 1.02 \cdot 10^7 \text{ Hz}$  which is close to that calculated in the draft calculation presented in this report and validates the orders of magnitude obtained with the equations for these preliminary calculations.

**Figure 73 : ANSYS simulation of the resonant frequency of the piezoelectric**



If one carries out the calculation of the resonant frequency of the structure of figure 5 which comprises, it, a free sole of Casimir  $S_{S2}$  parallel to a fixed surface  $S_{S3}$  and transmitting by a mechanical link finger the force of Casimir, one finds that the resonant frequency of this structure becomes:

$$\omega_{p1} = (4.73)^2 \sqrt{\frac{E_p I_p}{M_s l_p}} \Rightarrow f_{p1} = \frac{1}{2\pi} (4.73)^2 \sqrt{\frac{E_p I_p}{M_s l_p}} \quad (32)$$

With  $M_s$  = the total mass of the structure!  $M_s = \rho (S_p \cdot a_p + S_i \cdot a_i + S_s \cdot a_s) = \rho (l_p \cdot b_p \cdot a_p + l_i \cdot b_i \cdot a_i + l_s \cdot b_s \cdot a_s)$ .

With  $\rho$  = the density of : The piezoelectric material, of the connecting finger, of the Casimir electrode sole and  $S_p$ ,  $S_i$ ,  $S_s$  the longitudinal surfaces of this bridge. Indeed, the presence of the Casimir sole connected by the Casimir force

transmission finger in the middle of the piezoelectric bridge, modifies the resonant frequencies of this bridge, as if a fixed mass  $M_S$  were applied and fixed in the middle of the bridge.

The calculated resonance frequency then becomes for the same geometries and materials

$f_{s1} = 2.509 \cdot 10^6$  hertz. With these characteristics, an ANSYS simulation of this structure (figure 74) gives a close resonance frequency :  $f_{s1} = 2.62 \cdot 10^6$  Hertz

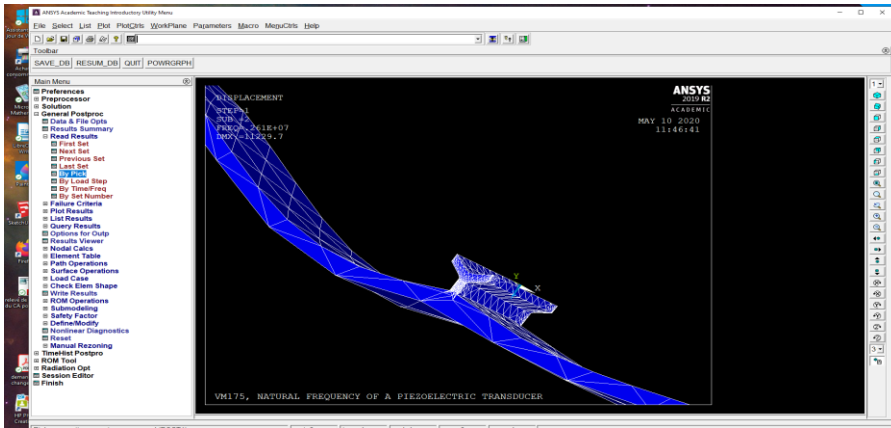


**Figure 74: ANSYS simulation of the resonant frequency of the complete structure**

This simulated resonant frequency is close to the calculated one. It is lower than that of a simple bridge by a factor of 3, which will affect the current that can be expected to be obtained from these vibrations of a piezoelectric structure.

Wachel and Bates [6] also give an approximate formula for the resonance of a bridge with a uniform mass distribution  $m = \rho \cdot S_p \cdot a_p$  on which a mass  $M$  is placed at its center.

The modification for a bridge embedded at both ends approximately follows the equation  $\omega_{s1} = \frac{\omega_{s1}}{1 + c M/m}$

With  $c$  a correction factor and  $c = 2.7$  for a bridge with both recessed ends. Which gives  $f_{s1} = 1.5 \cdot 10^6$  hertz.

This resonant frequency is not consistent with the ANSYS simulation and with the previous analytical calculation, we did not use it!

In this preliminary work, only equation (32) was used for the resonant frequency of the structure consisting of a piezoelectric bridge embedded at its two ends.

Coupled by a rigid finger to the free sole of the Casimir resonator, which is composed of a fixed electrode  $S_{S3}$  of the resonator and the surface  $S_{S2}$  at distance  $z_0$  from the other.

This mobile electrode transmitting to the piezoelectric bridge a unique and uniform Casimir force, depending only on its displacement in  $z$  and therefore remains parallel to the fixed surface  $S_{S3}$  (fig. 3,4,5).

This approach greatly simplifies these preliminary calculations because otherwise the curvature of the piezoelectric bridge makes the Casimir force strongly depend on the longitudinal and transverse positions  $x$  and  $z$  of the facing surfaces!